NTNU – Trondheim
Norwegian University of
Science and Technology

Experimental investigation of the superposition principle for a free surface roll damping tank

David Emanuel Elger

Marine Technology
Submission date: June 2014
Supervisor: Håvard Holm, IMT
Co-supervisor: Bjørnar Pettersen, IMT

Norwegian University of Science and Technology
Department of Marine Technology

Supervision of the thesis

NTNU
Norwegian University of Science and Technology
Department of Marine Technology

MASTER THESIS IN MARINE TECHNOLOGY

SPRING 2014

FOR

David Elger

In the thesis the candidate shall present his personal contribution to the resolution of problem within the scope of the thesis work.

The candidate shall study free surface stabilizing tanks used as antiroll tanks onboard ships. Physical investigations with an antiroll tank shall be done and special attention should be paid to how results from different tests can be superposed.

Both moments and forces are of interest, as well as free surface geometry.
The results should be compared against published experimental and numerical data if possible.

Theories and conclusions should be based on mathematical derivations and/or logic reasoning identifying the various steps in the deduction.

The candidate should utilize the existing possibilities for obtaining relevant literature.

The thesis should be organized in a rational manner to give a clear exposition of results, assessments, and conclusions. The text should be brief and to the point, with a clear language. Telegraphic language should be avoided.

The thesis shall contain the following elements: A text defining the scope, preface, list of contents, summary, main body of thesis, conclusions with recommendations for further work, list of symbols and acronyms, reference and (optional) appendices. All figures, tables and equations shall be numerated.

The original contribution of the candidate and material taken from other sources shall be clearly defined. Work from other sources shall be properly referenced using an acknowledged referencing system.

The thesis shall be submitted in two copies:

- Signed by the candidate
- The text defining the scope included
- In bound volume(s)
- Drawings and/or computer prints that cannot be bound should be organized in a separate folder.

Supervisor: Håvard Holm

Clarification of individuality

I hereby assure that I wrote this thesis independently, autographically and without using any other sources than stated.

_____

Date / Signature

Copyright © David Emanuel Elger and NTNU 2014

All rights reserved.

David Emanuel Elger

elgerdavid@aol.com

Preface

This master thesis was written at the Norwegian University of Science and Technology, Department of Marine Technology, to earn the degree Master of Science. The present work constitutes the graduation in the 2 Years International Master Programme in Marine Technology. A preceding project thesis is part of this thesis.

My special thanks go to Associated Prof. Håvard Holm and Prof. Bjørnar Pettersen who were willingly supervising me. I appreciate their support throughout the project thesis and the master thesis.

I am grateful for the opportunity to write this thesis in collaboration with the Norwegian Marine Technology Research Institute, MARINTEK, which was enabled by Ole Hermundstad. I want to give great thanks to Kjetil Berget and Dariusz Fathi from MARINTEK for a good introduction and supervision. I am grateful for the chance of using the rig at any time and for the possibility of exploring the tank performance step by step.

No less thanks to my parents who enabled my studies and supported me in many respects. Thanks to my friends who made the time here in Norway so special.

David Elger

Trondheim, 10 June 2014

Summary

Roll stabilizing tanks are widely used on offshore supply vessels and fishing vessels to ensure a better and safer working environment. However, the free surface of a partially filled tank is subject to sloshing. On one hand this is necessary for a roll damping tank, on the other it can lead to undesired effects such as damage to surrounding structures or a high noise level. It is therefore crucial to design such a tank in a proper way in order to dampen the roll motions of a ship most efficiently.

The focus of the present thesis lies in performing tests under pure roll and pure sway conditions with a model tank mounted on a “Two degree of freedom vessel motion simulator”. The tank was equipped with two damping grids. Each implemented experiment consisted of several tests with varying parameters. Three initial experiments were carried out to investigate the main characteristics of a free surface tank: testing the influence of different roll amplitudes with included damping grids, comparing the results with tests where the grids were absent, and testing the tank performance at different filling levels.

The objective of the present work is to detect what could be the reason for discrepancies between tests MARINTEK performed with a tank on the vessel motion simulator and a tank installed in a ship model and tested in irregular waves. The problem is approached by checking first in pure sway at periods close to resonance, where the water movement in the tank behaves linearly. Further it is investigated whether a superposition of periods including the resonance period gives the same result as a combined test. The studies are conducted with and without grids. As a preliminary investigation, five periods are superposed in sway and in roll. To date, no detailed research in this area has been realised and experiments of this type are done for the first time compared to previous studies.

The test results were plotted with a Matlab code and the damping moment curves

were evaluated. For the different roll amplitudes the tank achieves the highest damping at the highest roll amplitude of six degrees. The results show that the occurring moments for the tank without damping grids are much higher than with installed damping grids. The advantage of using damping grids is that the damping is available over a larger range of periods.

The comparison of different tank filling heights shows that higher moment amplitudes are achieved with a larger amount of water. However, a high water level gives very high damping at low periods, but only within a narrow range.

Furthermore, a sequence analysis was carried out and compared to literature. The major finding was that due to the installed damping grids less water reaches the other side of the tank in time to raise a large counteracting moment. The occurring hydraulic jump is delayed. This leads to the conclusion that both roll amplitude and configuration of the grids have to be considered together when designing a roll damping tank.

A superposition of roll and sway moments does not give the same result as a combination of roll and sway in one test. Three major findings resulted from the linearity checks and the superposition of different periods in sway: The damping grids – although introducing nonlinearities – help to keep the water movement linear in comparison to tests without grids. The resonance period can be included whereas the two neighbouring periods could not.

Contents

Nomenclature

A, B	Factors
a	Amplitude of displacement [m]
b	Tank breadth [m]
c	Damping force coefficient [Nms] in roll
c_{cr}	Critical damping [Nms]
g	Acceleration of gravity [m/s^2]
$\overline{GM}$	Metacentric height [m]
$\overline{GM}_T$	Transverse metacentric height [m]
$\overline{\delta GM}_T$	Reduction in the transverse metacentric height [m]
h	Water depth [m]
I_{WL}	Area moment of the water line [m^4]
k	Wave number [m^{-1}]
k	Restoring force coefficient [Nm] in roll
l	Tank length [m]
M	Moment [Nm]
M_a	Moment amplitude [Nm]
m	Inertia force coefficient [Nms^2] in roll
P	Excitation force [N]
P_a	Excitation force amplitude [N]
t	Time [s]
T_n	Natural period [s]
T_1	First natural period, resonance period [s]
x	Distance [m]

β	Frequency ratio [-]
ε	Phase angle [rad]
ζ	Free surface elevation [m]
η	Roll angle [rad]
$\dot{\eta}$	Velocity [m/s]
η_a	Roll amplitude [rad]
λ	Wave length [m]
λ	Scale [-]
ξ	Damping ratio [-]
ω	Circular frequency, load frequency [rad/s]
ω_0	Eigenfrequency [rad/s]
$\forall$	Displacement [m^3]

Definitions:

Metacentric height:

$$\overline{GM} = \overline{KB} + \overline{BM} - \overline{KG}$$

Area moment of the water line:

$$I_{WL} = \frac{l b^3}{12}$$

Wave number:

$$k = \frac{2\pi}{\lambda} = \frac{\omega^2}{g}$$

Period:

$$T = \frac{2\pi}{\omega} = \sqrt{\frac{2\pi\lambda}{g}}$$

Natural period:

$$T_n = 2\pi \Big/ \sqrt{\frac{\pi \cdot n}{b} g \cdot \tanh\left(\frac{\pi \cdot n}{b} h\right)}$$

First natural period, resonance period:

$$T_1 = 2\pi \Big/ \sqrt{\frac{\pi}{b} g \tanh\left(\frac{\pi}{b} h\right)} \quad \text{in general}$$

$$T_1 = 2b \Big/ \sqrt{g\,h} \quad \text{for shallow water}$$

Frequency ratio:

$$\beta = \frac{\omega}{\omega_0}$$

Wave length:

$$\lambda = \frac{2\pi}{k}$$

Damping ratio:

$$\xi = \frac{c}{c_{cr}}$$

Circular frequency:

$$\omega = \frac{2\pi}{T} \quad , \quad \omega^2 = kg \tanh(kh)$$

Abbreviations

CFD	Computational Fluid Dynamics
DLF	Dynamic Load Factor
LNG	Liquid Natural Gas
MARINTEK	Norwegian Marine Technology Research Institute
NTNU	Norwegian University of Science and Technology
RAO	Response Amplitude Operator
VERES	ShipX Vessel Responses programme

1 Introduction

In former times ships were stabilised in the wind by their huge sails and large keels. When ships began sailing with motor power they started to use bilge keels but these were not sufficient enough to compensate for the upcoming roll motions. It was already in 1880 when Watts and Froude suggested the use of water tanks for damping as reported by Van den Bosch and Vugts (1966). Nowadays, roll stabilizing tanks are widely used on offshore supply vessels and fishing vessels to provide a better and safer working environment. Tanks of different shape exist and they can be passively or actively controlled.

The movement of water within a container is called sloshing. Sloshing appears in almost every moving vessel which contains liquids with a free surface in a partially filled tank. Faltinsen (2009) pointed out that the liquid will move severely from one side to the other as a result of resonant excitation motions from the ship. As examined later, sloshing has a strong influence on the dynamic stability of a vessel.

Ship motions excited by waves can evoke sloshing in a tank which in turn will influence the ship motions from inside the ship. Ships equipped with a specially tuned tank utilize this effect to dampen their roll motions.

1.1 Motivation and objective

Since the 1960´s first liquid natural gas (LNG) tankers were built to serve Europe and Japan with a new carrier of energy. It became apparent that sloshing in cargo tanks resulted in one of the most critical ship loads. Until today these generated loads have remarkable influence on the tank walls and the supporting ship structure as reported

by Faltinsen et al. (1974) and Solaas (1995). Spherical and membrane tanks are the two mainly used geometries. A failure of such a tank can lead to brittle fracture of the surrounding structure due to a low temperature shock of the escaping liquid. Besides the risk of explosion the repair costs and out-of-service costs are high.

The phenomenon of sloshing appears not only in ships but also in many different applications and vehicles. Goudarzi and Sabbagh-Yazdi (2012) recently investigated sloshing in seismically excited tanks. Other storage tanks are installed on floating offshore units for oil and gas production. Tanks of wellboats contain living fish which has to be transported carefully to fish farms. Solaas (1995) mentioned sloshing in railway tanks. One can also find many articles written about sloshing in fuel tanks of rockets.

As can be seen from the described cases, cargo tanks apply manifoldly and sloshing becomes an important aspect. According to Solaas (1995), sloshing can involve large fluid motions with turbulences, braking waves and spray. These are highly nonlinear phenomenons and sloshing itself is therefore difficult to predict.

Besides the undesired sloshing in cargo tanks, sloshing is required in roll damping tanks to a certain amount. Still, many model tests are conducted to find the best configuration for a roll damping tank. Berget (2013) pointed out that model tanks tested with the vessel motion simulator at MARINTEK give slightly different results than tanks installed in a ship model and tested in irregular waves. It is speculated that these discrepancies are owed to the damping grids in the tank or to other nonlinear effects. Furthermore, MARINTEK assumes that the damping moment increases linear with increasing roll amplitude, referring to Van den Bosch and Vugts (1966).

The objective of the present work is to investigate what the reason for the above mentioned discrepancies could be. Accordingly, it was first checked at which tank motions the water movement in the tank behaves linear. Usually a test at MARINTEK

involves many frequencies in an irregular time series. So it is further investigated which frequencies can be superposed by keeping the water movement in the tank linear and under which conditions the water movement starts to become nonlinear.

1.2 Thesis structure

In the following chapters the theoretical aspects of a free surface tank will be discussed first. This will be done by describing mathematically how this kind of tank works and how its main dimensions can be designed physically. Then the flow through grids and effects of damping are described by a literature study.

The focus lies on the third chapter, performing own tests with a model tank to investigate the main characteristics of a free surface tank. A lot of studies were already done with different roll centres but this study is special as it shall describe the characteristics for pure roll and pure sway motions. The experimental procedure will be described including the test setup, calibration and test implementation. In the beginning, two tank parameters will be examined: the influence of different roll amplitudes and of different filling levels on the tank performance. Especially the water movement with the resulting forces and moments will be analysed. Further, linearity will be checked for different periods at and around the resonance period before superposition will be done with various combinations of periods. At the same time, a comparison is made how a tank with damping grids is performing in contrast to a tank without damping grids. The investigation of linearity and superposition, even with taking the effect of damping grids into account, is done for the first time compared to previous studies.

A comprehensive discussion of the achieved results follows in the fourth chapter. The significance of the findings for further work with the tank will be outlined in the subsequent conclusion. Finally, recommendations for further analyses with the tank

will be suggested.

2 Literature review

Before looking deeper into the topic of free surface tanks it is shortly explained why more than one natural period exists. After a short distinction of free surface tanks and U-tube tanks, the function of a free surface tank is described. An important aspect is thereby the occurrence of a hydraulic jump and the resulting counteracting moment over one period of roll. Designing a free surface roll damping tank is not trivial and depends on many factors. A theoretical background is presented how to design the main dimensions of a free surface tank physically, and how it can be implemented in praxis.

The flow through grids and effects of damping are described by a literature study as well as restrictions in experiments and calculations due to complicated fluid physics. Last in this chapter it is elucidated when the principle of superposition is valid.

2.1 Natural periods

Natural frequencies or eigenfrequencies describe the modes in which a body or fluid can oscillate when excited. The modes are characteristic wave patterns as shown in figure 1. The relationship of any period T and frequency ω is

$$T = \frac{2\pi}{\omega} \tag{1}$$

The natural periods for a roll damping tank with arbitrary water depth are given by

$$T_n = 2\pi \Big/ \sqrt{\frac{\pi \cdot n}{b} g \cdot \tanh\left(\frac{\pi \cdot n}{b} h\right)} \tag{2}$$

with *n* as a positive integer, tank breadth *b*, gravity constant *g*, *and* water depth *h*. T_1 represents the highest natural period since increasing *n* in the denominator of the fraction gives lower period values.

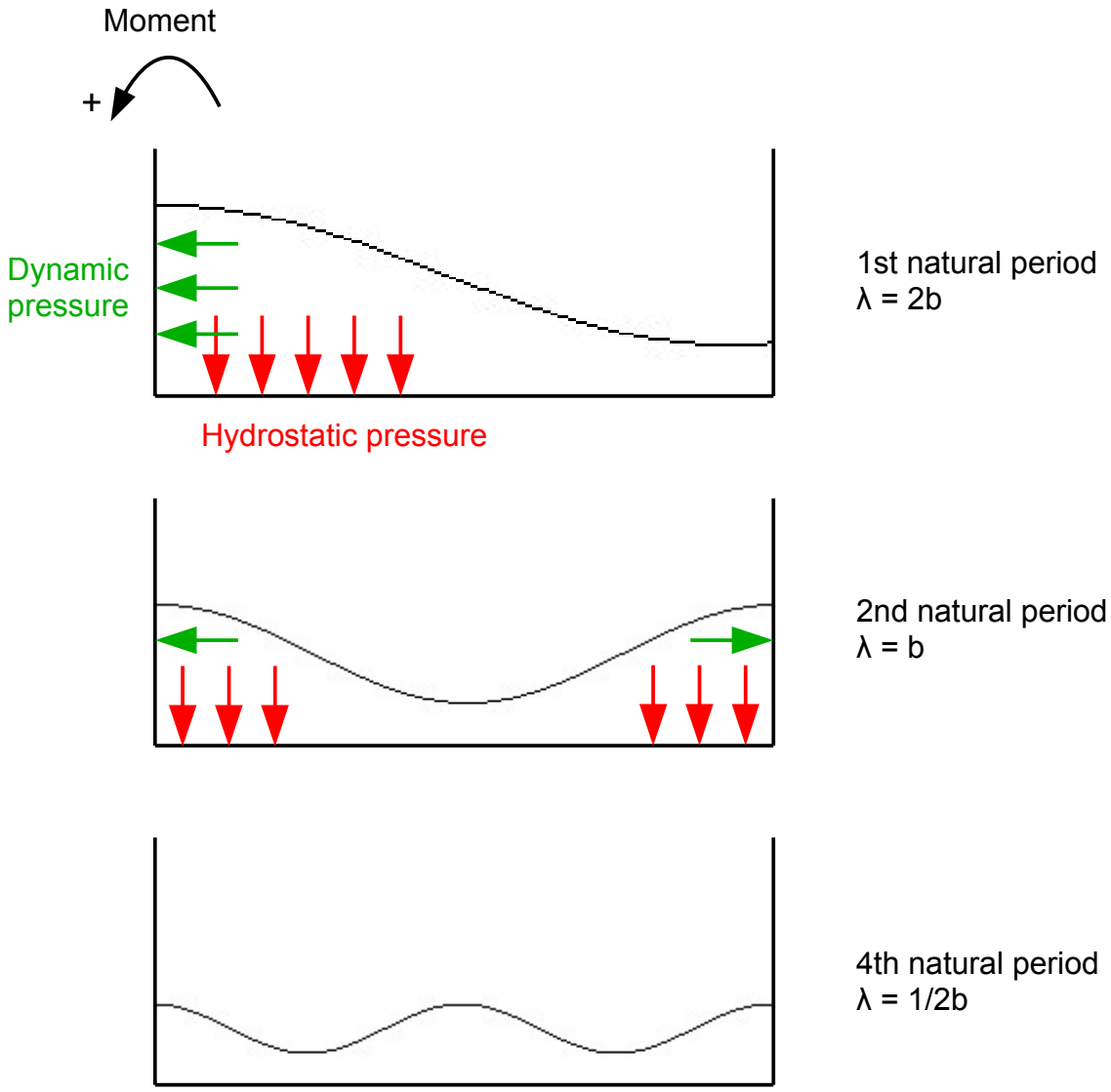

Figure 1: Natural periods in a tank

Petterson (2013) and Henderson (2014) relate the wave length λ to the tank breadth *b* as

$$n\lambda = 2b \tag{3}$$

According to this relationship, the typical wave patterns for the natural periods can be drawn as in figure 1. For *n* = 1 for the first natural period in the upper part of the figure, the longest possible wave is given whereby only one half of the wave can be seen within the tank. According to Strandenes (2014) there is most of the water concentrated on one side of the tank which gives high dynamic and hydrostatic

pressure forces resulting in a high moment. The first natural period gives therefore the highest damping moment when the tank is installed on a ship. In the following, the highest natural period is also referred to as the resonance period as excitation at this period leads to resonance.

For the second natural period in the middle of figure 1, the forces stay in equilibrium and give no damping moment. There is one whole wave in the tank but with a lower amplitude than for the first, highest natural period. The lower the periods or higher the frequencies get, the more waves with an even lower amplitude will be in the tank as exemplified in the lower part of the figure.

Henderson (2014) pointed out that waves can be reflected in a way such that the water seems to stand still at certain locations in the tank while the surrounding medium is moving up and down. These nodal points are illustrated in figure 2 and a so called standing wave pattern is formed. However, at any other frequency than a natural frequency, the response of the medium will be irregular and non-repeating.

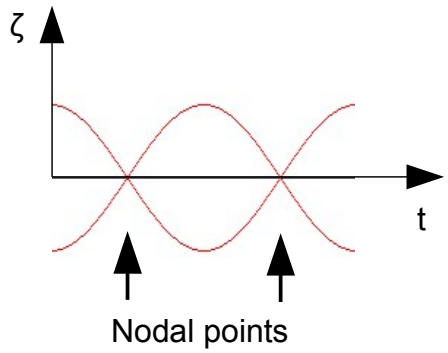

Figure 2: Second natural period

2.2 Roll damping tanks

Free surface tanks, as the right one in figure 3, are rectangular and only partly filled with water such that a free water surface exists. They are passive damping tanks but the damping can be influenced by the filling height, which can be adjusted accordingly to the natural roll period of the ship as discussed later. Often, damping grids are included to restrict the water movement to a certain amount to avoid too severe sloshing. These tanks are higher located in the ship, often close to the bridge, because here the roll motion of the ship, which shall be damped, is higher. There, the tank is more effective and can be reduced in size compared to an installed tank below the centre of rotation. The horizontal position of the tank in the ship is not an issue except for trim considerations because the effect of the roll damping moment is acting on the whole ship.

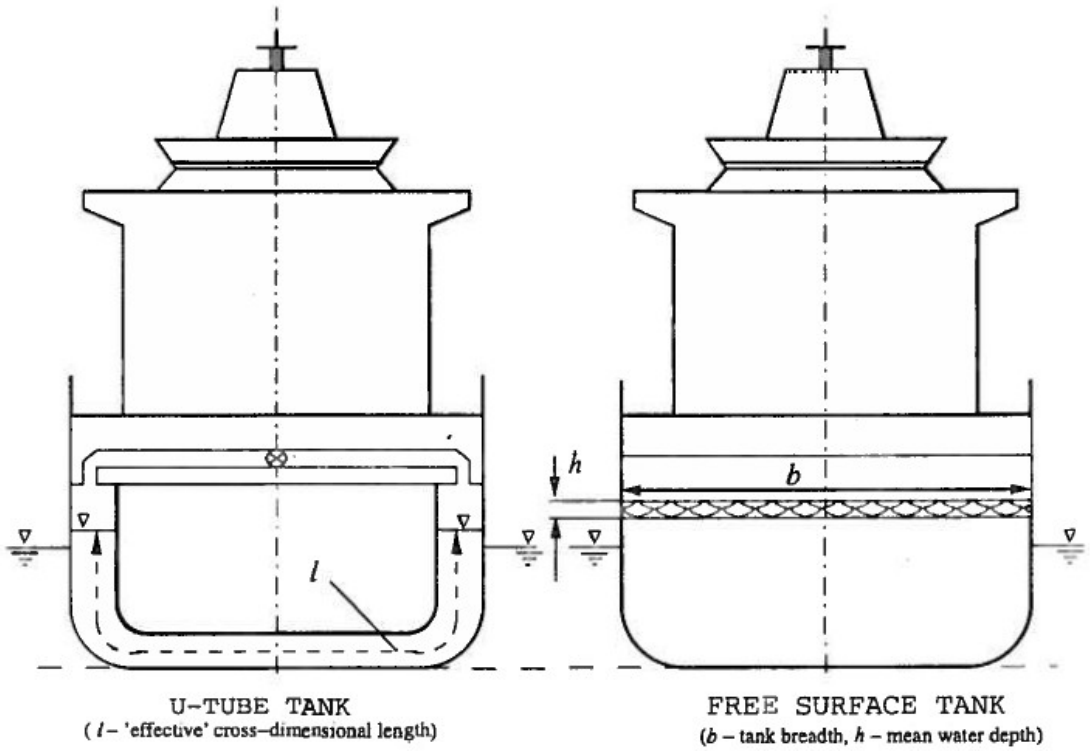

Figure 3: U-tube tank and free surface tank (Faltinsen, Timokha, 2009)

When a passive roll damping tank is used, a reduction in roll motion has amongst others the following advantages as listed by Winkler (2011) and Faltinsen, Timokha (2009):

- Higher passenger and crew comfort and consequently higher safety
- Risk of parametric roll is significantly reduced
- Less cargo damage
- Roll reduction of 40-75 % at resonance condition
- It works even at zero forward speed
- Most cost efficient compared to active fins and bilge keels
- No special maintenance or spare parts required
- Reduced fuel consumption due to less roll motion and less resistance compared to fins and bilge keels

The following disadvantages of a free surface tank can be mentioned:

- Free liquid surface
- Reduction of the metacentric height $\overline{GM}$
- Additional weight of 1-2 % of ship displacement
- Reduction of space and cargo carrying ability

Besides straight, rectangular free surface tanks U-tube tanks are often installed. Figure 3 shows both of them schematically. Common is that both use the cross-sectional breadth but the free surface tank is usually higher located than drawn in the figure. U-tube tanks consist of a U-shaped fluid channel. An air channel connects both ends of the fluid channel and a valve in the middle controls by means of air pressure the liquid filling level at both ends of the tank. It is classified as an air controlled passive tank whereas actively controlled tanks also exist. Moaleji and Greig (2007) reported two cases of active controlled tanks: In the first one, a turbine driven blower provides air pressure to push water from one side of the tank to the other. In the second case, a continuously rotating impeller is located in the water

channel. In combination with control valves water is moved actively to the specific tank side.

Controlling the fluid with valves in an active tank achieves more damping than a passive tank can provide. In addition, it was noticed that a passive tank only dampens the roll motion of a ship around the ship´s resonance frequency but increases the roll motion in fact at other frequencies than the resonance frequency as further described in chapter 2.7. This problem is solved by active controlled tanks. Though, for larger ships the amount of stabilising water, which has to be moved, increases and the required valves would become impracticably large.

Further, Moaleji and Greig (2007) pointed out that a U-tube tank avoids two of the main problems a free surface tank is accompanied with: the hardly controllable fluid sloshing, as well as the reduced stability due to the location above the centre of gravity and the shifted mass during slow side motions. On the contrary, Iglesias, Rojas and Rodríguez (2003) quoted that a U-tube tank can be difficult to tune for changing loading conditions.

2.3 Function of a free surface tank

One may think that the water filling level in a roll damping tank must be actively controlled related to steadily changing environmental conditions to ensure proper damping of the ship roll motions. This is not the case because the ship rolls with a constant period according to its “stiffness” related to the centre of gravity and the metacentre which depend on the loading condition. The tank filling level has therefore be only adjusted to dampen the roll amplitude within the concerning period when the loading condition has changed.

Due to roll motions of the ship, the fluid in the tank will flow from one side to the other

across the tank. The shifting mass will exert an own roll moment on the ship. By a smart design of the tank this roll moment can be used as a damping moment which counteracts the initial roll motion of the ship as stated by Moaleji and Greig (2007). Thereby a so called hydraulic jump occurs when the lowest natural frequency of the tank is near the excitation frequency. The flow motion with a hydraulic jump is schematically illustrated by Faltinsen and Timokha (2009) in figure 4.

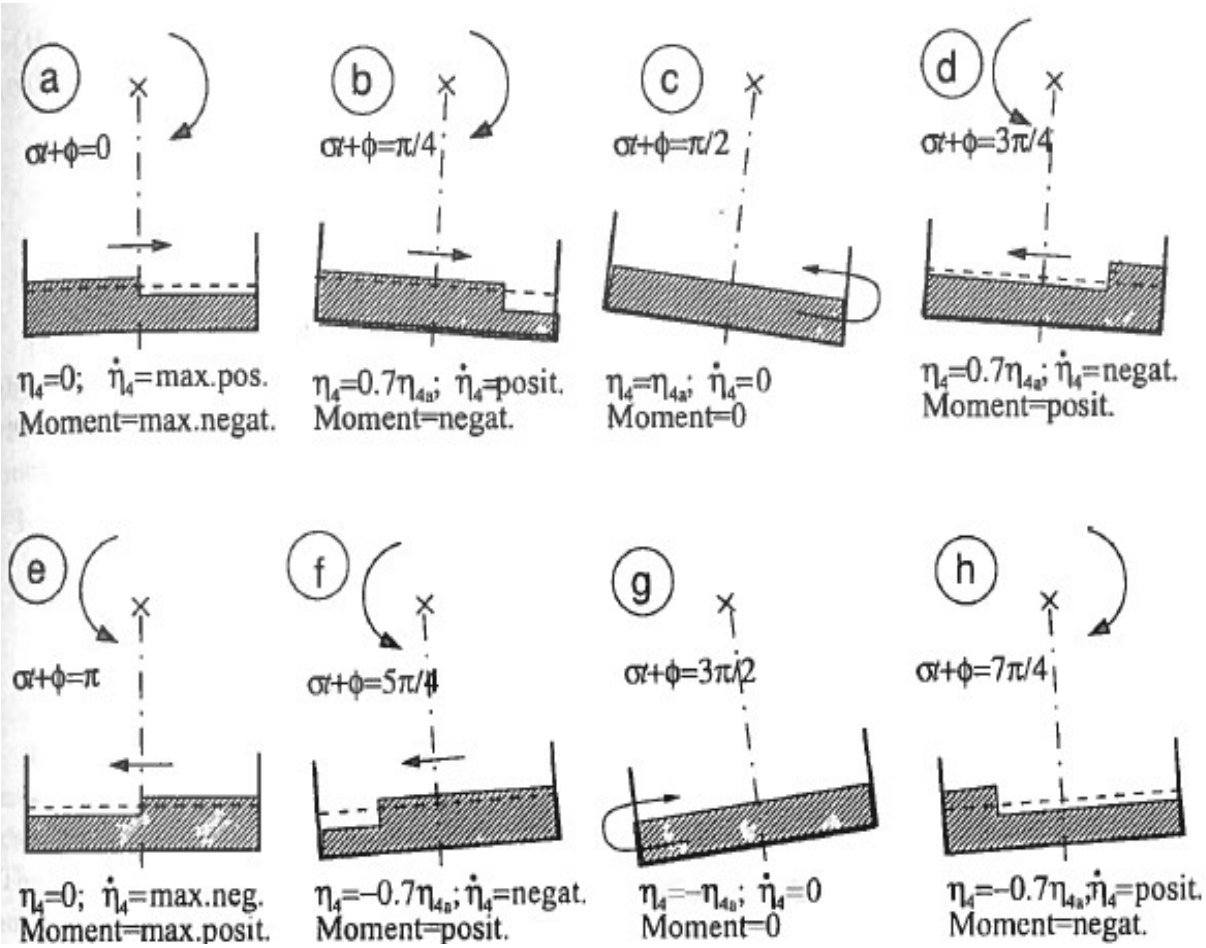

Figure 4: Position of the hydraulic jump during one period of roll at tank resonance (Faltinsen, Timokha, 2009)

The position of the hydraulic jump changes over time during one roll period. The roll angle η_4 can be described as

$$\eta_4 = \eta_{4a} \sin(\omega t) \tag{4}$$

Then, the roll velocity becomes

$$\dot{\eta}_4 = \omega \eta_{4a} \cos(\omega t) \tag{5}$$

In the initial position (a) in figure 4 the roll angle η_4 of the tank is zero and thereby ωt = 0. It follows that the cosine in equation 5 becomes one which gives the maximum positive roll velocity $\dot{\eta}_4$. The moment is maximally negative and thereby counteracting the positive roll motion, indicated by the arrow around the centre of roll.

Figure 4 clarifies that the hydraulic jump is around the middle of the tank in (a) and (e) when the roll angle is zero and the roll velocity has a maximum. At this point, the moment has also a maximum. As Van den Bosch and Vugts (1966) stated, the hydraulic jump has a great (positive) influence on the fluid transfer and therefore on the counteracting moment. The larger the roll amplitude is, the larger is the hydraulic jump and thereby the moment. The dependence of the damping moment on the roll amplitude can be approximated by the square root because the strength of the hydraulic jump is proportional to the square root of the roll amplitude. The damping moment is thereby not increasing linear with the roll amplitude, which in contrast is assumed by MARINTEK, referring to a conclusion from Van den Bosch and Vugts (1966).

A more detailed description about height, position, and velocity of the hydraulic jump can be found in Faltinsens and Timokhas book “Sloshing” (2009), chapter 8.8.2, Steady-state hydraulic jumps.

2.4 Physics: Design of a free surface tank

When external forces create sloshing in a tank, a roll moment will be induced by the tank on the vessel. This roll moment of the tank will cause roll damping when it

counteracts the roll moment of the ship, especially at the resonance period of the ship. Faltinsen and Timokha (2009) explained that effective damping of ship roll motions can be achieved when the highest natural sloshing period of the tank is designed to be close to the natural roll period of the vessel.

The resonance frequency of a free surface tank can be easily modified by changing the water level in the tank. Therefore a free surface tank is well suited for ships with a wide range of transverse metacentric heights $\overline{GM}_T$ due to very different loading conditions. It is even common to use two roll stabilizing tanks when the ratio of maximum $\overline{GM}_T$ to minimum $\overline{GM}_T$ is often larger than two in different load cases. Such a tank is usually installed relatively high in the ship because the roll velocities are more intense there. This can mean a reduction of 15-30 % of the transverse metacentric height $\overline{GM}_T$ which means less stability. For steady healing ships in a curve or due to strong side wind the water in the tank will flow to one side and keep staying there which reduces the moment righting lever. In spite of this disadvantage, the free surface tank provides acceptable roll motions for crew, passengers, and cargo.

When designing a free surface tank the main dimensions water depth *h*, tank breadth *b* and tank length l have to be determined. Faltinsen (1993) reported that *b* is often chosen to be the cross-sectional breath of the inner ship hull where the tank shall be placed.

The dispersion relation for finite water is valid with

$$\omega^2 = kg\tanh(kh) \tag{6}$$

The highest natural period T_1 is related to the wave length

$$\lambda = 2b = 2\pi / k \tag{7}$$

which represents a standing wave in the tank as elucidated by Pettersen (2013).

Then, the highest natural period T_1 is in the proximity of the natural roll period of the

ship and becomes with equations (6) and (7)

$$T_1 = 2\pi \Big/ \sqrt{\frac{\pi}{b} g \tanh\left(\frac{\pi}{b} h\right)} \tag{8}$$

According to Greco (2012), the water depth *h* is usually small compared to the tank breadth *b* so that shallow water conditions apply which means that $h / b \rightarrow 0$ and therefore

$$\tanh(\pi h / b) \approx \pi h / b \tag{9}$$

Referring to Faltinsen (1993), the natural period can then be written as

$$T_1 = 2b \Big/ \sqrt{g h} \tag{10}$$

where it can be clearly seen, how the water depth *h* and the tank breadth *b* influence the natural tank period. So, the performance of the tank can be adjusted to different roll periods due to changing loading conditions, by simply regulating the water depth in the tank. The following figure 5 based on equation (8) illustrates that the natural period increases with increasing tank breadth *b* for a given filling level *h*. For a given breadth *b* the natural period will decrease for increasing *h*.

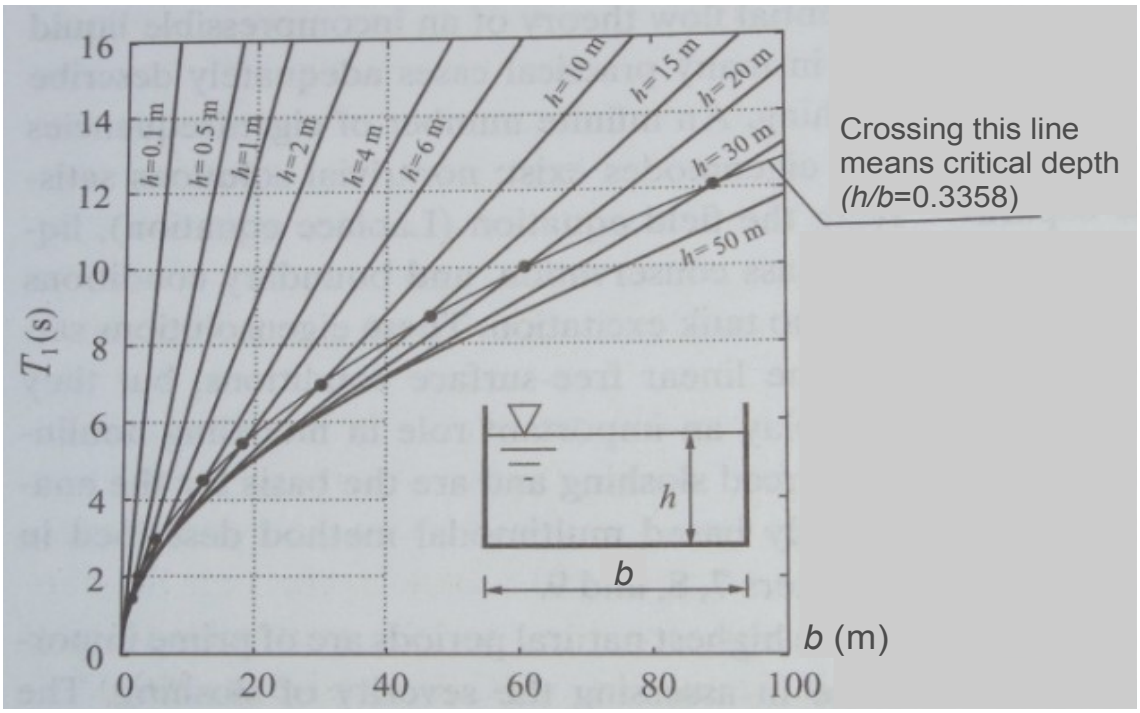

Figure 5: Natural sloshing period for a rectangular tank versus the tank breadth b for different filling levels (Faltinsen, Timokha, 2009 and Greco, 2012)

Now, *h* can be determined by requiring that the natural period of the tank shall be equal to the roll period of the ship:

$$(T_n)_{tank} = (T_n)_{ship} \tag{11}$$

Following Faltinsen (1993), the expression for the filling level *h* can then be calculated in dependency of the natural roll period for the current loading condition:

$$h = \frac{1}{g}\frac{4b^2}{(T_n)^2_{ship}} \tag{12}$$

Finally, the length l has to be chosen. In quasi-steady conditions, which means that the oscillation frequency is much lower than the lowest natural frequency of sloshing in the tank, there will be a reduction $\overline{\delta GM}_T$ of the transverse metacentric height $\overline{GM}_T$. Faltinsen and Timokha (2009) categorise the ratio $\overline{\delta GM}_T$ / $\overline{GM}_T$ to lie typically between 0.15 and 0.3. Pettersen (2013) pointed out that $\overline{\delta GM}_T$ is defined as the ratio between the area moment of the water line and the displacement:

$$\overline{\delta GM}_T = \frac{I_{tank}}{\forall_{ship}} \quad \text{where} \quad I_{tank} = \frac{l b^3}{12} \tag{13}$$

Knowing this relation, l can be found. Here, it becomes also obvious why the tank preferably should go over the whole breadth of the ship.

When looking into the unsteady effects of sloshing in a free surface tank, Faltinsen and Timokha (2009) suggested to assume initially that the roll motion is uncoupled of other motions. In reality there is a close coupling between the sway, roll, and yaw motions.

2.5 Tank design in industry

There might be different ways in how to implement a tank design for a real ship with the above outlined theory. As one example, the design routine of the Norwegian Maritime Research Institute MARINTEK is briefly delineated here.

MARINTEK uses the ShipX Vessel Responses (VERES) programme to include the effect of motion control systems on the ship motions. Different types of tanks can be handled. Either model test data from a given tank or data from systematically performed tests stored in a database can be taken as input for designing a tank using the VERES programme.

The user manual written by Fathi (2012) gives a guidance on how a rough design of a free surface roll damping tank is determined according to the sea performance of the actual ship. First, the ship motion transfer function is found in VERES which is defined by the given vessel geometry and the loading condition. Mass and position of the tank are already included but the free surface effects are of course not incorporated because the original ship performance shall be treated. Berget (2014) adds that also the sea state where the ship shall operate is an important factor in the transfer function, as larger waves will lead to larger roll amplitudes of the vessel. By plotting the transfer function one can find the natural roll period of the ship.

Second, tank geometry and maximum filling height are specified. Additional options as damping grids can be chosen. The programme then calculates which filling level is optimal for each roll period. Berget (2014) points out that an important assumption is made: It is assumed that the roll damping increases linear with increasing roll amplitude, also at resonance.

Third, by knowing now the natural roll period of the ship the optimal filling level can be read out of a plot from the second step. Finally, the modified ship transfer function

with included roll reduction can be plotted. If the achieved damping should not be sufficient, a longer tank as well as a higher location of the tank would increase the effect of the roll damping moment. Sometimes, a second tank is installed. Such operating vessels have often bilge keels in addition as initial configuration. Some of these ships cannot operate with the tank when the $\overline{GM}$-requirements are not fulfilled. Bilge keels need to be included in the ship motion calculations.

2.6 Known experiments and flow through grids

Lee and Vassalos (1996) investigated the damping effect of baffles in a tank. The different types of baffles with different opening sizes are shown in figure 6. Figure 7 shows the response amplitude operator (RAO) for roll over the frequency for the different kinds of baffles in figure 6. Moaleji and Greig (2007) explained that the undamped roll amplitude becomes very high without a roll stabilizing tank. A tank without any baffles shows in curve two a high increase in roll motions at frequencies much lower than the natural frequency. A semipermeable baffle seems to give the best effect in roll damping.

Furthermore, a baffled tank shows wider natural resonance peaks. “The roll reduction depends solely on the level of the water inside the tank. In the case of a baffled tank, the natural resonance peak is not as sharp as the unbaffled case and the response tends to get smoother as the water height increases compared to the baffle height. The baffles generate large amplitude travelling waves, and dissipate energy by generating vortices in the water. The baffled tank acts as a strong damper and results in almost 50 % roll reduction.” (Moaleji, Greig, 2007)

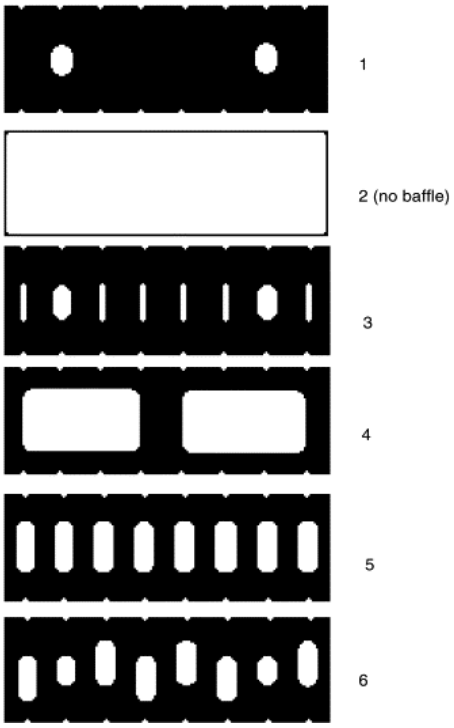

Figure 6: Tested baffle configurations (Lee, Vassalos, 1996)

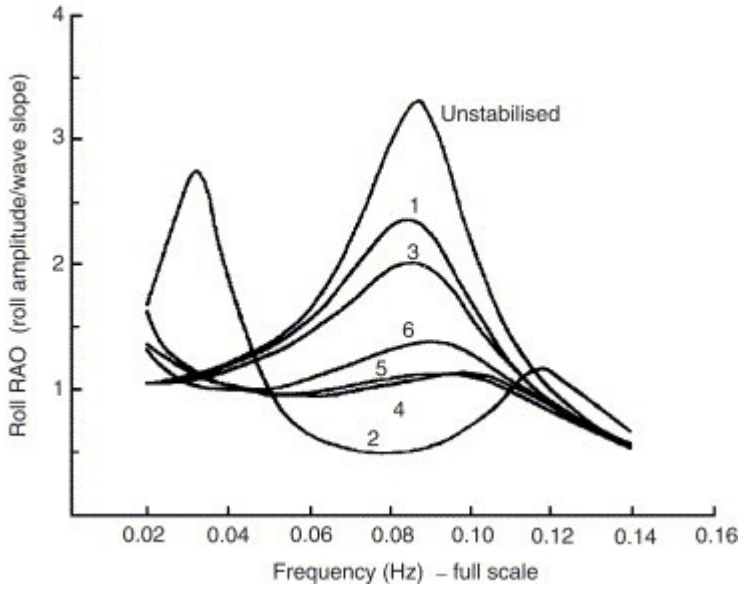

Figure 7: Estimated response amplitude operator (RAO) of a vessel (Lee, Vassalos, 1996)

A typical RAO for a ship already fitted with bilge keels is exemplified by Lewis (1989) in figure 8. The unstabilised ship has a roll damping ratio of 0.05 as in figure 10. At low frequencies the roll amplitude of the ship is very low such that the fluid in the passive roll damping tank simply follows the ship motions. Remarkably, the tank has a large damping effect when the ship is excited on its resonance frequency. However, a small destabilising effect by the tank is recorded below a frequency ratio of 0.7 and above 1.25.

Abramson (1969) stated that the effectiveness of such slosh-suppressing grids depends on their configuration and on factors as shape, size, stiffness, perforations, gaps, number, and location in the tank. They have an influence on the sloshing amplitude and frequency and therefore on the amplitude and acceleration of the tank motion. Additional parameters are tank size and geometry as well as the physical properties and filling level of the fluid.

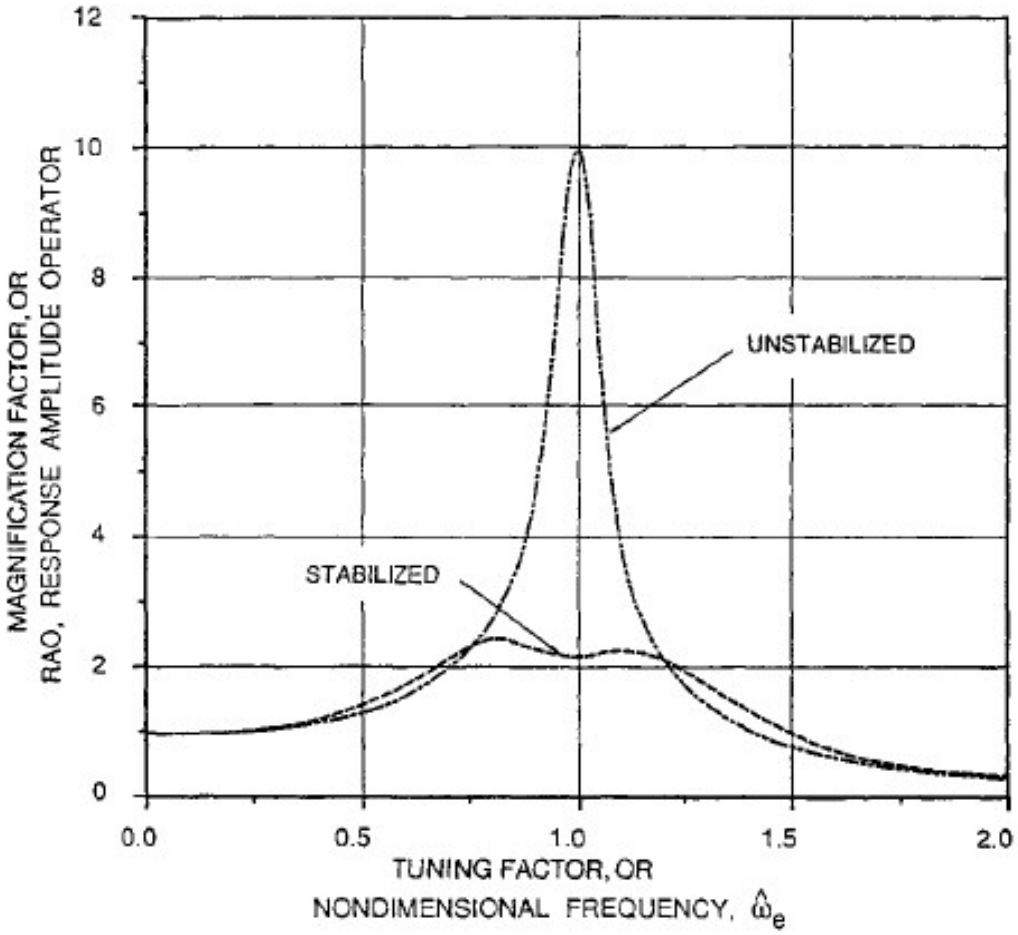

Figure 8: Roll response of a ship with and without a passive roll damping tank (Lewis, 1989)

Det Norske Veritas investigated with Faltinsen et al. (1974) impact pressures and lateral hydrodynamic forces in prismatic and spherical LNG tank models without baffles, also in full scale. They could show that parameters like tank acceleration, tank geometry, and liquid fill depth are of importance when designing a safe LNG cargo tank.

Apparently, the velocity potentials for pure roll and pure sway motions were calculated as from Faltinsen (1974) and Solaas (1995) but experiments for the separated motions have not been conducted, yet.

2.7 Damping

Damping is given when the moment is negative to the velocity as illustrated before in figure 4 on page 11. According to Larsen (2014), the tank is moving with a roll angle η_4:

$$\eta_4 = \eta_{4a} \sin(\omega t) \tag{14}$$

The measured moment is

$$M = M_a \sin(\omega t - \epsilon) \tag{15}$$

with a phase shift ε between roll angle and moment. The moment can be split into

$$M = M_a \cdot A\sin(\omega t) + M_a \cdot B\cos(\omega t) \tag{16}$$

The first part after the equal sign of equation (16) represents a part of the excitation force which is needed to give a forced motion on the tank. The sine components are inertia and restoring forces as in the equation of motion (18) for roll which applies for a tank in combination with a ship:

$$m\ddot{\eta}_4 + c\dot{\eta}_4 + k\eta_4 = P_4 \quad \text{or} \tag{17}$$

$$-\omega^2 m\eta_{4a}\sin(\omega t) + \omega c\eta_{4a}\cos(\omega t) + k\eta_{4a}\sin(\omega t) = P_{4a}\sin(\omega t - \epsilon) \tag{18}$$

In equation (18), inertia forces plus damping forces plus restoring forces equal the excitation forces which can be phase shifted to the other terms. The factor *B* in the last part of equation (16) finally is the damping component of the moment in the tank as this cosine term is in phase with the cosine term of the equation of motion (18) where this part represents the damping in the system. There is a 90° phase difference between the tank motions and the stabilizing moment as illustrated in figure 9 because the cosine term of the moment is 90° phase shifted to the sine term in equation (14) for the tank motions. By adding a stabilizing moment to the unstable roll motion the roll motion will become well stabilized as on the last line of figure 9.

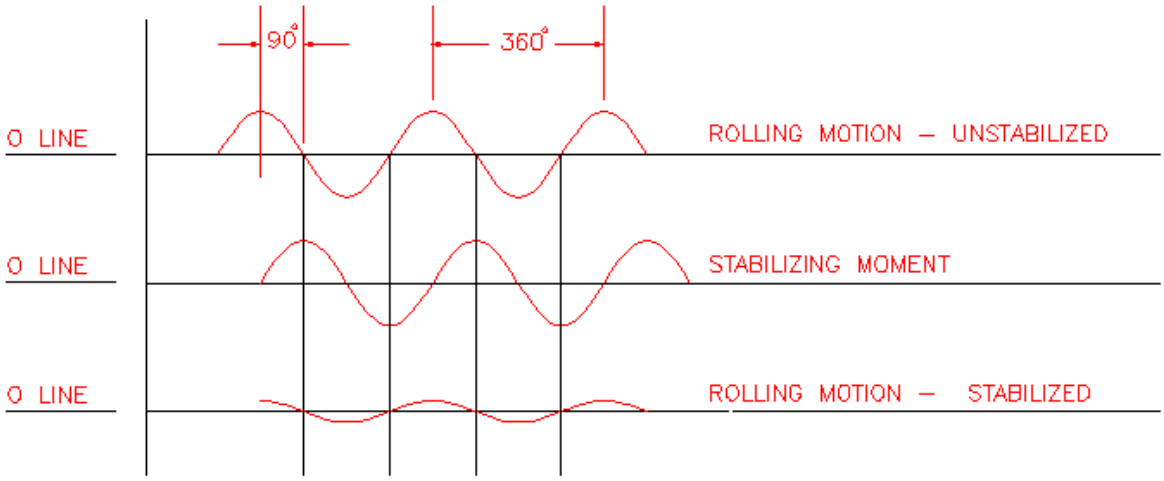

Figure 9: Achieving 90° phase difference for a stabilized motion (Winkler, 2012)

As Larsen (2012 and 2013) outlined, a system will oscillate with the same period as the exciting force which can be a harmonic function as in equation (18). The amplitude of the displacement can be found by

$$a = \frac{P_a}{k} \cdot DLF \tag{19}$$

Here, P_a / k is the static displacement which will occur when the system is hidden with a load amplitude P_a. The dynamic load factor (DLF) can enlarge or reduce the displacement as the DLF is depending on the frequency ratio β and the damping ratio ξ. The frequency ratio β is defined as the ratio between the load frequency ω and the eigenfrequency ω_0:

$$\beta = \frac{\omega}{\omega_0} \tag{20}$$

The damping ratio ξ is defined as the ratio between the damping coefficient c and the critical damping c_{cr}:

$$\xi = \frac{c}{c_{cr}} \tag{21}$$

For a damped system in forced oscillation as it is the case for a roll damping tank, the DLF becomes

$$DLF = 1 \Big/ \sqrt{\left(1-\beta^2\right)^2+\left(2\xi\beta\right)^2} \tag{22}$$

The dependency on both the frequency ratio β and the damping ratio ξ can be seen. Formula 22 can be plotted as in figure 10 where the DLF varies for different frequency ratios and for different damping ratios which are given in percent on the right hand side of the figure where the order of the numbers complies with the order of the lines. This figure points out that the response of a system will be very large when the load frequency equals the eigenfrequency such that the frequency ratio equals one. This case is called resonance. For lower load frequencies than the eigenfrequency, the DLF approaches one which means that here the displacement of the system will follow the slow excitation in phase. A so called static condition is reached. At the other end the graph approaches zero because the excitation frequency is too high for the mass of the system to follow. For this reason it is an inertia dominated system in that range. A high load frequency gives then only small response amplitudes. As Larsen (2014) concluded, the damping of a system is only for the resonance range of importance.

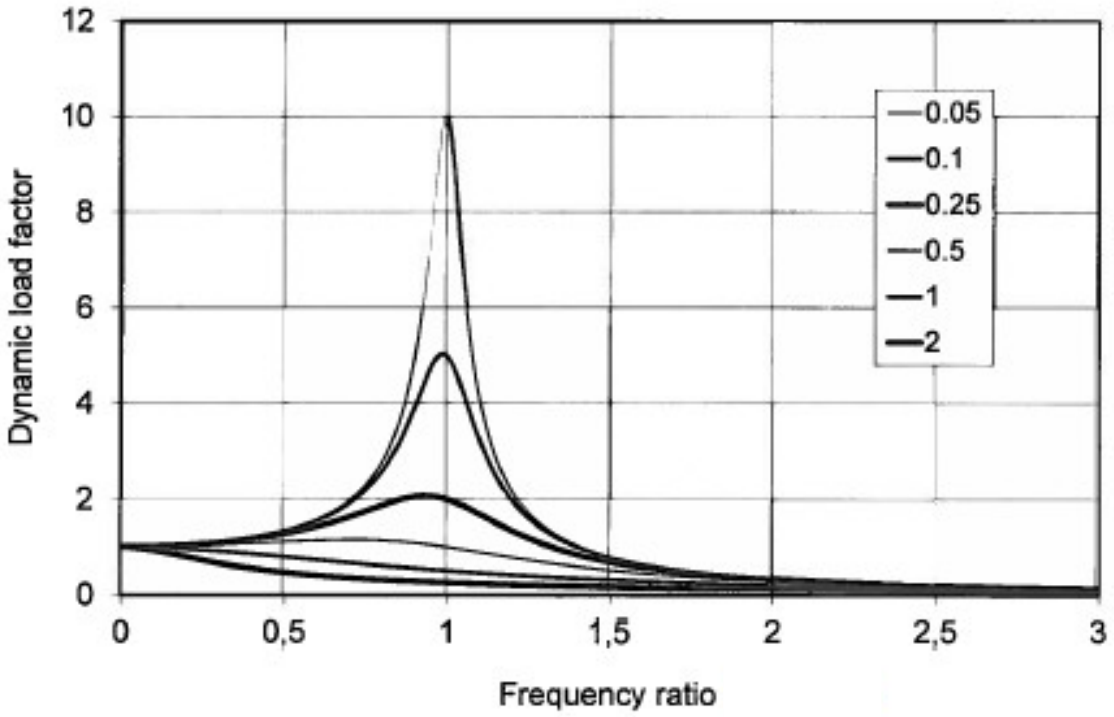

Figure 10: Dynamic load factor as function of the frequency ratio for given damping ratios (Larsen, 2012)

Corresponding to this issue, figure 11 exemplifies how large the phase shift between load and response will be for different frequency ratios and for various damping. For a frequency ratio smaller than one, load and response are almost in phase for low damping and the term “quasi static response” is used. At resonance the response is 90° phase shifted to the excitation. Thereafter both are opposite in phase for a frequency ratio greater than one.

The phase shift is depending on the load frequency but not on the load´s amplitude. The phase shift is also depending on the damping in figure 11 as well as the response amplitude in figure 10.

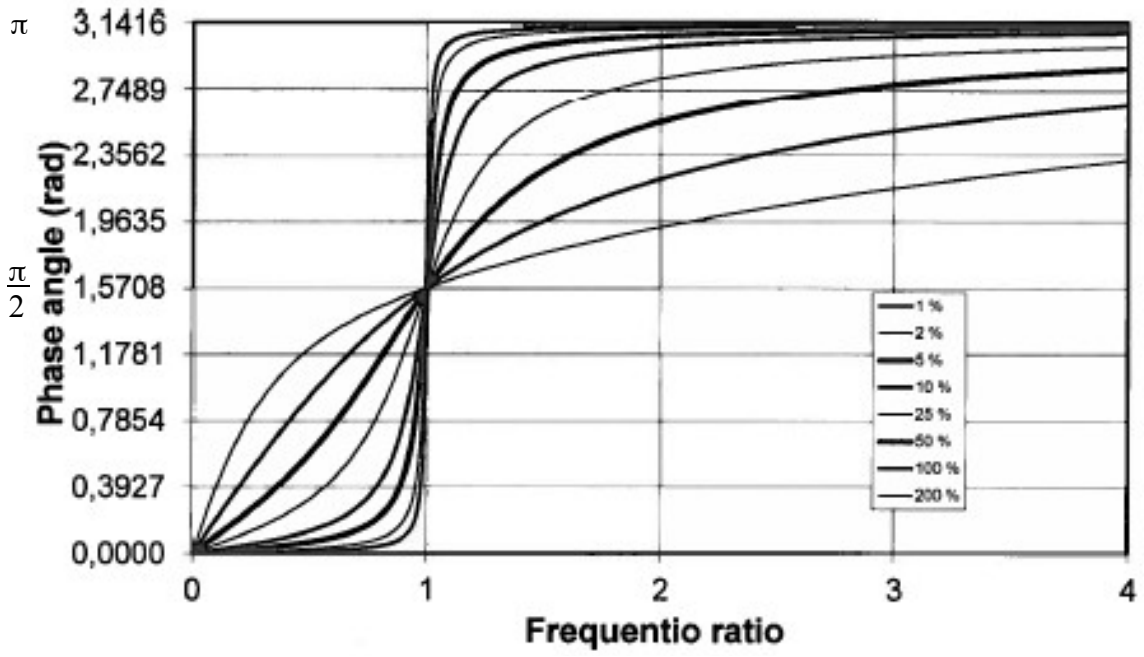

Figure 11: Phase angle between load and response as function of the frequency ratio for given damping ratios (Larsen, 2012, modified)

Inside the tank there is another type of damping which has a great influence on the water movement through the tank and therefore on the performance of the tank. Besides flow through grids damping is also caused by viscous boundary-layer flow along the tank walls. As Faltinsen, Timokha (2009) and Solaas (1995) further list,

damping of the fluid motion is related to wall roughness, the fluid viscosity itself and the free surface boundary layer. Breaking waves induce damping by turbulent energy dissipation.

2.8 Fluid physics – restrictions in experiments and calculations

Faltinsen and Timokha (2009) regarded the hydrodynamical part of sloshing as complicated due to the high complexity of the water movement within the restricted tank. For its fully understanding a combined knowledge about theory, computational fluid dynamics (CFD) and experiments are required. Still, tank design is based on experiments. Furthermore, it is not fully understood which impact the scaling from model to full scale has on the sloshing pressure. When designing the tank, also the structural mechanics and their interaction with the hydrodynamic forces on the tank have to come into account.

Celebi and Akyildiz (2002) mentioned two major problems when using computational approaches to sloshing: The boundary conditions change at the fluid tank interface and nonlinear motions have to be considered at the free surface. Nevertheless, the achieved numerical solutions agreed quite well with experimental results while the analytical solutions did not.

Abramson (1969) concluded that a theoretical analysis of liquid-resonant frequencies of sloshing in segmented tanks usually yield higher values than measured values because of the association of nonlinear effects with finite-excitation amplitudes.

2.9 Validity of superposition

Computational solutions for calculating the flow within a tank may be obtained analytically or numerically. As Solaas (1995) described, the analytical solutions are mainly based on potential flow theory which means that the Laplace equation is solved by using boundary conditions at the tank walls and the free surface. Potential theory is valid for an inviscid and incompressible fluid without rotation. The velocity potential gives the pressure of the water on the tank walls. Forces and moments are obtained by integrating the pressure.

Linear solutions may be only valid for small oscillations and where the excitation frequencies are not close to resonance. For excitation frequencies equal to resonance the linear theory predicts infinite response. Furthermore, inviscid flow in potential theory means that there is no friction, and therefore no damping of the fluid motions is predicted. This lack can be compensated by introducing an additional damping term to the linear solution. In a first comparison between theory and experiments, Faltinsen (1974) could show a compliance for the water filling height to tank breadth ratio h/b up to 0.5.

As a first conclusion, potential theory can be used to obtain solutions as long as the excitation frequencies are far away from the resonance frequencies. Also, the rig amplitudes should be small to keep the waves nearly linear. As soon as the water movement becomes more violent or the hydraulic jump occurs, nonlinear effects appear.

When potential theory can be used, two solutions can directly be added to obtain a third solution. The so called superposition principle is valid. If two velocity potentials from different motions like roll and sway are added, a phase difference between them will have to be considered. A phase angle may then be introduced in one of the velocity potentials.

Van den Bosch and Vugts (1966) went even a step further by claiming that the principle of superposition is valid when treating ship motions in irregular waves as long as the ship is equipped with a roll damping tank and is therefore performing only small rolling angles. The water movement in the tank can thereby be still markedly nonlinear.

3 Tests with the “Two degree of freedom vessel motion simulator”

In this chapter a test series with a roll damping tank in pure roll and pure sway movement will be described. The tank was installed on top of a movable table, the so called “Two degree of freedom vessel motion simulator” (rig).

Normally, the centre of roll is located at the centre of gravity of the ship which is often below or above the roll damping tank. This means that the testing rig has normally to combine roll and sway movements in order to simulate a roll centre which is not located at the tank. To the best of our knowledge, tests with roll damping tanks in pure roll or even in pure sway have not been performed before. For testing the water behaviour in the tank in pure roll, the centre of roll was laid to the bottom of the tank. For the pure sway direction the code for the movement of the rig had to be rewritten which shows that this option had not been considered to be tested before.

First, the test setup will be explained with a verification of the transducers and the rig. Thereafter the test procedures are elucidated. Finally, the results will be described in detail.

3.1 Test setup

The tank breadth *b* was defined as lying along the y-axis such that the tank could roll around the x-axis as the ship would drive in x-direction. Consequently, a positive roll moment would point towards the positive y-direction as drawn in figure 12.

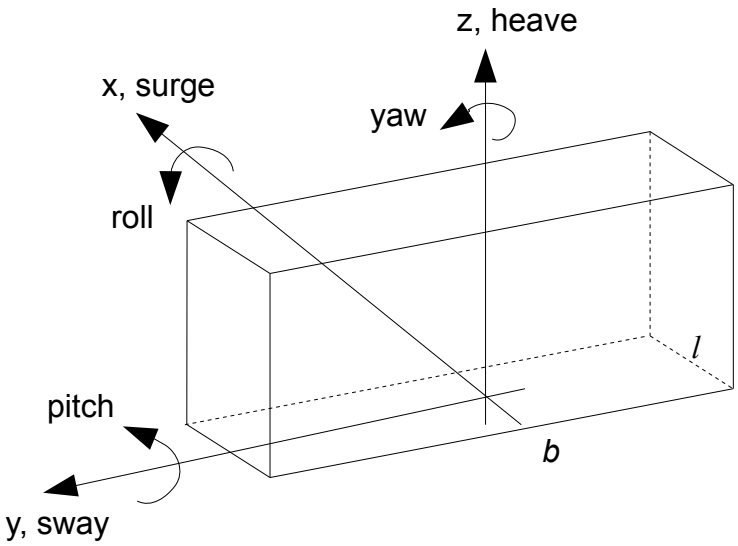

Figure 12: Definition of the tank´s coordinate system with motion modes

The rig in figure 13 was the main part of the setup. According to MARINTEK (2014) the rig was driven by two electric servo motors which means that each of the two degrees of freedom could be driven separately. There were three transducers (full bridge strain gauges) attached to the supporting plate of the rig: one for the measurement of horizontal forces and two for measuring vertical forces.

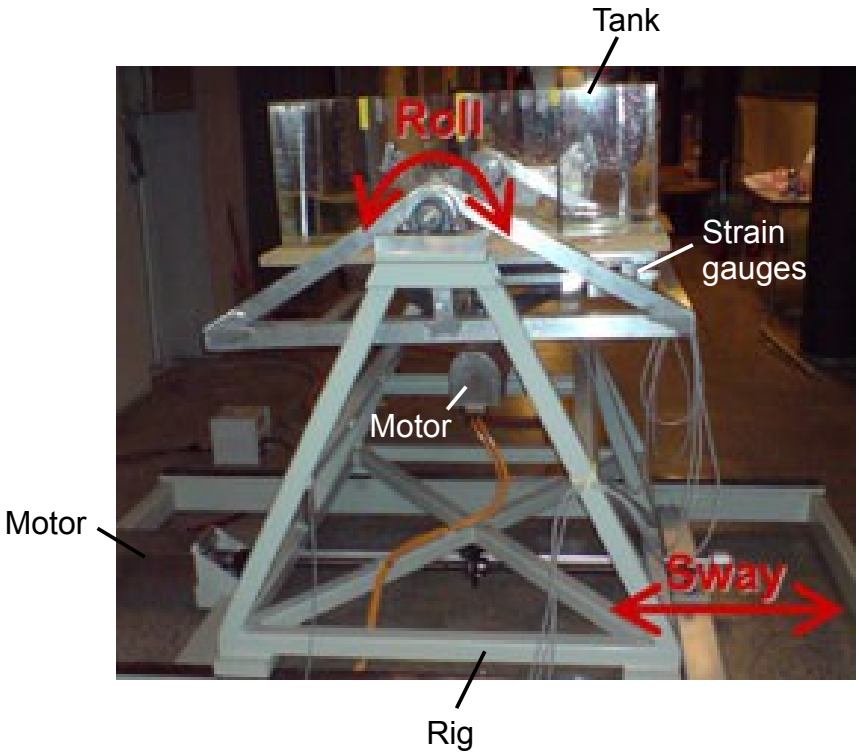

Figure 13: Test setup, rig with tank (MARINTEK, 2014, modified)

The upper part of the test setup is sketched in figure 14 to exemplify the used centres of rotation with their according moment arms. The distances are not drawn in scale.

It must be noted that the rotation centre of the rig was higher located than the bottom of the tank around which the tank should rotate for a pure roll motion. That meant that the rig had to move in addition in sway direction to simulate a rotation centre at the bottom of the tank. The distance from rig rotation centre to tank rotation centre was measured with around 0.07 m and recorded in the software. Subsequently the rig was run and the movement of the tank around its centre of rotation was confirmed by using a laser measurement device. The laser point was directed to the desired centre of roll on the tank bottom, and the input data for the rig were modified until the tank moved around this centre of roll.

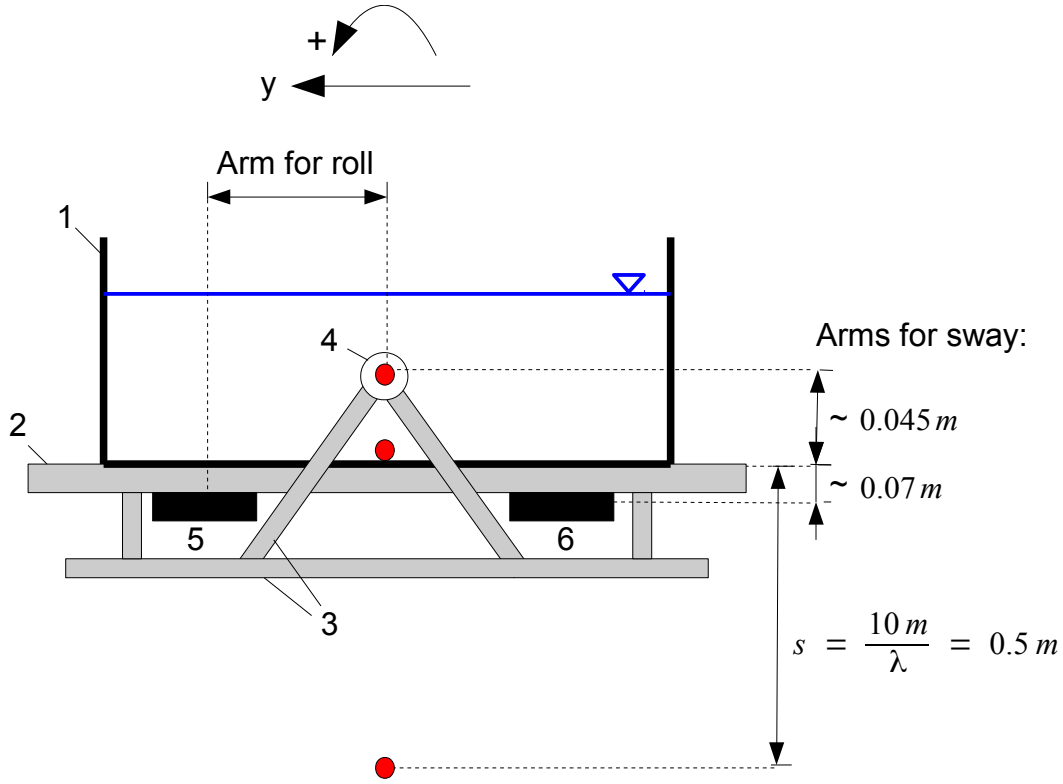

Legend:
1) Model tank
2) Table
3) Movable frame in roll
4) Rig rotation axis for roll
5) Two transducers measuring vertical forces for roll
6) One transducer measuring horizontal forces for sway
● Used rotation centres
λ Scale 1:20

Figure 14: Schematic test setup with moment arms and centres of rotation

The used tank on top of the rig was made of perspex and had the following dimensions:

Breadth: 1000 mm

Length: 175 mm

Height: 291 mm without cover panels

The tank was unrealistic high to avoid water slamming against the cover panels. This

would have made the water motions within the tank much more complicated. Actually, the tank on board should not be built smaller due to lack of space as it is often done. One should avoid slamming because this results in noise and vibrations which harm the performance of the crew. Instead, skewed and perforated panels can be installed in the upper corners. The height of the model cover panels could be adjusted such that real tank dimensions could have been achieved if desired. In the implemented tests the cover panels were fixed to the highest possible location to ensure mostly free water movement but avoiding water from splashing out of the tank.

Two damping grids out of aluminium divided the tank into three parts of the same size. The damping grids were purpose-built and self designed to have a water permeability of 50 %. The grids are shown in figure 15 and the technical drawing can be seen in figure 45 in appendix A.

Figure 15: Damping grids with permeability of 50 %

Two computers were used in the setup. One for driving the rig and one for recording

the measurements. The data as scale, distance from tank bottom to ship centre of gravity, tank breadth and amplitude of roll motion which were necessary for configuring the movements of the rig were recorded in an Excel spreadsheet. Time series were then created with a macro. The resulting binary file was loaded from the computer which operated the rig.

The applied frequencies were around 1.2 Hz in model scale and the sampling frequency during measurements was 0.02 s or 50 Hz. An amplifier strengthened the output signal from the transducers to +/-5 V and a converter changed the signal from analogue to digital before it was recorded by the second computer. Amplifier and converter were mounted in one unit. An overview of the complete setup with its components is given in figure 16.

Seven channels gave input to the data acquisition: time, two for the vertical forces in z-direction, side force in y-direction, roll and sway motions conducted from the rig, and roll torque.[1]

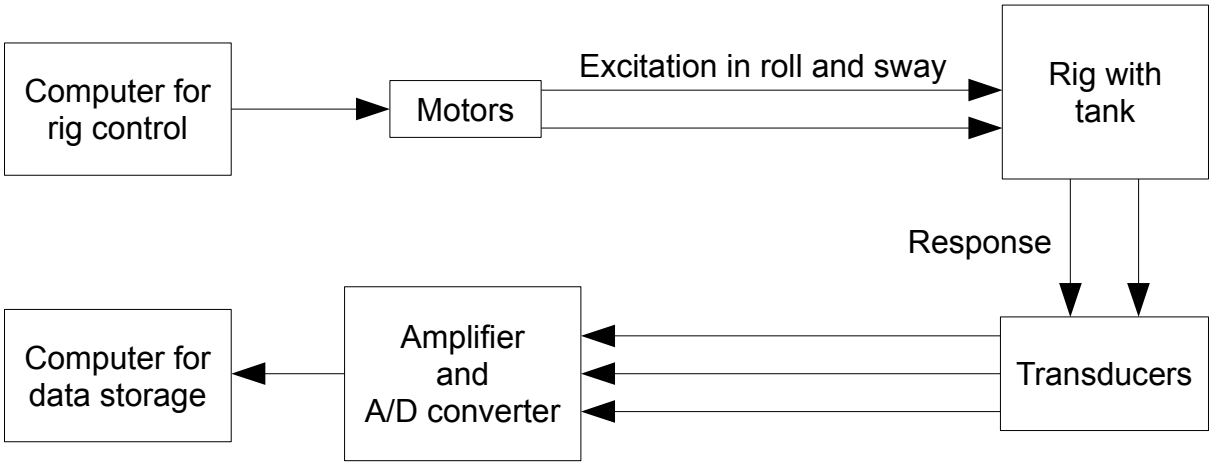

Figure 16: Components of the test setup

Before mounting transducers onto the experiment facility they are normally calibrated first. This is carried out by measuring their output while applying a certain force on

1 Torque is the average of the vertical forces measured by two transducers and multiplied by an arm to get the roll moment.

them. Next, a calibration factor can be calculated and implemented into the measurement programme. This was done by the construction workers who built up the rig and inserted the transducers the first time. Since then they are fixed but the calibration could be verified as shown in table 1. After a first zero setting of 60 s a digital force gauge was pushed against the tank supporting plate. The peak value and the corresponding measured value from the strain gauges were noted. Three measurements were done in each direction to check the accuracy over a large range of the transducers. The results lay in an acceptable range of two percent.

Table 1: Verification of the transducers

Force direction	**Input from digital force gauge in N**	**Measured output from the transducers in N**
In positive y-direction (side force)	35.3	35.47
	61.7	62.18
	119.5	119.65
In negative y-direction	31.9	-32.14
	66.2	-66.36
	98.8	-98.67
In positive roll direction (two transducers for vertical forces)	31.3	15.02 + 15.24 = 30.26
	62.1	29.95 + 31.44 = 61.39
	89.7	44.45 + 45.81 = 90.26
In negative roll direction	30.4	-15.02 - 15.89 = -30.91
	64.7	-31.94 - 32.97 = -64.91
	113.6	-56.21 - 57.19 = -113.40

The accuracy of the rig itself could also be verified by moving the rig with the software into a static position and then measuring the deflection. For an angular deflection a digital protrector (level) was used and for a lateral deflection a ruler was sufficient. The results are stated in table 2. For all these measurements it had to be

proven that the transducers or the rig went back to zero deflection after applied motions.

Table 2: Verification of the rig

Rig moving direction	**In the software stated deflection**	**Measured deflection**
In positive roll direction	1.55 deg	1.63 deg
	4.13 deg	4.37 deg
	6.96 deg	7.35 deg
	0.038 deg	0.07 deg
In negative roll direction	-2.19 deg	-2.32 deg
	-4.05 deg	-4.26 deg
	-6.87 deg	-7.22 deg
	-0.07 deg	-0.06 deg
In positive sway (y-) direction	9.98 mm	10 mm
	21.56 mm	21.5 mm
In negative sway direction	-13.99 mm	-14 mm
	-20.27 mm	-20.5 mm
	0.37 mm	0.5 mm

3.2 Experiment procedure

Figure 17 gives an overview of all experiments which will be described and discussed in the following, categorized in sway and roll as well as without and with damping grids. Pure roll and sway tests were implemented. Each experiment consisted of several tests with varying parameters like amplitude, filling level or period.

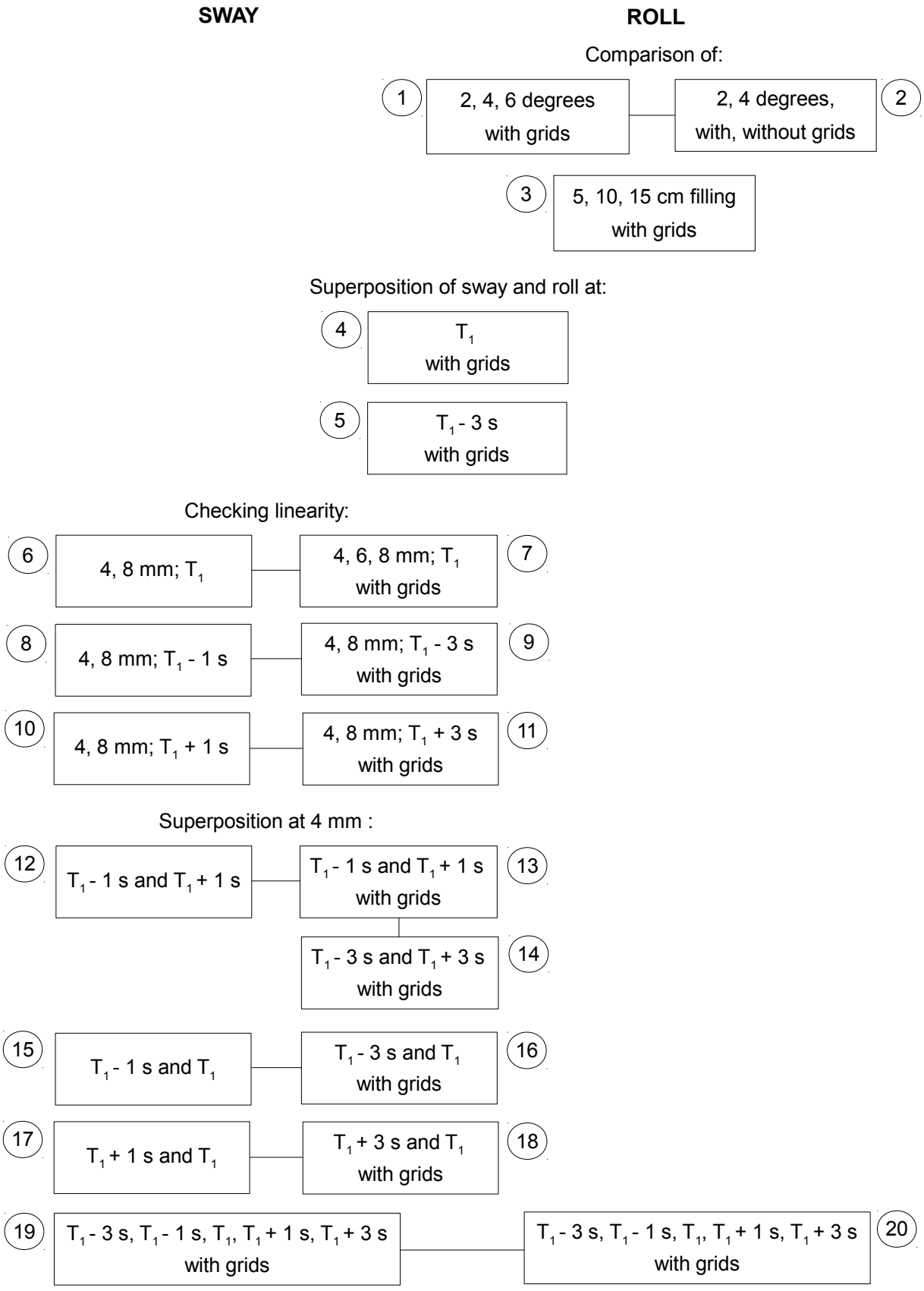

Figure 17: Overview of the performed experiments; T_1 as resonance period

In the first three experiments two tank parameters were examined: the influence of different roll amplitudes and different filling levels on the tank performance. In the fourth and fifth experiment a superposition of pure roll and pure sway movements was tried. Beforehand, this gave no satisfactory results so that systematic checks for linearity were done in the sixth to the 11th experiment. It was examined at which periods around the resonance period linearity is given. T_1 stands for the resonance period of nine seconds in full scale. Linearity can be checked by looking whether the response of a tank in four millimetres sway is half of the response of a tank in eight millimetres sway motion. Pure sway was chosen to keep the tank geometry the same during the rig motions. Thereafter, different periods at and around the resonance period were superposed in miscellaneous combinations in the 12th to the 18th experiment. It was thereby made a comparison on how a tank with damping grids is performing in contrast to a tank without damping grids. Finally, all five periods were superposed at once for sway in experiment 19 as well as for roll in experiment 20.

The forces from the fluid in the tank were obtained by subtracting the acting forces from the empty tank on the transducers from the forces of the filled tank. First, series of the empty tanks were tested before water was filled in. A logical test order, covering the first five experiment series in figure 17, was made as a test matrix in table 3 before starting with any test. This saved time when the tank filling level had not to be changed between or within experiment series. The complete test matrix for the total work is listed in appendix B.

The tests which were performed as listed in table 3 were then combined in the result analysis for the investigation of different parameters such as the influence of different roll amplitudes or different water filling levels. Most of the tests were done twice for a subsequent accuracy analysis. The two damping grids were included in each test in table 3 unless otherwise stated. Pure roll in the test matrix means roll motions around the roll centre at the inside tank bottom. For a superposition of roll and sway motions the tank was rolled around a new point, the lowest in figure 14 on page 30, to include a sway motion in the rig movement as described above. This new point was the

centre of gravity of a virtual ship. Thus, *s* in table 3 is the distance between the inside tank bottom and the centre of gravity, here 10 metres in full scale.

Table 3: Test matrix

Test number	**Parameters**
1103	Empty, pure sway
1104	Empty, pure roll, 4 deg
1105	Empty, pure roll, 2 deg
1106	Empty, pure roll, 6 deg
1107	Empty, *s* = 10 m, 4 deg
1108	10 cm water, pure roll, 2 deg
1109	10 cm water, pure roll, 4 deg
1110	10 cm water, pure roll, 6 deg
1111	10 cm water, *s* = 10 m, 4 deg
1112	10 cm water, pure sway
1113	10 cm water, pure roll, 2 deg, without grids
1114	10 cm water, pure roll, 4 deg, without grids
1115	15 cm water, pure roll, 4 deg
1116	5 cm water, pure roll, 4 deg

When speaking of superposed motions or moments, the output of two separate time series were added numerically with a new time series as result. When mentioning combined motions or moments, it is referred to one time series where two parameters were joined in the input signal from the beginning. The combined time series was taken as a “true”, in reality appearing, reference which showed whether an assumption of superposition was correct or not. For a superposition the different time series had to be in the correct phase to each other which was ensured by a Matlab script, further explained in appendix C.

For the linearity check in the experiments six to 11 the first natural period was

calculated for the tank with formula 10 on page 14:

$$T_1 = \frac{2b}{\sqrt{gh}} \tag{23}$$

The model tank has a breadth of 1 m and a water filling height of 0.1 m. The scale is 1:20 such that the highest natural period in full scale lies around nine seconds:

$$T_{full\ scale} = \frac{2 \cdot 1\,m \cdot 20}{\sqrt{9.81\frac{m}{s^2} \cdot 0.1\,m \cdot 20}} = 9.03\,s \tag{24}$$

Time is scaled by the square root of the scale λ:

$$t_{full\ scale} = \sqrt{\lambda} \cdot t_{model\ scale} \tag{25}$$

Then, the resonance period T_1 becomes for the model tank

$$T_1 = \frac{9.03\,s}{\sqrt{20}} = 2.02\,s \tag{26}$$

The tank without damping grids was excited in this frequency and stopped from moving. The wave travelled for a long time further through the tank without being damped significantly. As explained in chapter 2.7, the damping is very low at the resonance frequency and therefore very important to account for when designing structures. The time was taken for one wave period which showed accordance with the calculated natural period.

Linearity was investigated at the periods of ±1 s and ±3 s in full scale around the resonance period. The periods for the model tank became then

$$\begin{aligned} T_1 - 1\,s &= \frac{8\,s}{\sqrt{20}} = 1.79\,s & \qquad T_1 - 3\,s &= \frac{6\,s}{\sqrt{20}} = 1.34\,s \\ T_1 + 1\,s &= \frac{10\,s}{\sqrt{20}} = 2.24\,s & \qquad T_1 + 3\,s &= \frac{12\,s}{\sqrt{20}} = 2.68\,s \end{aligned} \tag{27}$$

Linearity was checked by looking whether the response of the tank in four millimetres sway was half of the response of the tank in eight millimetres sway at the same period. Without damping grids one second below and above resonance were checked for linearity in the eighth and tenth experiment. With damping grids in the

ninth and 11th experiment three seconds below and above resonance were chosen to be for sure far away from resonance to investigate how the grids influence the water movement.

The transducer for measuring the sway forces was located approximately seven centimetres below the tank bottom. The sway forces had therefore to be multiplied by a negative arm of seven centimetres in the analysis to achieve a positive moment around the centre of rotation located at the tank bottom for most of the tests, as drawn in figure 14 on page 30. Later, other centres of rotation were also used. The output of the two transducers measuring the vertical forces was averaged and already multiplied by a horizontal arm within the measuring software Catman. This roll moment and the moment from the sway force were added to achieve the total roll moment in the plots.

Before each test a zero measurement of the transducers was done because it was observed that they “drifted” a small amount. The time series for the first five experiments were created with the necessary input parameters as described above. One series contained a sequence of 19 periods which was in full scale: 4, 5, 6, 6.5, 7, 7.5, 8, 8.5, 9, 9.5, 10, 11, 12, 13, 14, 16, 19, 22 and 25 s. The amplitude was kept the same for all periods during one test. The rig used three cycles for reaching the required amplitude for each period as shown later in figure 19 on page 44. For each period there were then 20 s (model scale) for full-amplitude rig motions before the rig slowed down within three cycles to the start position. There was a ten second time interval between each period for allowing the water to calm down.

For all further tests starting with the sixth experiment a simple sinusoidal time series with a duration up to five minutes was created for the rig. Each series contained one period and one amplitude as listed in table 5 in appendix C starting with test number 3001. For the combined tests two time series with their specific periods were added by keeping the amplitude constant for both. As before, three cycles were used to reach the required amplitude.

3.3 Test results

The description of the test setup in chapter 3.1 is applied to all tests. Two slightly different test procedures are described in chapter 3.2. Therefore, the resulting data of the various tests are directly analysed and interpreted in this chapter.

The first experiments have been investigating the movement of water with the resulting forces and moments for pure roll in a free surface tank with damping grids. Two parameters were examined: Which influence have different roll amplitudes or different filling levels on the tank performance?

In the fourth and fifth experiment a superposition of roll and sway was done. The results were not satisfactory. As a consequence, a linearity check at and around the resonance period with following superposition was done. At last, five periods were superposed in sway and in roll.

3.3.1 Testing of different amplitudes

For analysing the effect of different amplitudes in the first experiment the tests with the test numbers 1104, 1105 and 1106 for the empty tank from table 1 were needed. Then, the tests 1108, 1109 and 1110 for a tank with ten centimetres filling level could be compared after having subtracted the forces of the empty tank tests.

The following phenomena can be observed in a tank with damping grids, here exemplarily described for an amplitude of four degrees:

- First amplitude of 4 s (full scale): one standing wave with $\lambda = b$ in the tank
- 6 s: Short waves start travelling from one side of the tank to the other. The flow

becomes more violent with the following periods.

- 7.5 s: One big wave moves from on side to the other. The hydraulic jump can be identified.
- 8.5 – 10 s: The waves hit the cover panels at the tank ends (not the case for an amplitude of two degrees).
- 9 s: Strong turbulences occur when water passes the damping grids.
- 10 s: The hydraulic jump stopped, two waves travel through the tank.
- 11 s: Two waves travel through the tank, more up and down than moving forward, they swing also in x-direction. This shows that nonlinearities are involved.
- 12 s: More than two waves. The water follows the tank inclination.
- 14 s: Small waves on top, the water level rises and falls with the rig movement.
- 19 s: No longer waves, the water level rises and falls with the rig movement but still large horizontal particle movement of about a quarter of the tank breadth.

It is useful to plot three graphs from the sampled data. The top graph in figure 18 shows the phase of the moment relative to the rig motion in degrees over the roll periods. For the first period of four seconds and for the large periods towards the end, there is nearly no phase difference because either the water is too inert to follow the rig motions or it can easily follow the motions at large periods. The phase of the moment can be read out of the recorded time series after the measured forces are multiplied by the lever arm to the centre of gravity. In figure 18 the moment is expressed as moment per unit roll to make the values comparable with other amplitudes of roll. The total moment can be found by multiplying with the amplitude of roll motion. The amplitude of the moment plotted in the middle graph can also be read out of the time series. The bottom graph finally shows the damping by multiplying the negative total moment by the sine of the phase of the moment from the top graph.

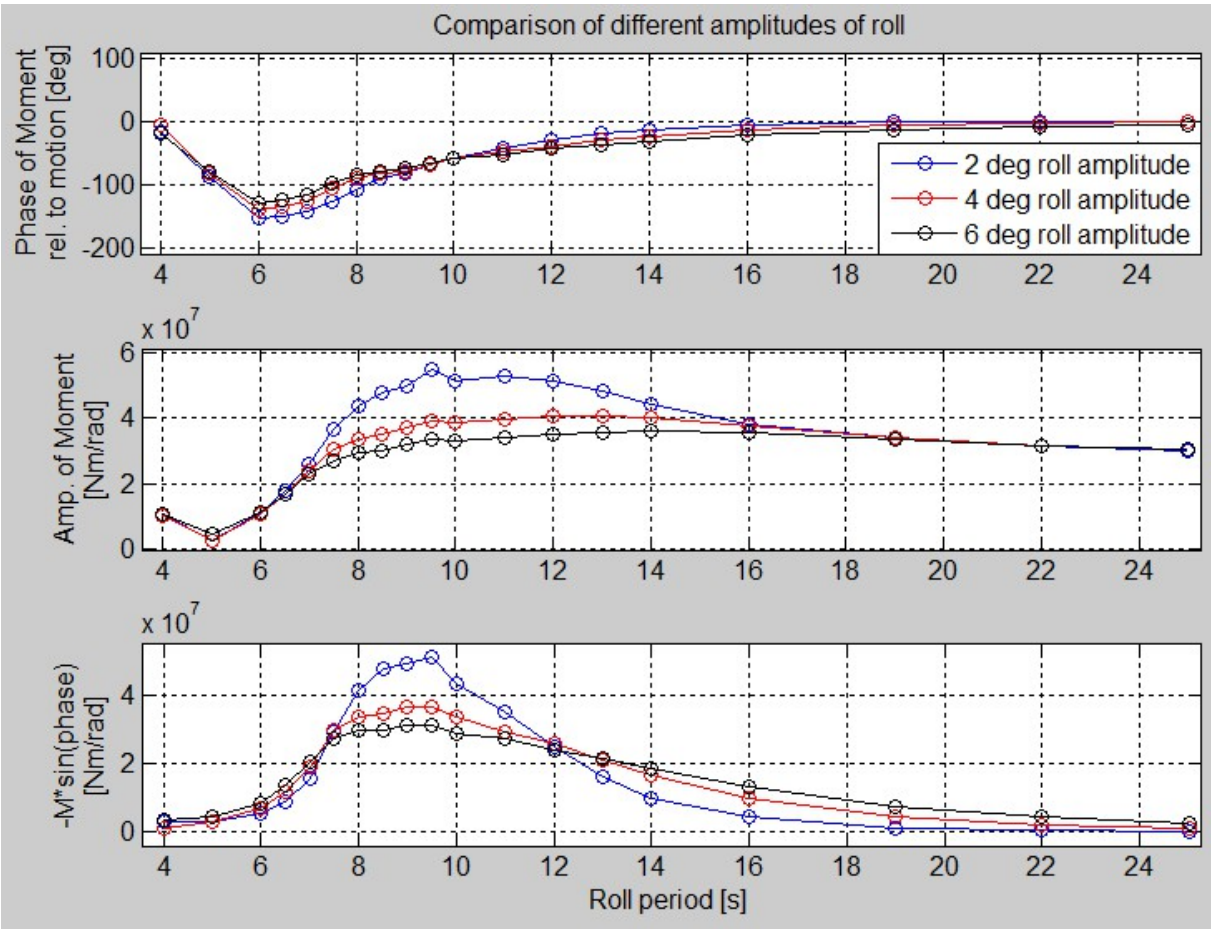

Figure 18: Comparison of different amplitudes of roll with damping grids; first experiment

As mathematically derived in chapter 2.7, most damping is achieved when the moment of the water in the tank is 90° out of phase with the ship motions. Where the phase of the moment in the top graph of figure 18 has a value of -90°, the bottom graph shows a maximum damping moment around a roll period of nine seconds.

The curves in the bottom graph of figure 18 have to be looked at separately because they were unified by the amplitude of roll. When multiplying each curve by its roll amplitude it is clear that the black curve multiplied by six gives higher values than the blue curve multiplied by two. A higher roll amplitude represented by the black curve gives therefore higher damping moments, also for a tank with damping grids.

Another aspect can be seen from the bottom graph in figure 18: The distances between the single curves are not equal. The damping moment increases not linear with the roll amplitude.

The above outlined theory in chapter 2.7 can be compared to own achieved results by looking at a sequence in detail. Chosen is a period of 8.5 s at four degrees roll. The zoomed part of figure 19 illustrates the phase shift of nearly 90° between the roll motion of the rig and torque for one period. Related pictures of the fluid flow through the tank during exactly this period are shown in figure 20 and can be compared with figure 4 on page 11 which describes the fluid flow in theory. In addition, the different phases a-g) from the pictures in figure 20 can be found in figure 19 for a better understanding.

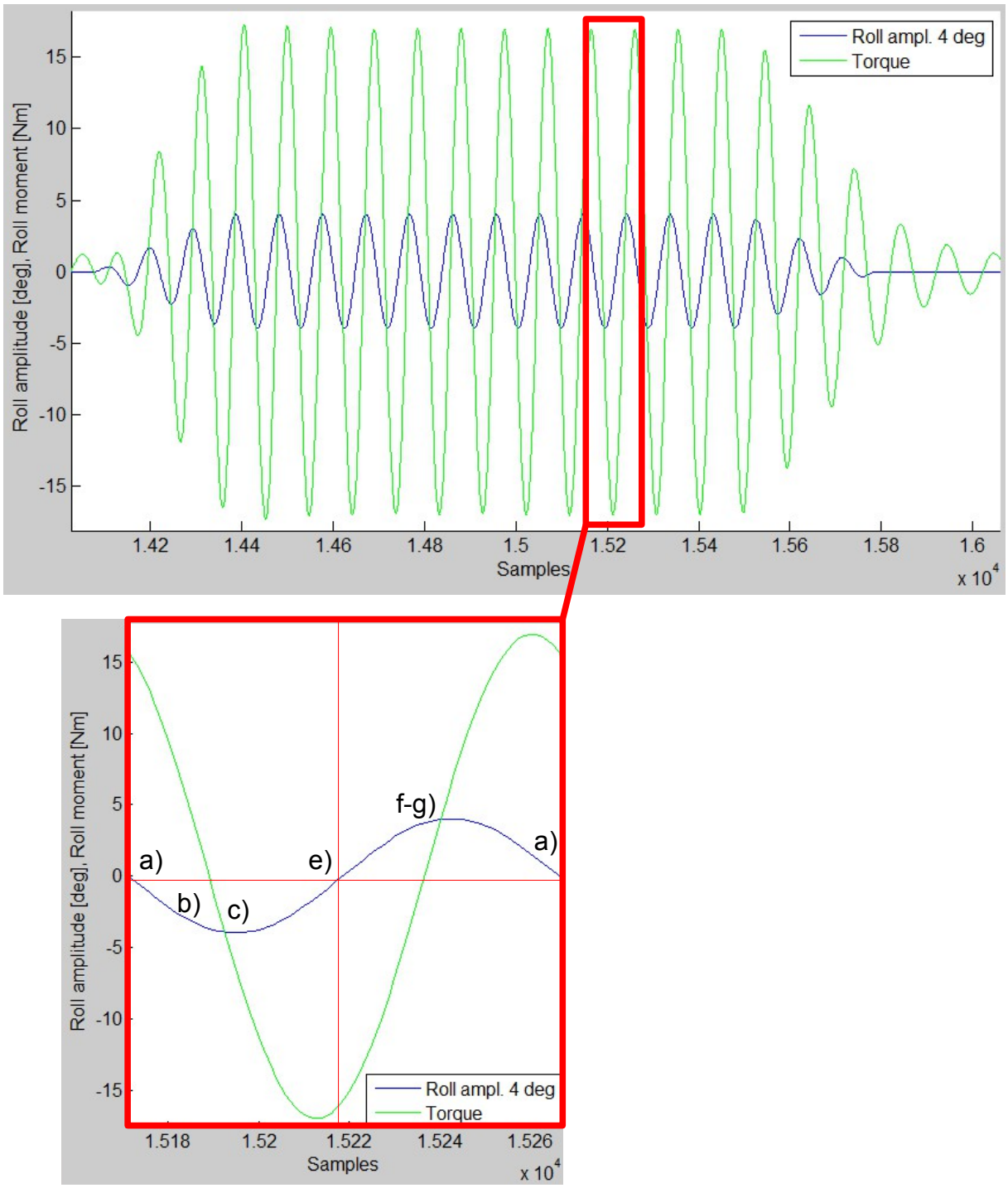

Figure 19: Results from test 1109, four degrees amplitude, pure roll, period 8.5 s. The numbering corresponds to the numbering in figure 20.

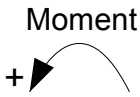

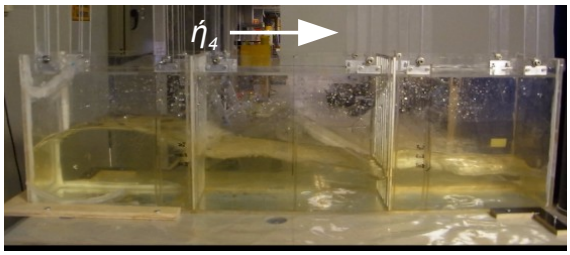

a) $\eta_4 = 0$; $\dot{\eta}_4$ = max. negative.
Max. positive Moment has passed.

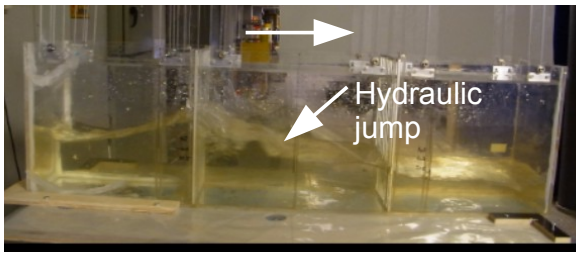

b) $\eta_4 < 0$; $\dot{\eta}_4$ = negative.
Moment goes towards zero.

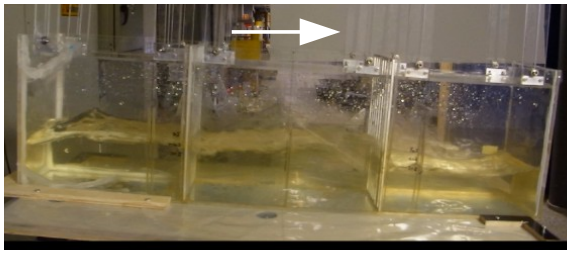

c) $\eta_4 = \eta_{4a}$; $\dot{\eta}_4$ still negative.
Moment has passed the zero point.

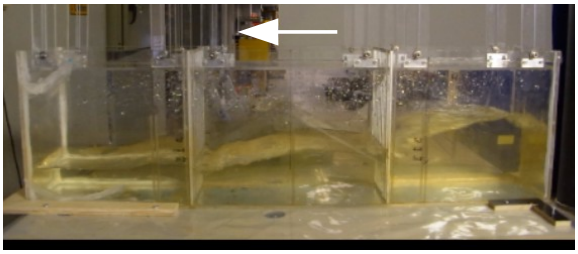

e) $\eta_4 = 0$; $\dot{\eta}_4$ = max. positive.
Max. negative Moment.

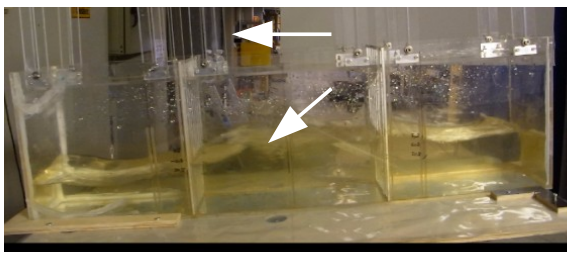

f-g) $\eta_4 > 0$; $\dot{\eta}_4$ = positive.
Moment nearly 0 because tank reached nearly $\eta_4 = \eta_{4a}$.

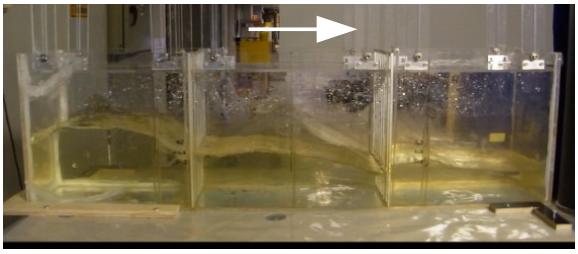

a) $\eta_4 = 0$; $\dot{\eta}_4$ = max. positive (negative for the next period).
Max. positive Moment.

Figure 20: One roll period corresponding to the red selected period in figure 19 for test 1109, four degrees amplitude, pure roll, period 8.5 s. The numbering corresponds to the numbering in figure 4. (η_4 roll motion of the tank; $\dot{\eta}_4$ roll velocity of the tank; η_{4a} roll motion amplitude)

When the tank is in its initial horizontal position as in figure 20 a) the main amount of water is on the left hand side of the tank and the maximum moment has just passed. Following the black line in figure 19, the roll amplitude becomes negative which means that the left hand side of the tank is moving upwards. The weight of the water causes a positive moment[2]. Before the tank reaches its most deflected position in figure 20 c) the water already moves towards the right hand side and a negative moment is developing. The maximum negative moment is developed before the tank reaches its horizontal position in figure 20 e) and figure 19. This can be explained by the damping grids which hinder much of the water to reach the other side in time. So, when the water is rushing back there is already quite an amount of remained water on the other side which is visible in figure 20 e). For the case without damping grids described by the next test the maximum moment occurs exactly with a 90° phase shift.

Due to the damping grids the hydraulic jump in figure 20 b) has not yet reached the middle of the tank at zero roll angle as illustrated in figure 4 on page 11. The water behaviour is time shifted compared to the theory. While the tank deflection corresponds to figure 4 g) the water movement is still that from figure 4 f). This delay might be one reason for lower damping moments compared to a tank without grids as investigated in the next experiment.

3.3.2 Testing of different amplitudes with and without grids

Two additional tests were done to see what happens when the damping grids are removed. The empty tank without grids was not extra tested because they were symmetrically placed and the difference in weight was negligible as Berget (2013) stated. In the second experiment, the two amplitudes of two and four degrees are compared with each other in figure 22 for existing grids and removed grids. The

2 When comparing with the theory in figure 4 on page 11, note that the coordinate system for the tank is reversed to that used in figure 4.

occurring moments for the tank without damping grids are significantly higher than with installed damping grids.

For the tests without damping grids very large sloshing against the cover panel is observed. Side forces of around 50 N were measured at four degrees roll motion. If much more water would reach the cover panel the moment curve would be cut horizontally as Berget (2013) mentioned. The maximum possible amount of water which can stay on one side of the tank would be reached. This has to be considered for high filling levels. A moment curve cut did not occur in this test.

Figure 21 illustrates the severe sloshing at four degrees roll amplitude without damping grids. The wave is running up the tank side, along the cover panel and then splashing back towards the tank middle as indicated by the arrow in the figure. The impact on the free surface is also good to see.

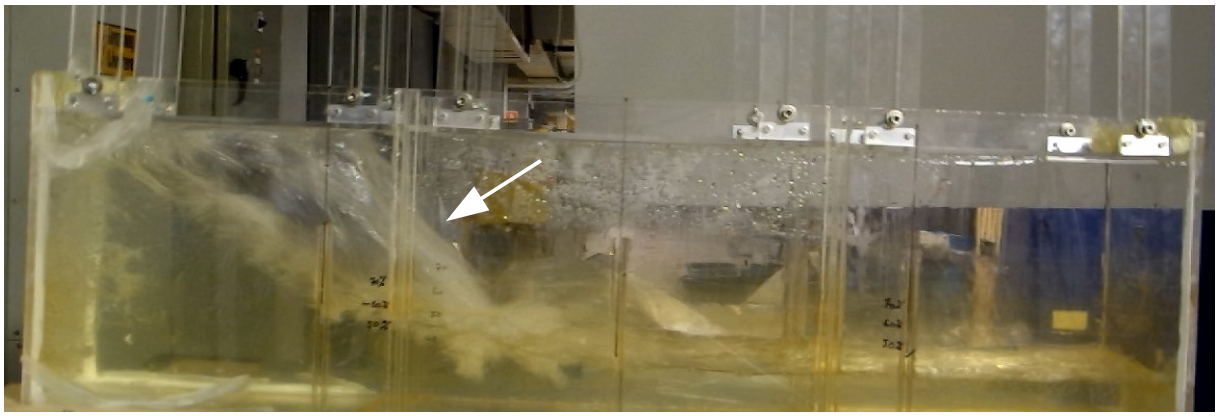

Figure 21: Four degrees pure roll without grids: water hitting the cover panel and sloshing back as a wave

Furthermore, a break-in of the curve for two degrees roll motion without grids is observed for the period of 8.5 s in figure 22.

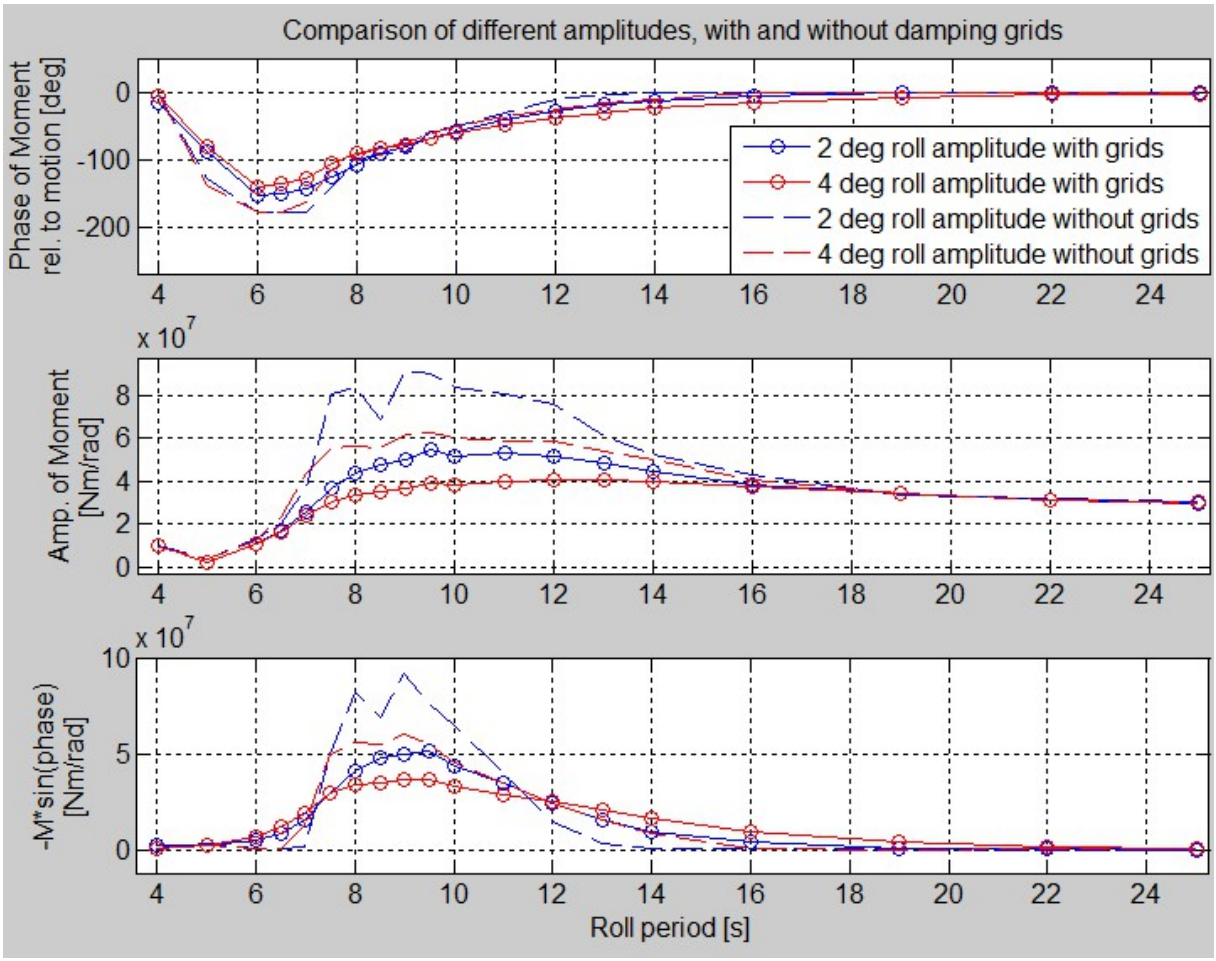

Figure 22: Comparison of different amplitudes, with and without damping grids; second experiment

3.3.3 Testing of different filling levels

For comparing different filling levels in the third experiment, the tests 1109, 1113 and 1114 for four degrees roll amplitude in table 1 were used. Only one empty tank test with test number 1104 was needed because the applied motions and therefore the forces from the empty tank remained the same.

Normally, different filling levels are stated in percent of the total tank volume and a rough benchmark for a good operating tank is said to be 60 %. Since the tank height

of the model was not to scale the common ratio h/b was used. MARINTEK has a data base consisting of systematically performed tests for 0.04 ≤ h/b ≤ 0.16. The scale for this tank was 1:20 and with a breadth of one meter it was decided to test water heights of 0.05, 0.10 and 0.15 m. According to Faltinsen et al. (1974) these water heights lie within shallow depth theory represented by h/b ≤ 0.2.

The comparison of different tank filling heights shows in the middle graph of figure 23 that higher moment amplitudes are reached with a larger amount of water. The bottom graph of figure 23 reveals that a high water level gives very high damping at low periods but only within a narrow range. A very little amount of water has still an effect on vessels with long roll periods but these vessels then normally do not need an additional damping device. A good damping seems to be given with a water height of ten centimetres. The damping is relatively high and lasts over a wide range of periods. As can be seen in equation (12) on page 15, the filling height should be chosen accordingly to tank breadth and natural roll period. This will then give the optimal water height. However, it must be noticed that equation (12) is valid for tanks without damping grids. Equation (10) is validated by this experiment where the natural period of the tank, recognised by the largest value of a curve in the bottom graph, increases with decreasing water depth.

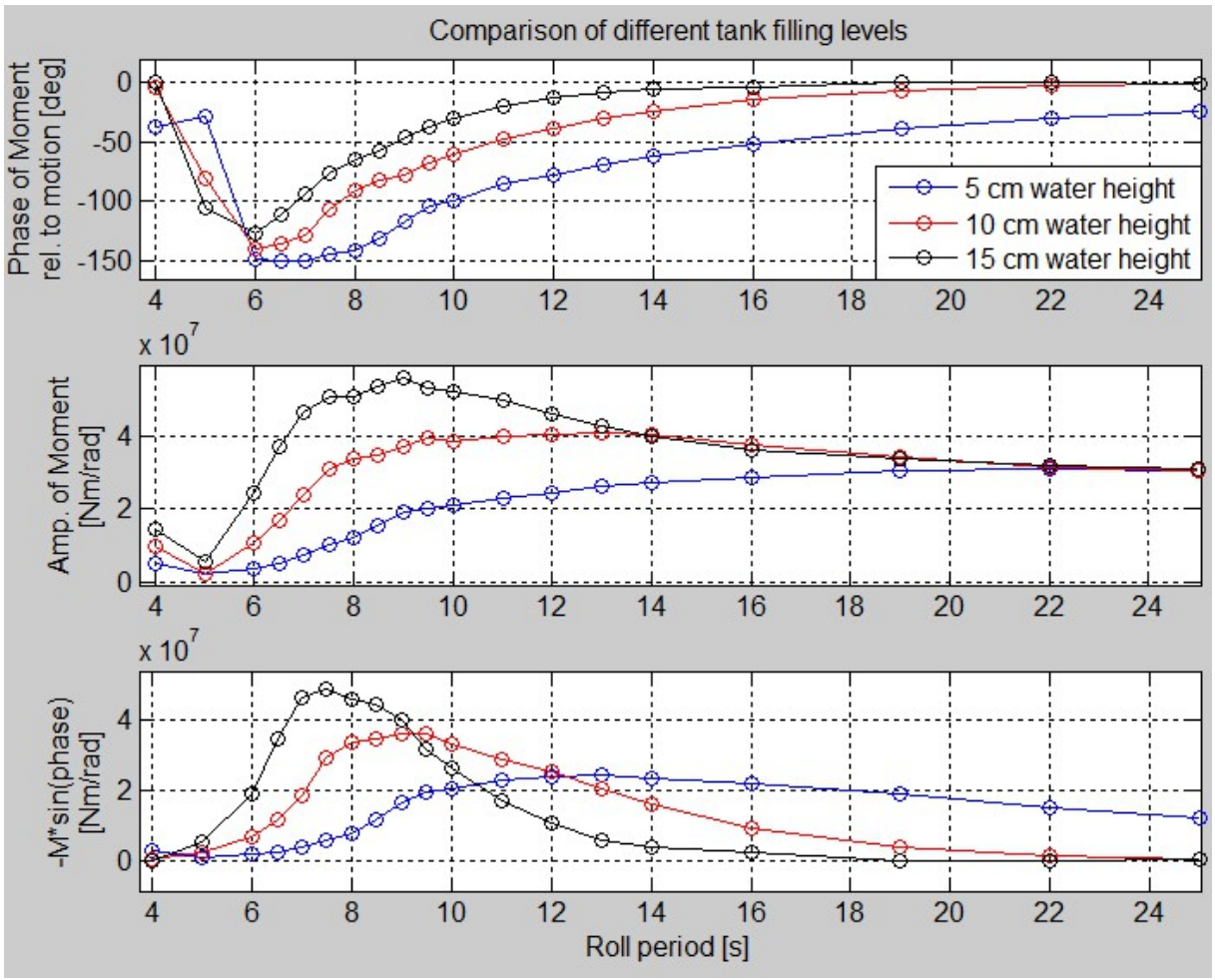

Figure 23: Comparison of different tank filling levels; third experiment

3.3.4 Superposition of roll and sway

As a first try, two single rig movements in roll and in sway were superposed to one combined motion. The interest consisted in seeing whether a theoretically accomplished superposition by the computer gives a comparable result to a performed test with combined motions.

Test 1104 with four degrees roll from before and test 1112 for pure sway were taken for the fourth and the fifth experiment, both with damping grids. To get a combined

motion of roll and sway in test 1111 the rig was rolled around a virtual centre of rotation, ten metres below the tank bottom in full scale. To simulate this deep centre of rotation the rig had to include sway motions. As before, all 19 periods were tested. For the analysis two periods were selected by looking at figure 18 on page 42: On one hand, the resonance period was of interest which was represented by the highest moment of the red curve for four degrees of roll in the third part of that figure. The resonance period was found to be around nine seconds. On the other hand, the third point on a roll period of six seconds in the first graph of that figure was chosen as it is far away from resonance. In the following, the periods of nine seconds at resonance and of six seconds far away from resonance were analysed which corresponds to the fourth and fifth experiment in the overview on page 35.

The centre of rotation was chosen to lie on the inner tank bottom. The horizontal forces measured by the transducer located below that point had to be multiplied by a negative arm of 0.07 m for a positive moment as drawn in figure 14 on page 30. The forces for the combined motion, however, had to be multiplied by the distance from the transducer to the deeper located centre of rotation.

Figure 24 joins the resulting total roll moments of the single tests in the fourth experiment. The blue curve represents the roll moment from the roll test and green stands for the roll moment obtained from the sway test. Computational superposition of these two test results gives the pink curve which finally can be compared with the dashed red curve from the combined test. It can be clearly seen that the tank accomplishes higher roll moments in the combined test than what a computational superposition would give.

The excerpt in figure 24 is chosen in a way that the black motion curves of the rig start with a maximum. The maxima of the moment curves are almost 90° phase shifted to the right which is in accordance to the calculated value in chapter 2.7 where the highest damping occurs. However, the roll moment for the combined test follows the rig motions a bit closer.

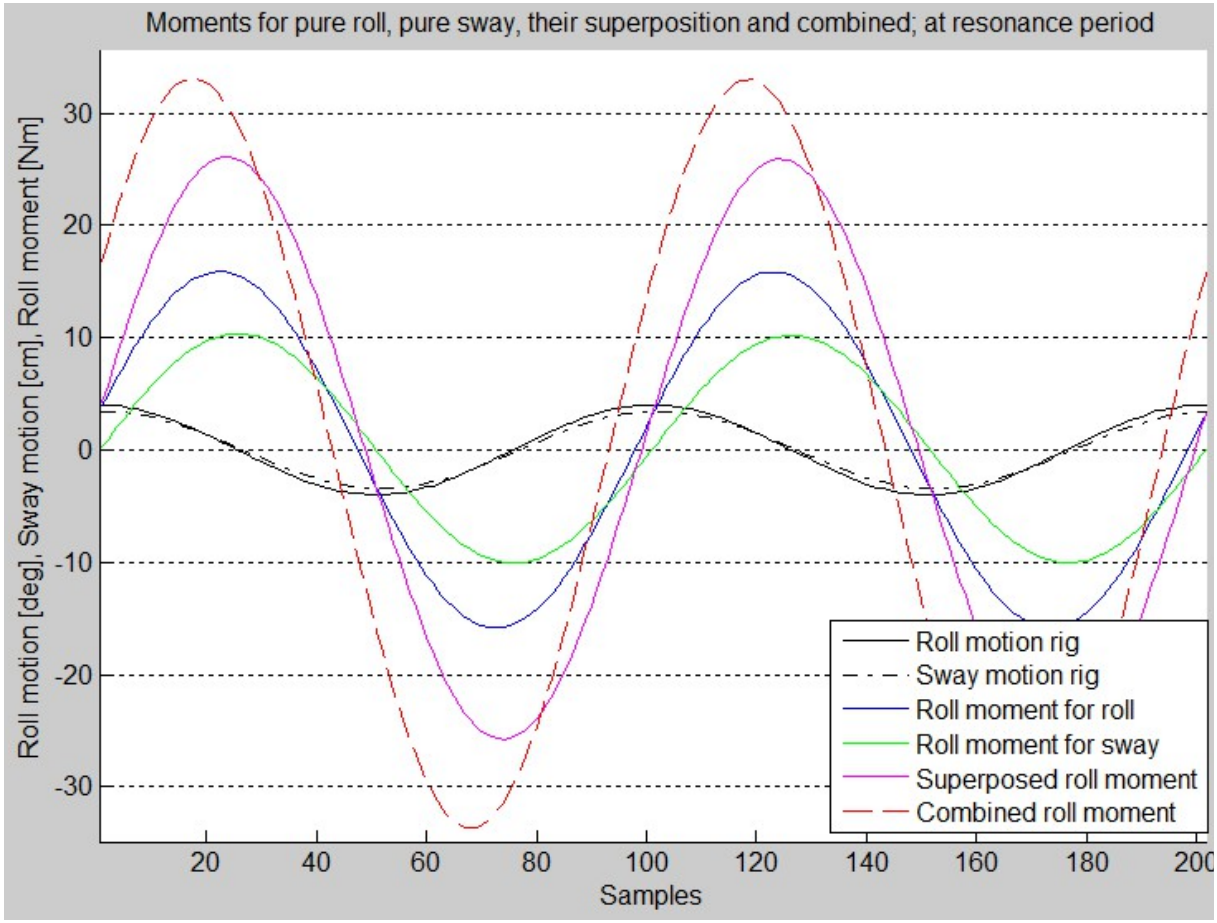

Figure 24: Superposition of roll and sway at the resonance period, with damping grids; fourth experiment

The peaks of the curves look mostly to be in phase with each other, this is less the case in the next experiment in figure 25. Although a period three seconds below the resonance period is analysed, the curves stand more different in phase to each other. In total they are now more than 90° phase shifted to the rig motions. Furthermore, the roll moment of the sway motion in green is now higher than that of the roll motion in blue which was the other way around for the previous experiment. In total the magnitude of the moments is half as high as at the resonance period. After this incongruity it seemed to be logic to conduct simpler experiments but strategic placed around and at the resonance period.

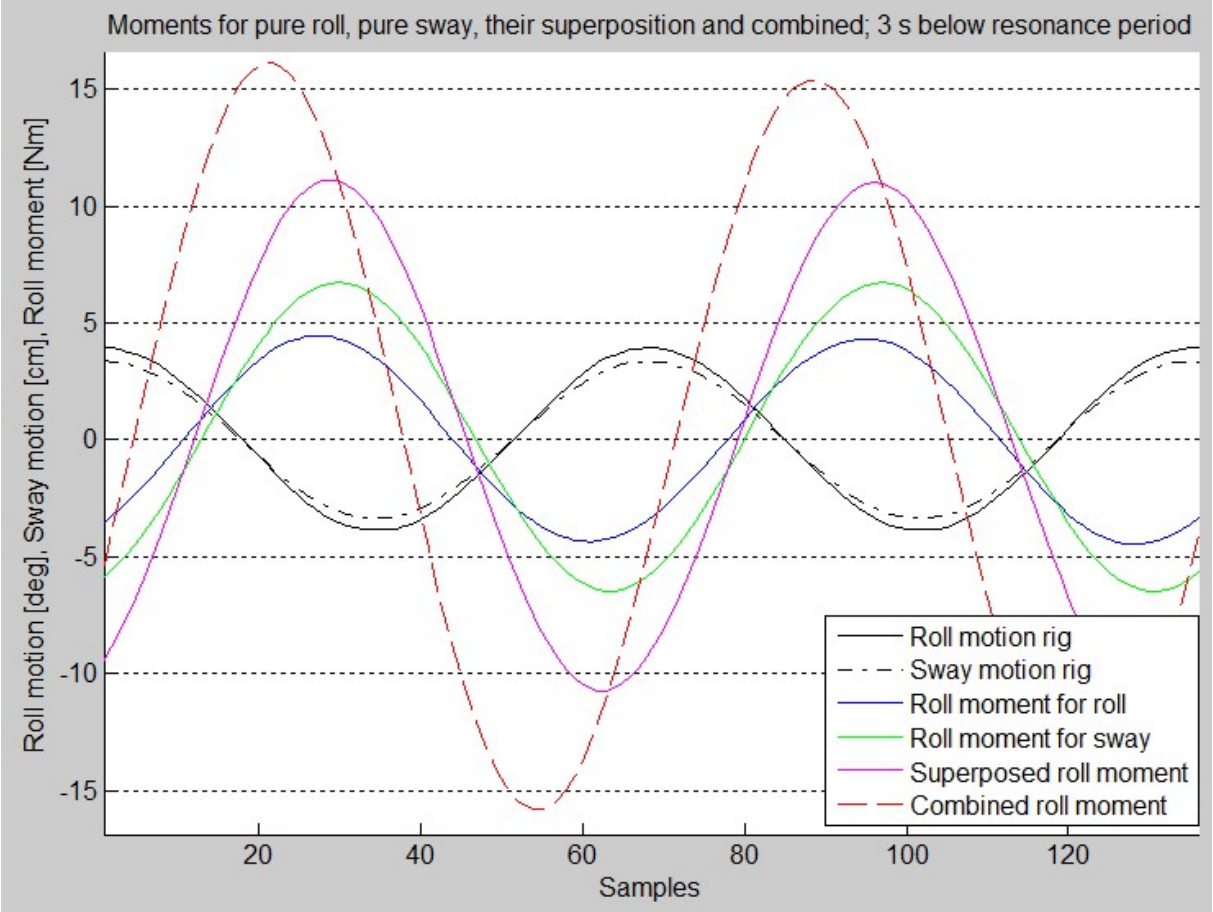

Figure 25: Superposition of roll and sway at three seconds below the resonance period, with damping grids; fifth experiment

When looking at all tested periods as a time series it was noticed that the rig did not reach an amplitude of four degrees for the first three cycles of the pure roll test and that it was slightly higher towards the end. For the sway test it was the same, after an amplitude of 0.033 m in the beginning the rig finally reached an amplitude of 0.035 m. The input for the sway motion was given as two degrees and $\tan(2) = 0.035\,m.$

For the combined test the amplitudes were increasing in the same manner such that there was no significant disadvantage from this at all. Admittedly, it must be mentioned that the rig performed 0.038 m amplitude in the combined test which means a discrepancy of three millimetres to the pure sway test. This can be explained by figure 26 and by calculating the distance *x* which the rig should perform

when the rotation centre is located *s* = 0.5 m below the tank bottom. The actual rotation axis of the rig lies even 0.045 m higher. The roll angle has to be four degrees as for the pure roll test. Thus the sway amplitude is calculated as

$$(0.5\,m + 0.045\,m) \cdot \tan(4) = 0.038\,m \tag{28}$$

For a proper superposition the pure sway test should have the same amplitude which is received by

$$\arctan(0.038) = 2.18\,° \tag{29}$$

Thus the input for the pure sway motion amplitude should have been 2.18° which was discovered after the data analysis. Nevertheless, three millimetres less in the sway amplitude were regarded as negligible as the total roll moment would have been only slightly higher. This would not change anything on the fact that the superposed and the combined roll moment feature a high difference.

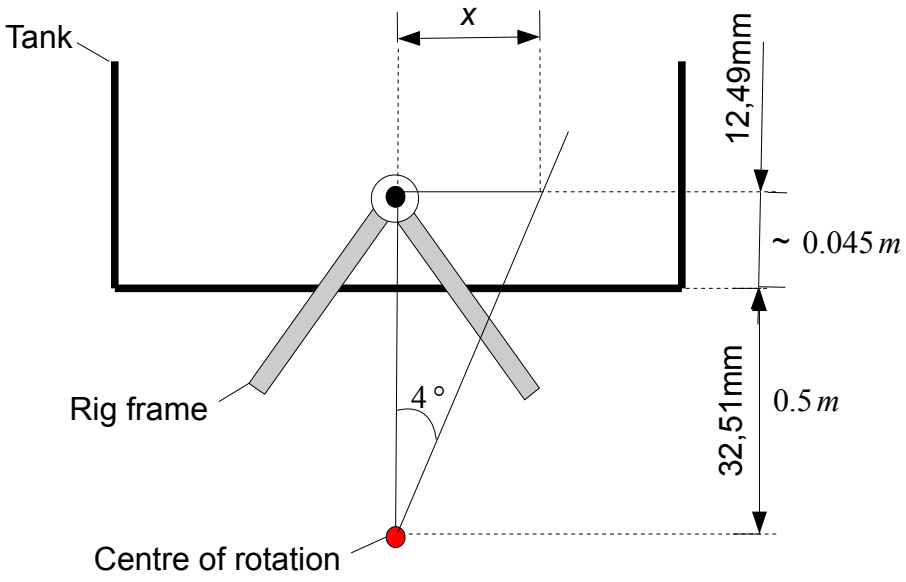

Figure 26: Sketch for calculating the sway amplitude x

3.3.5 Linearity check at the resonance period

The last investigation of the two periods suggests that a superposition of roll and sway motions does not give the same outcome as if both were combined in one test. To probe the cause of this large difference it was sensible to investigate the tank performance systematically for sway motions. First it was checked at which periods the water movement is linear before superposing two and more different periods. It was thereby distinguished between tests with and without damping grids.

Linearity was checked by reviewing whether the tank response at four millimetres sway amplitude is half the response of eight millimetres amplitude. Experiment six investigated this issue at resonance without damping grids and the result is visible as an excerpt of an itself repeating time series in figure 27. The solid lines correspond to the eight millimetres sway motion in black and the dashed lines to the four millimetres sway motion. Shown are the sway force in green resulting from the dynamic water pressure against the tank side walls and the roll moment in blue resulting from the static water pressure on the tank bottom. The total roll moment in red was received by adding both where the sway force had to be multiplied by a small arm to get a moment as described in chapter 3.2.

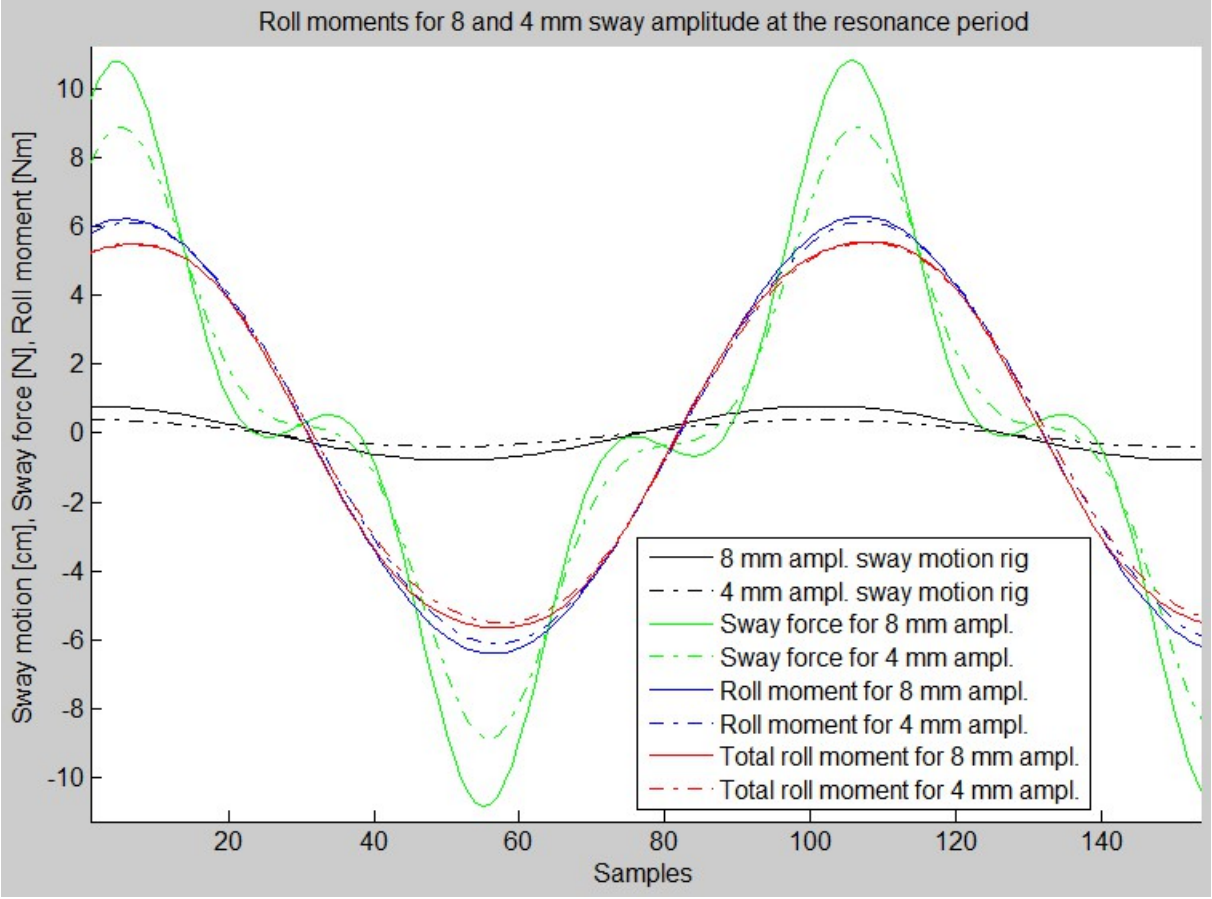

Figure 27: Roll moments for eight and four millimetres sway amplitude at resonance with damping grids; sixth experiment

The excerpt in figure 27 starts with a maximum in the rig motions. The maxima of the moment curves are a bit phase shifted to the right. From linear theory one would expect that the roll moment halves when the tank motion is cut in half. The sway moment experiences only a small reduction while the roll moment in blue remains nearly unchanged likewise the total roll moment in red.

The serrated signal of the measured forces was filtered with a frequency of 1.2 Hz. The roll moments in blue and red are like sinusoidal curves but the peak of the sway force is narrower and local maxima are visible around the zero line. With a filter frequency of 2.5 Hz these local maxima could have been suppressed. In order to show the physics of the tank and the actual happening the filter frequency was kept at the initial value.

Figure 28 explains the emergence of the unsymmetrical local maxima at both sides of the side force graph in figure 27. The green line in figure 28 shows the measured side force due to water motion which was zero for a while when the tank passed its starting position. The blue line represents the inertia forces of the empty tank which had to be subtracted from the water induced forces to obtain comparable values. Due to the different shapes of these two graphs and a small phase shift which can be seen at the left edge of the figure, the final side force with the characteristic small maxima in red appears.

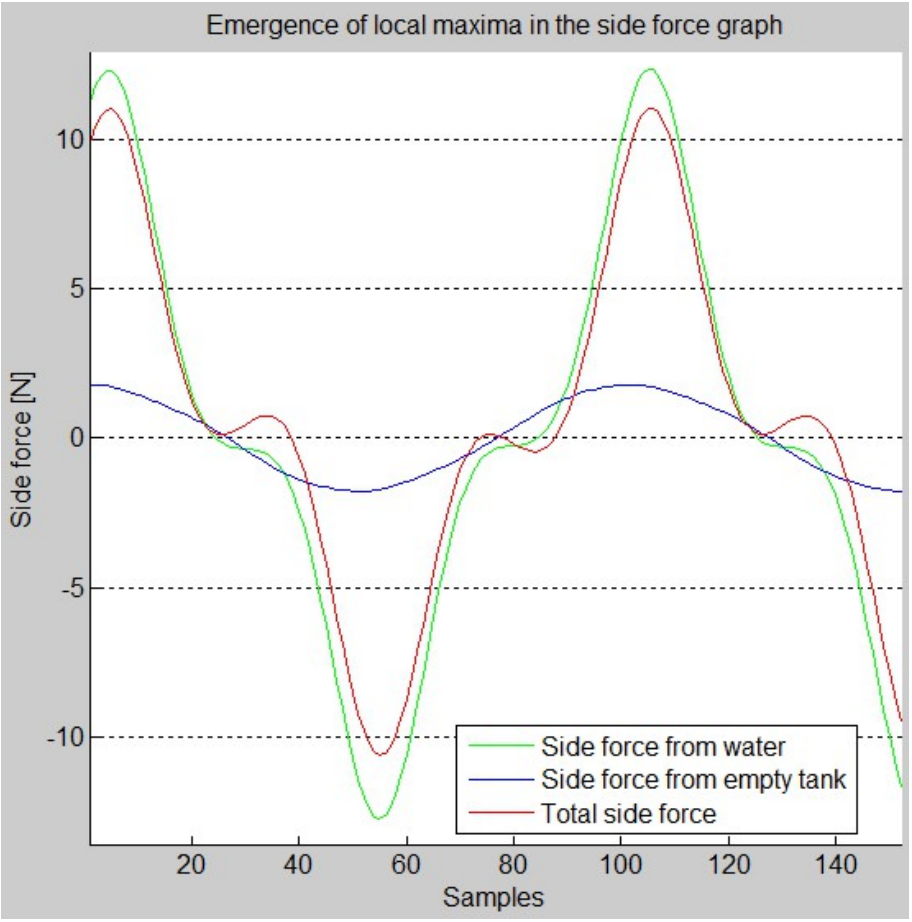

Figure 28: Emergence of local maxima in the side force graph

When using damping grids for the same experiment and with a sway amplitude of six millimetres in addition, figure 29 was generated, representing the results of the seventh experiment. The rig motions are drawn in black, the total roll moments for the

three amplitudes in red. With the damping grids there is now a larger phase shift between the roll moments and the sway motions of the rig and also between each roll moment in comparison to figure 27. The amplitudes of the moments are no longer one value as before but still they proceed not linear, the distances between them are not the same. Conditioned by the damping grids the double peak of the sway forces resulting in a strange pattern in the previous experiment in figure 27 is damped out and vanished.

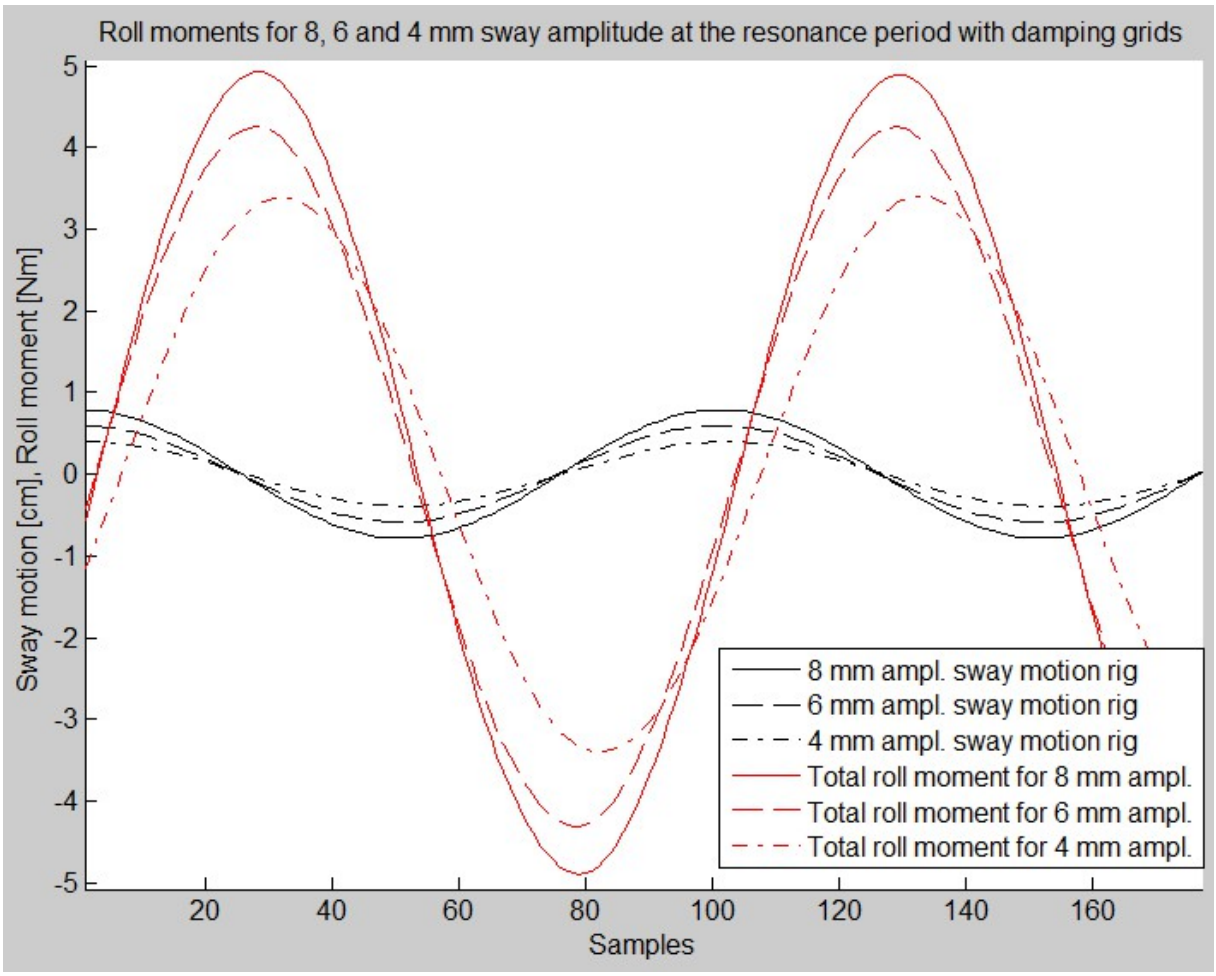

Figure 29: Roll moments for eight, six and four millimetres sway amplitude at resonance with damping grids; seventh experiment

The filter frequencies were adjusted for each channel of the different tests to present the curve shapes as close to reality as possible. For this experiment for example, the

highly serrated signals from the channels for roll and sway were both filtered with 2.5 Hz for the tests of eight, six and four millimetres sway amplitude. Only the channel for roll for the test with six millimetres sway amplitude was filtered with 1.2 Hz. In the description of the following experiments the single filter frequencies will not be mentioned any more. The data are filtered usually with 1.2 Hz, above resonance often with 2.5 Hz. In conclusion, the water motions are not linear at resonance, neither without nor with damping grids as the two last experiments showed.

3.3.6 Linearity check below the resonance period

The experiment from the last chapter at resonance confirmed the suspicion that the response of the tank is not linear at resonance. Next, just one second below the natural period was tested in the eighth experiment. The result in figure 30 displays the rig motions for eight and four millimetres amplitude of sway in black and the corresponding forces in the same line stile. The blue line represents the roll moment. The sway force in green is added with a very small negative arm to the roll moment such that the total roll moment in red is the final line close to the single roll moment in blue.

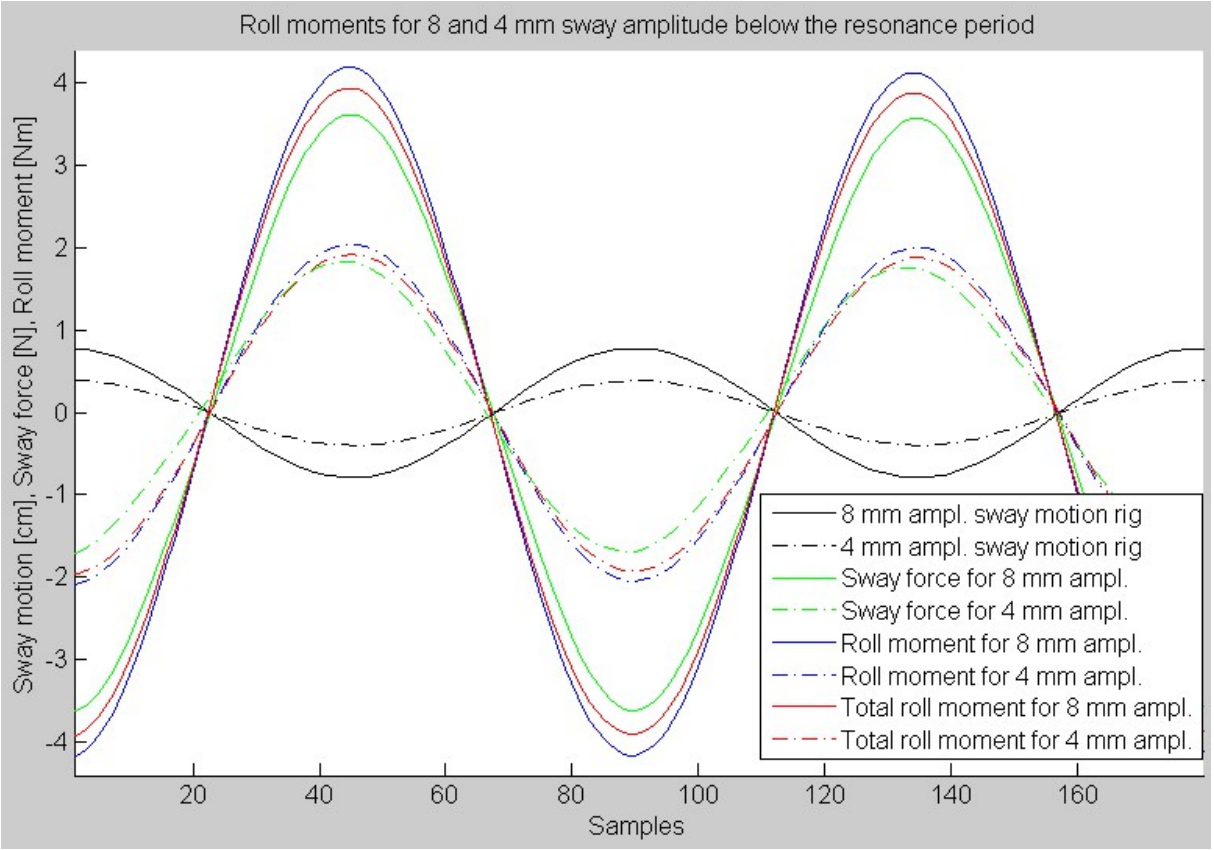

Figure 30: Roll moments for eight and four millimetres sway amplitude one second below the resonance period without damping grids; eighth experiment

Just one second below the resonance period the water behaviour in figure 30 looks completely linear. The forces and moments in the dashed lines due to four millimetres sway motion are almost exactly half the forces and moments of the eight millimetres sway motion in the solid lines. So, half the amplitude gives half the response and the water movement is linear at this period. Another observation is that the forces and moments in figure 30 are exactly 180° out of phase with the tank motions.

The same experiment was accomplished with damping grids but three seconds below the resonance period to be sure that resonance had no more influence. It was feared that the damping grids would introduce more nonlinearities. In fact, the result looks almost the same as for the experiment without damping grids and is shown in figure 46 in appendix D. The resulting amplitudes are approximately one fourth of the amplitudes without damping grids and they are a bit less than 180° phase shifted.

Still, half the sway motion gives exactly half the roll moment and the water movement is linear even with damping grids.

3.3.7 Linearity check above the resonance period

The second last experiment validated that the water movement one second below the resonance period is linear for a tank without damping grids. The tenth experiment examined whether this is also the case for one second above the resonance period.

Noteworthy, a double peak occurs in the green line for the sway force in figure 31. At eight millimetres sway amplitude there are two waves visible travelling close to each other in the tank such that the side force experiences a double peak when the waves are reaching one end of the tank. This phenomenon is much more distinct at eight than at four millimetres sway amplitude. The roll moment in blue however appears in one wider peak because the water stays longer on one tank side due to the double wave. The multiplication of the sway force with the small arm has no large impact on the total roll moment in red which proceeds close below the single roll moment. Half the rig amplitude gives more than half the response. Consequently, the water movements are not linear one second above the resonance period. Unlike the previous experiment, the forces and moments are exactly in phase with the tank motions.

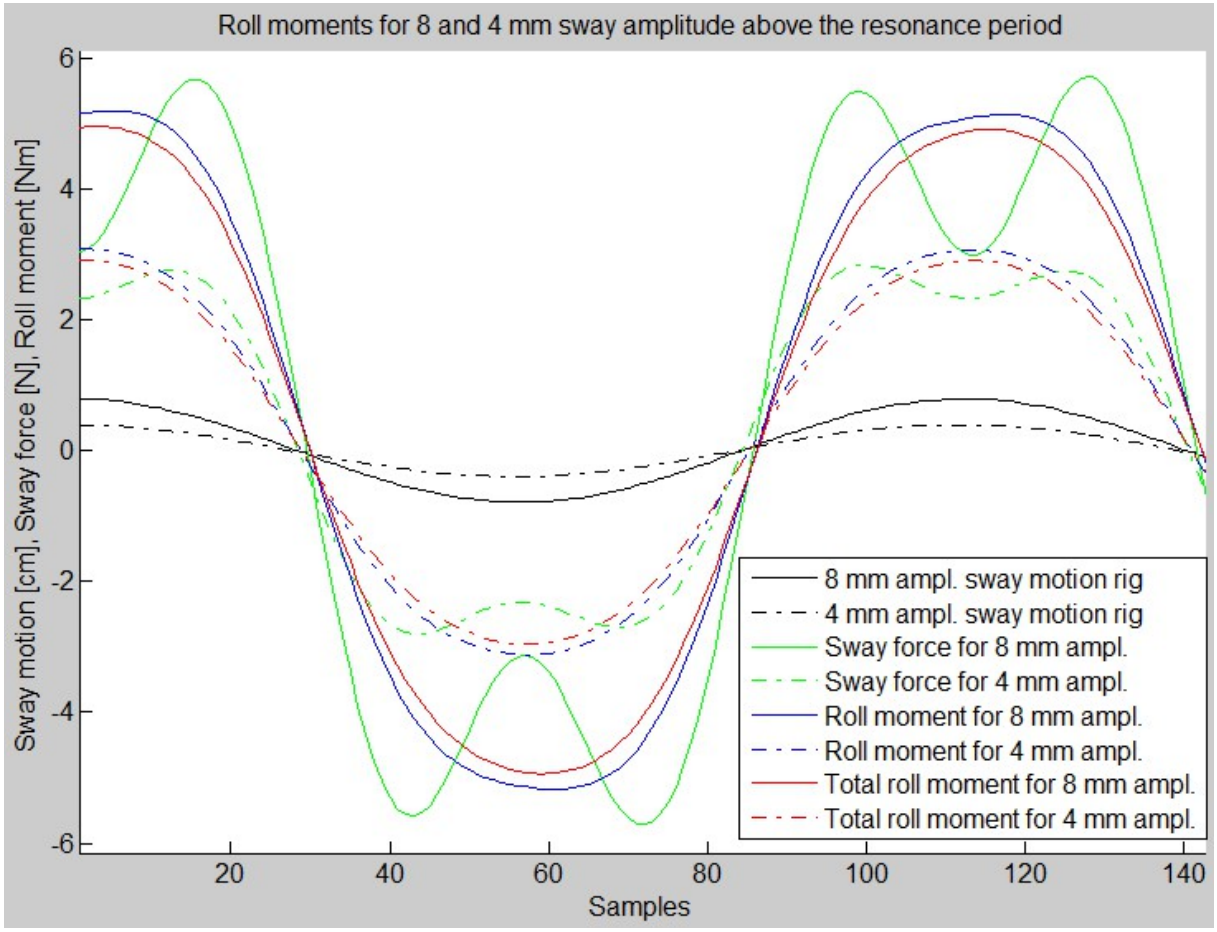

Figure 31: Roll moments for eight and four millimetres sway amplitude one second above the resonance period without damping grids; tenth experiment

Nevertheless, the signals were very serrated with the result that the filter frequencies were adjusted for this analysis. The roll moment was filtered with a frequency of two Hertz and the sway forces with 2.5 Hz. If one wants to merge the double peak into one peak, a filter frequency of 1.2 Hz has to be taken. As the physics of the water shall not be hidden it was decided to show the double peak in figure 31. The filter should only take the noise in the high frequency range on top of the main signal away as shown in figure 32. It is therefore called low pass filter.

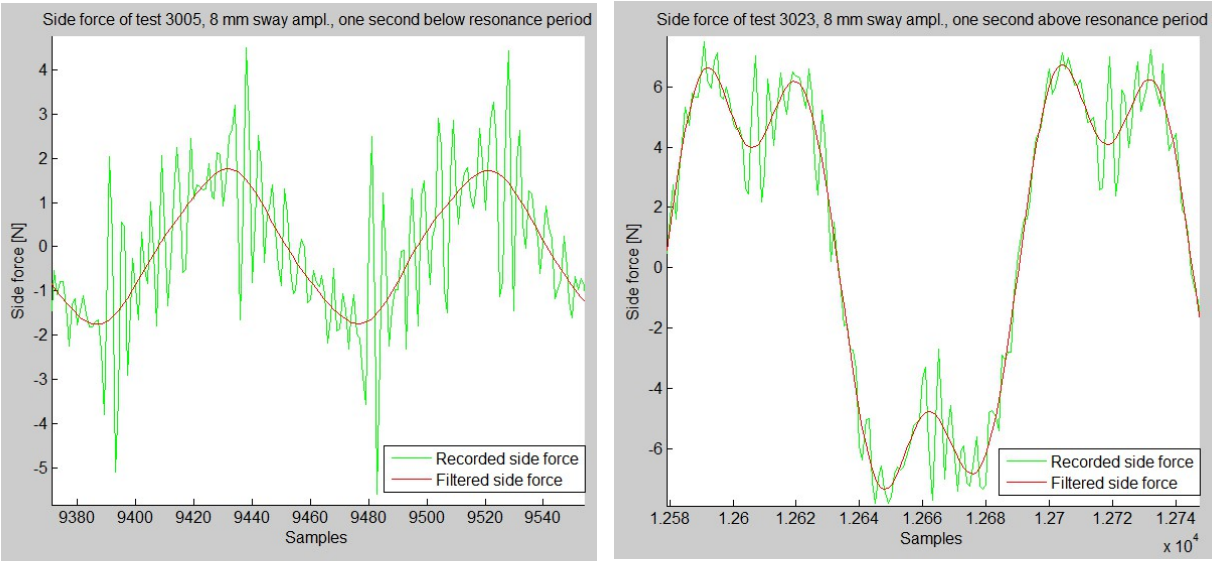

Figure 32: Sway forces filtered with a filter frequency of 2.5 Hz

Figure 32 compares the sway forces from the tests for one second below and one second above the resonance period without damping grids. Before doing the tests, one might think that the forces will look nearly the same because they have an equal distance to the resonance period, but this is absolutely not the case. For periods above the resonance period, the forces can reveal double peaks. The filtered forces in the red curves are further used in the result analysis.

A similar experiment was accomplished with damping grids and three seconds above the resonance period. The amplitudes are minimal phase shifted due to the damping grids but are mainly in phase with the tank motion. The corresponding figure 47 of the 11th experiment is placed in appendix D because the result is like for the previous experiment with damping grids at three seconds below the resonance period. In spite of the nonlinearities in figure 31, the associated experiment with damping grids eventuated in linear water behaviour. So, both experiments with damping grids below and above the resonance period displayed linear water characteristics.

3.3.8 Superposition of sway motions below and above the resonance period

After having checked for linearity in the previous experiments it can now be seen for which frequency combinations superposition is valid. The combination of two frequencies at eight millimetres sway amplitude led to sloshing against the cover panel. To keep the water motions as linear as possible, the following tests were done at four millimetres amplitude where the saturation was avoided.

Two frequencies are combined in the 12th experiment, first one second below and one second above the resonance period. When two simple sinusoidal signals with different frequency but with the same amplitude interfere, the outcome is a signal where frequency and amplitude change in time but the originated pattern is repeating itself periodically which is called beating. The signal is swelling by reaching higher amplitudes and decreasing to a very low amplitude before it starts to swell again. The generated superposition of the two different sway periods with the same amplitude of four millimetres is the starting point of consideration in the first part of figure 33. A detailed accomplishment of this superposition can be found in appendix E.

The sample counting in figure 33 starts at zero. In fact, an extract after 6000 samples was chosen to analyse a more stable range. The top graph in the figure shows an exact accordance of the two superposed and the combined sway motion of the rig. It indicates that the superposition of the two regular time series successful with no significant phase shift. So, besides a visualisation of the performed rig motions this first part works also as a control that the correct parts of each single time series were chosen to give the right superposition of the moments.

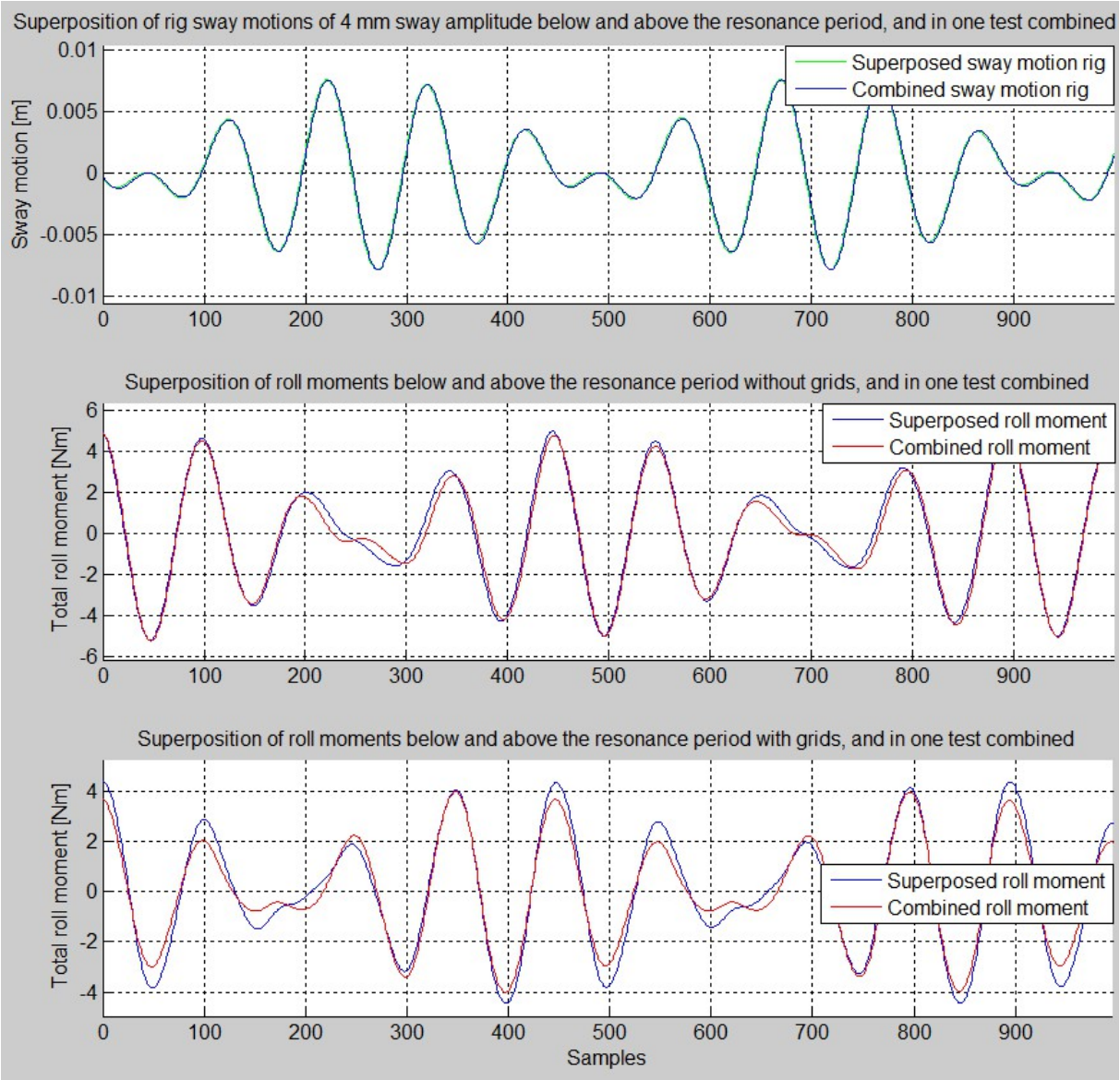

Figure 33: Superposed roll moments one second below and above the resonance period, without and with damping grids; 12th and 13th experiment

The combined motion reveals sections of larger amplitudes followed by sections with lower amplitudes where the two single sinusoidal signals neglect each other as described above. The middle part of figure 33 displays the total roll moment one second below and above the resonance period without damping grids. Looking at the two first parts of the figure likewise, the coherence between rig motions and resulting roll moment can be explained. Starting for instance with the sample number 400 the wave and thereby the roll moment are nearly fully developed. The wave continues

travelling through the tank even when the rig motion has nearly stopped at sample number 500 due to the superposition of the two frequencies. However, when the rig started to move again, it was observed that the rig movement is out of phase with the current wave such that the wave is forced to slow down. The wave started to develop again at sample number 700. For this 12th experiment the roll moment is high for low rig motions in sway.

The graph in the middle of figure 33 compares the superposed with the combined total roll moment one second below and above the resonance period without damping grids. Where the wave is developed, the superposed roll moment is in very good coherence with the combined one. In the middle of the large rig motions, the superposition does not match exactly with the combined case. Above all, linearity is seen to a great extend and superposition is valid.

The same experiment was repeated with damping grids to see whether superposition of two frequencies close to resonance is also valid for a tank with grids since MARINTEK is working mostly with tanks which have damping grids included. For a close comparison of the two experiments, the excerpt of the 13th experiment with installed grids is added to figure 33 as the bottom graph. It belongs to the same sway motions in the top graph as the experiment without grids in the middle graph. Comparing the last two graphs with respect to the rig motion in the top graph, the damping grids cause a shift of the roll moment but closer to the rig motion. Due to the damping grids the water can react faster on the excitation because the current sloshing is faster damped out. As an example, the rig almost stopped to move at sampling number 500. The following excitation needs some time to effect a change in the water motion without damping grids at sampling number 700 because the kinetic energy of the wave lets the wave travel further through the tank. The grids on the contrary dampen the water motion such that the new excitation can already be implemented into the fluid at sampling number 600 in the bottom graph of the figure. In accordance to this, the combined roll moment in red shows lower amplitudes than the superposed one in the bottom graph as soon as the rig decreases its motion. In

general, the achieved moments are barely lower for the case with damping grids. More distinct as for the experiment without damping grids is the mismatch of superposed and combined roll motion where they have very small amplitudes around the sampling numbers 200 and 600 in the bottom graph.

Overall, a validity of superposition is questionable for the 13th experiment with damping grids just one second below and above resonance. In the 14th experiment, the distance to the resonance period was therefore increased to see whether superposition of the frequencies three seconds below and above the resonance period is valid for a tank with damping grids. Superposing these two frequencies gives a regular wave pattern which repeats itself. During the experiment it could be observed that one part of the pattern nearly stopped the water motion while the following part excited the water again as drawn in figure 34. Indeed, the roll moment amplitude in the second part of the figure decreases rapidly and increases again shortly after the remarkable rig motions. In spite of this, the superposition of both frequencies in blue mirrors the combined roll moment in red quite well. Superposition is therefore valid far away from resonance.

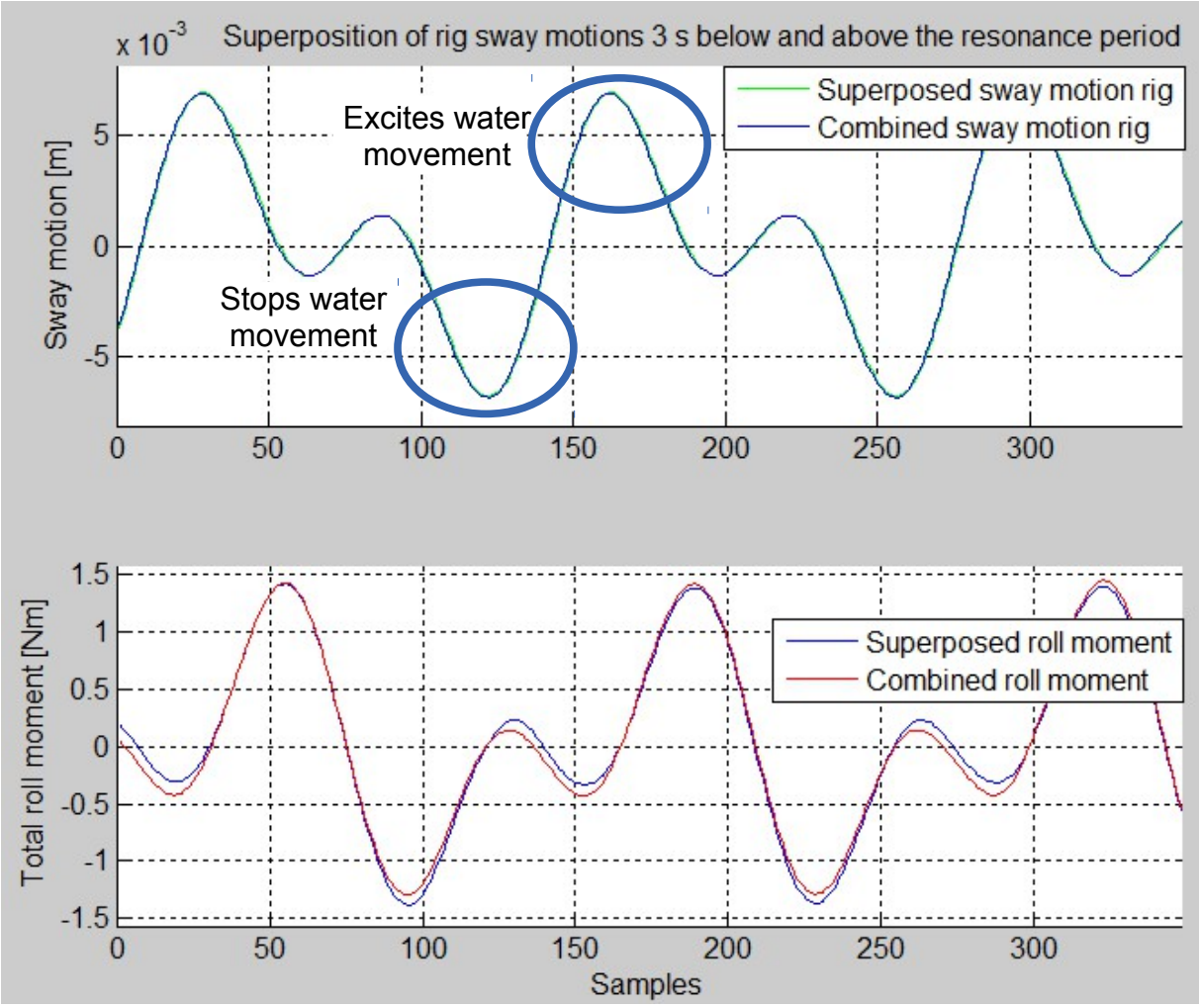

Figure 34: Superposition of sway motions (upper graph) and roll moments (lower graph) at four millimetres amplitude, three seconds below and above the resonance period, with damping grids; 14th experiment

3.3.9 Superposition of sway motions below and at the resonance period

In the 15th experiment the resonance period was included and superposed with a period one second below the resonance period in a tank without damping grids. In the upper part of figure 35 the beating of the signal can be seen very well in an excerpt taken towards the end of around 16000 samples. The superposed sway motion matches with the combined one in contrast to the roll moments in the lower

part. The superposed roll moment does not coincide with the combined one when the rig executes large amplitudes after the sampling number 500. Phase and amplitude differ. After this excitation period of the rig the wave starts to develop, not least because the resonance period is included. The roll moment curves start to align in phase and amplitude. First, before 1000 samples the superposed roll moment in blue reveals higher values than the combined roll moment, thereafter it becomes the other way around. For some sequences the combined roll moment achieves higher values (at the sampling numbers 200 and 1800) while in other sequences the superposed roll moment is higher (at sampling number 1000). As soon as the resonance period is included but the damping grids not, the water movement is no longer linear and superposition is not valid.

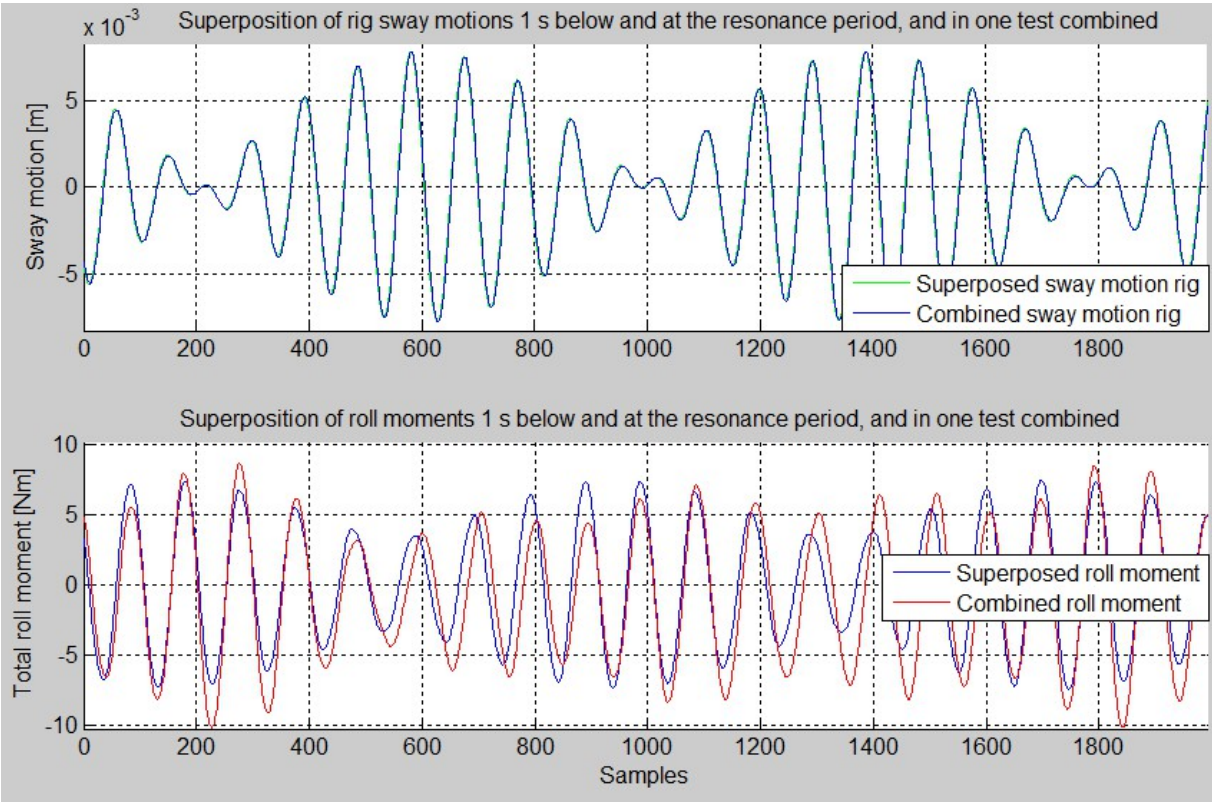

Figure 35: Superposition of sway motions (upper graph) and roll moments (lower graph) at four millimetres amplitude, one second below and at the resonance period, without damping grids; 15th experiment

Next, the damping grids were added and the 16th experiment was performed with the

resonance period and the period three seconds below resonance. The large distance between the periods was chosen because it was seen in the 13th and 14th experiment that the water movement with damping grids is linear three seconds below but nonlinear one second below the resonance period. One period with linear water movement and the resonance period should be superposed.

Although the resonance period is included, the resulting water movement is completely linear because the two roll moments added together in the lower part of figure 36 give the same output as the combined test. For the sway motions at four millimetres amplitude it was somehow not managed to superpose the two single graphs correctly and a very small discrepancy occurred between the superposed and the combined sway motion in the upper part of the figure. To ensure accurate working and to have control about the output in Matlab, the upper part about the rig motions is always displayed in the figures. Besides this, the graph gives an idea of the motions the rig performed which were different for each superposition.

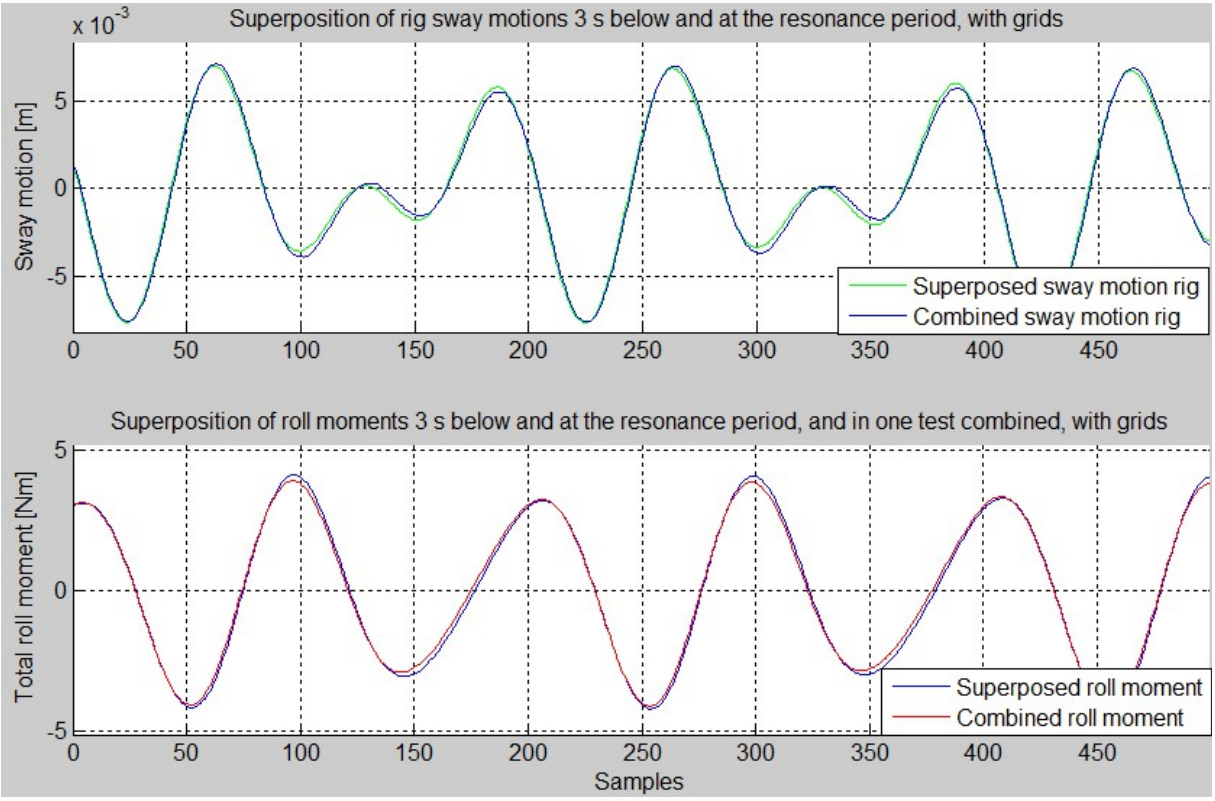

Figure 36: Superposition of sway motions (upper graph) and roll moments (lower graph) at four millimetres amplitude, three seconds below and at the resonance period, with damping grids; 16th experiment

3.3.10 Superposition of sway motions above and at the resonance period

The last described experiment without damping grids investigated the superposition of sway motions one second below and at the resonance period. This 17th experiment will now examine whether the tank gives the same performance for a superposition of sway motions one second above and at the resonance period.

With the progression of the experiments it could be recognised that a resonance period plus a higher period gives much more violent sloshing than it is the case for lower periods. The included resonance period leads to higher moment amplitudes.

For periods above resonance the measured force signals are more serrated and a double wave occurs. In this experiment the two waves met in the middle of the tank with the result that the surface elevation is rising and falling twice within one period of tank motion. This strong double peak, first only known for the sway forces, now also distinct in the roll moment, could no longer be ignored and was not hidden by a filter in the analysis of figure 39.

It was noticed that time series consisting of two frequencies have two slightly different sequences within one repeating pattern which was especially visible at the differing moment. One time series consists of many patterns as in figure 37. At a first glance, they look the same but one can find variations between them, especially in the intermediate parts. The superposed periods are periodically, thus the patterns of the superposition are periodically as well, but their repetition is extended over a larger period of time. In the upper part of figure Fehler: Referenz nicht gefunden the first and the fourth pattern of figure 37 are compared. The development of their amplitudes is slightly different. However, the first pattern is repeated in the last pattern of figure 37 as plotted in the lower part of figure Fehler: Referenz nicht gefunden.

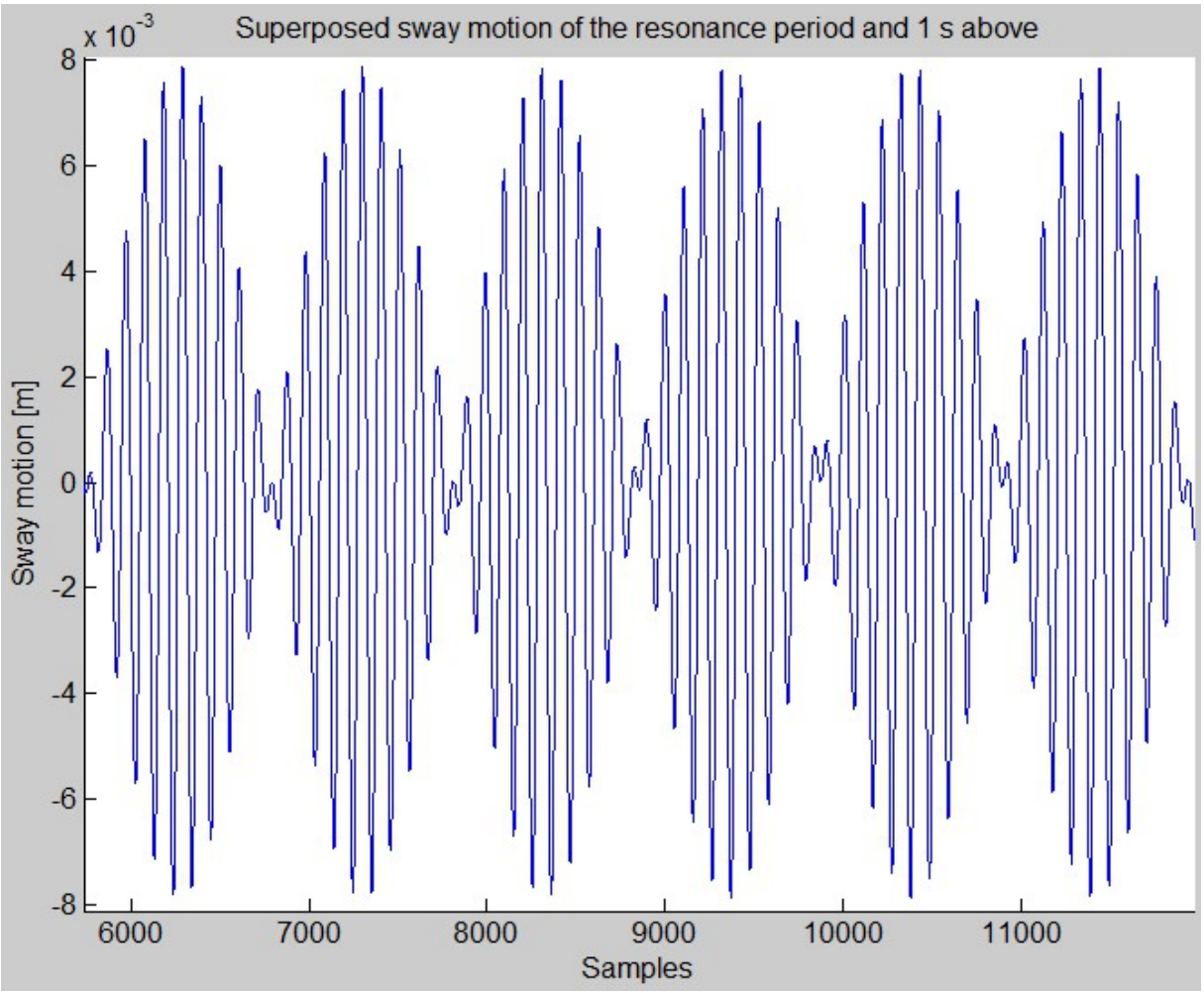

Figure 37: Rig motion patterns in the superposed sway motion of the resonance period and one second above

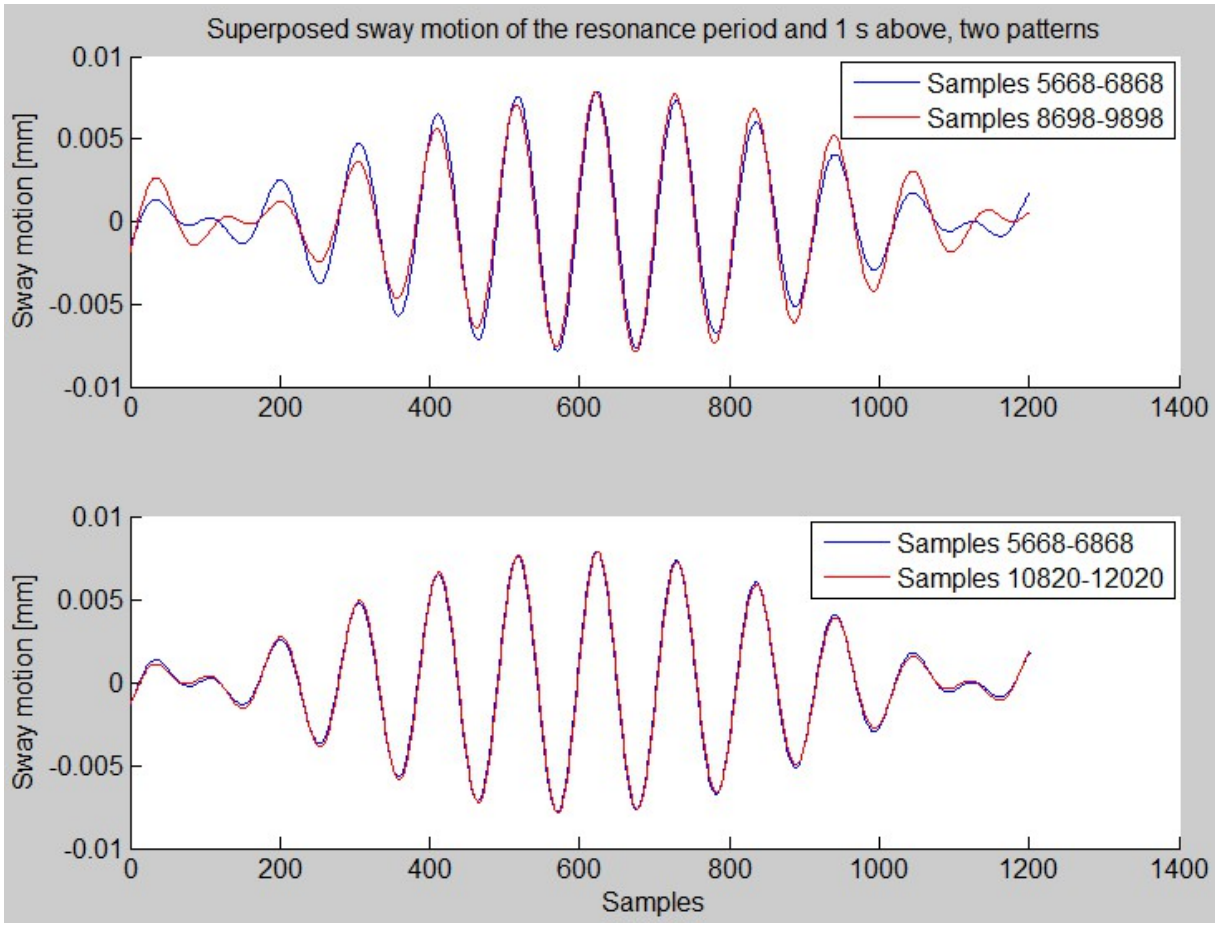

Figure 38: Comparison of two patterns from figure 37

For a moment analysis, such a pattern is examined in the upper part of figure 39. One can see that the superposed and the combined moments are in phase at the sampling numbers 600 and 1800. By contrast, they are completely out of phase in the intermediate part around sampling number 1200 before they will be back in phase in the next following pattern. The amplitude of the combined moment is mostly larger than that of the superposed one. The patterns vary slightly as described above. Figure 39 reveals that more than one pattern should be considered in a moment analysis.

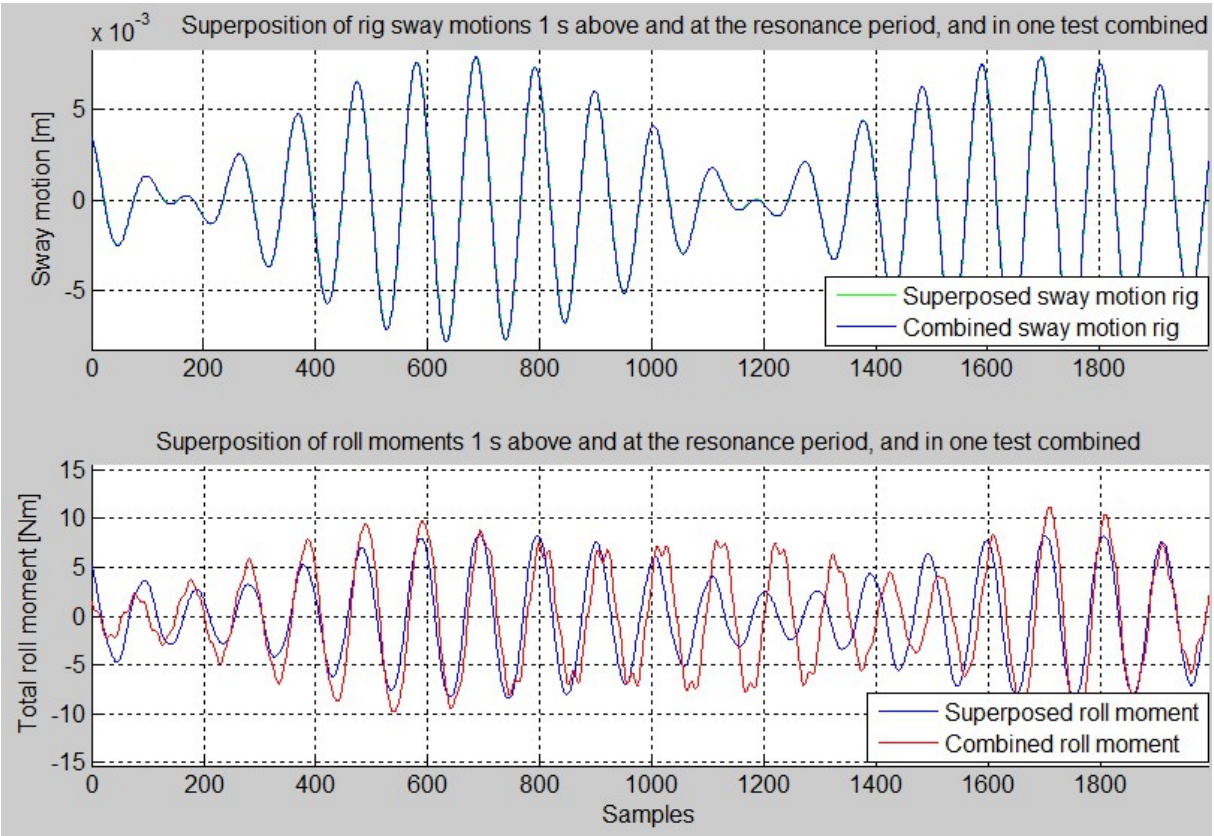

Figure 39: Superposition of sway motions (upper graph) and roll moments (lower graph) at four millimetres amplitude, one second above and at the resonance period, without damping grids; 17th experiment

The sloshing for the combined motion in the lower part of figure 39 looks very different from the sloshing which appears when the single periods are superposed. The combined roll moment in this experiment shows double peaks but only once stronger distinct within one pattern. This is a good example for how nonlinear and difficult to predict sloshing of just two different frequencies can be.

The 18th experiment with damping grids and sway motions at three seconds above and at the resonance period gave similar results to that of three seconds below and at the resonance period in the previous chapter. The roll moment is linear and the corresponding figure 49 is listed in appendix E.

3.3.11 Superposition of five periods in sway and roll

In the coming two last experiments all five up to now used periods were superposed at once and tested in a tank with damping grids: Three seconds and one second below the resonance period, the resonance period itself, and one and three seconds above the resonance period. The 19th experiment tested them based on four millimetres sway and the 20th experiment based on four degrees roll.

In figure 40 the sway motion of the rig looks very irregular. In comparison to the other experiments, high amplitudes of maximal 18 mm in sway were achieved due to the superposition. The phases of the superposed and the combined roll moment match but the superposition gives higher amplitudes than the combined motion. Small changes in the moving direction of the rig have no large influence on the response of the roll moment. They might lead to a wider response as around sampling number 1600. The complexity of the motion time series makes it difficult to predict the next wave in the roll moment after a performed sway motion.

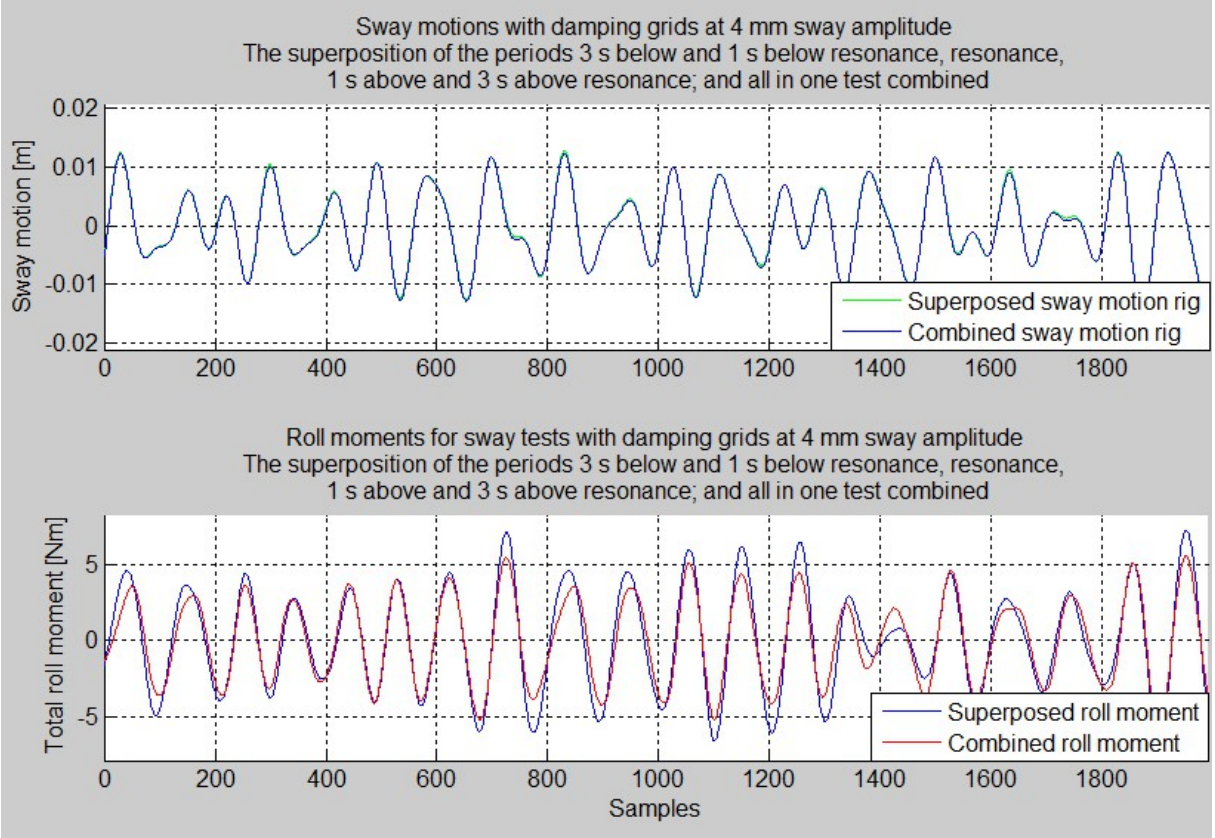

Figure 40: Superposition of sway motions (upper graph) and roll moments (lower graph) at four millimetres amplitude, all five up to now used periods, with damping grids; 19th experiment

Overall it is questionable whether superposition is valid or not. For some sequences like after the sampling number 400, the roll moment is fully linear but directly afterwards, the amplitude heights differ quite a lot.

For the same experiment with four degrees roll instead, the resulting curves in the lower part of figure 41 are diverging more. The curves for the roll moments are slightly more serrated even with a high filter frequency of 2.5 Hz.

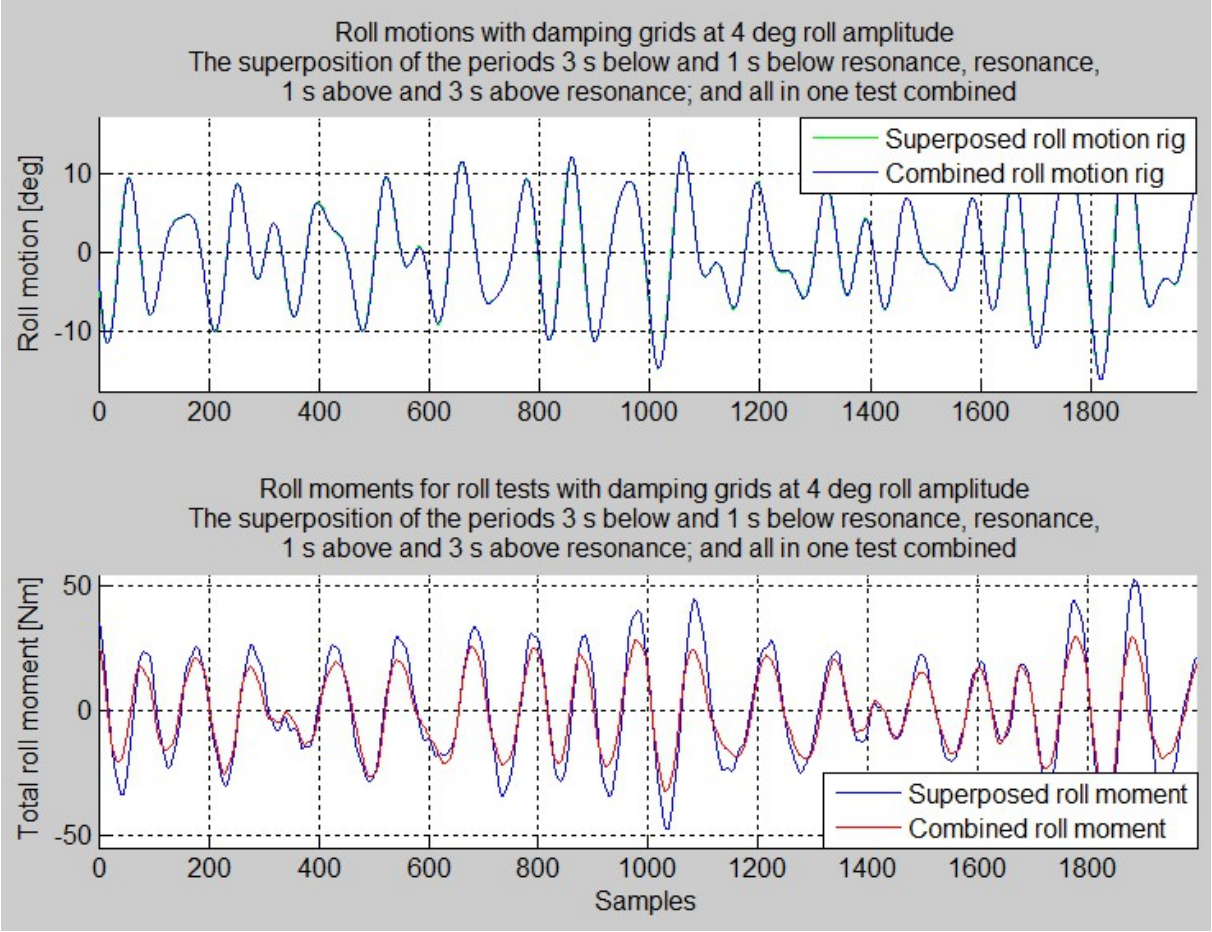

Figure 41: Superposition of roll motions (upper graph) and roll moments (lower graph) at four degrees amplitude, all five up to now used periods, with damping grids; 20th experiment

Maximal 18 mm sway in the previous experiment were now maximal 18 degrees roll as amplitude. A sequence of the water movement at such high amplitudes is given in figure 42. The water rolled heavily in the tank by partially hitting the cover panel in the pictures 3 and 4.

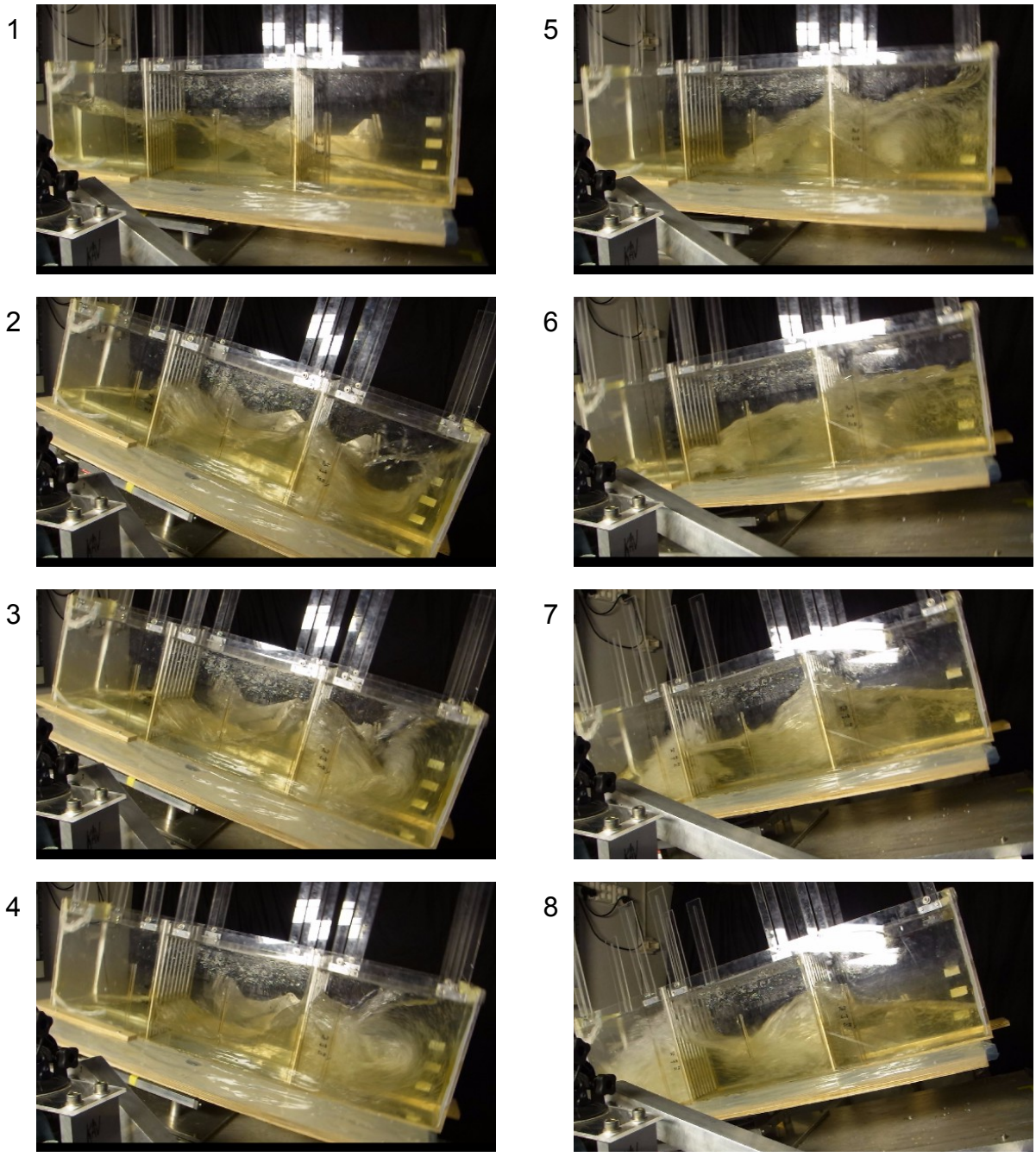

Figure 42: Sloshing at high roll amplitudes

Although the water movements in the tests of the single periods in table 4 are harmless, the final superposition of all five periods leads to unpredictable high sloshing. The tests with each single period had to be performed in order to superpose the single, total roll moments afterwards and to compare them with the combined test where the input file for the rig contained already a superposition of all frequencies.

Table 4: Test matrix for five periods in roll

Test number	**Period in full scale [s]**	**Observations**
3102	T_1 - 3	The rig motion is too fast, the water cannot follow.
3104	T_1 - 1	One wave travels through the tank.
3106	T_1	The cover panel is slightly reached by the water.
3108	T_1 + 1	The wave is breaking right before the first grid when coming down from one tank side.
3110	T_1 + 3	The rig motion is too slow, the water concentrates on the sides; the water surface changes in x-direction.
3112	T_1 - 3, T_1 - 1, T_1, T_1 + 1, T_1 + 3	High saturation and violent sloshing at large amplitudes.

The tests in table 4 were based on four degrees roll and a filling level of 10 cm. The two damping grids were mounted. T_1 was the resonance period of nine seconds in full scale. All tests together were used for the analysis of the 20th experiment.

3.3.12 Summary of the test results

In the first three experiments the physics of the tank were analysed. It was discussed how the roll moment varies when the roll amplitudes of the rig or the water filling level are changed and what happens when the damping grids are taken out. A superposition of roll and sway motions did not give the same result as a combined test which rose the question when in general the water movement in the tank behaves linear and a superposition as a consequence can be valid. The sixth to the 11th experiment analysed this issue systematically for pure sway before the next superposition experiments were done. The always present questions about linearity

could be answered for each experiment and the overview of the experiments from the beginning in figure 17 on page 35 can now be extended into an overview of linearity in figure 43. The results of the experiments in green are linear, those in red are nonlinear. For the two experiments in black linearity is questionable. Therefore, the 13th experiment was repeated further away from resonance which then gave linearity.

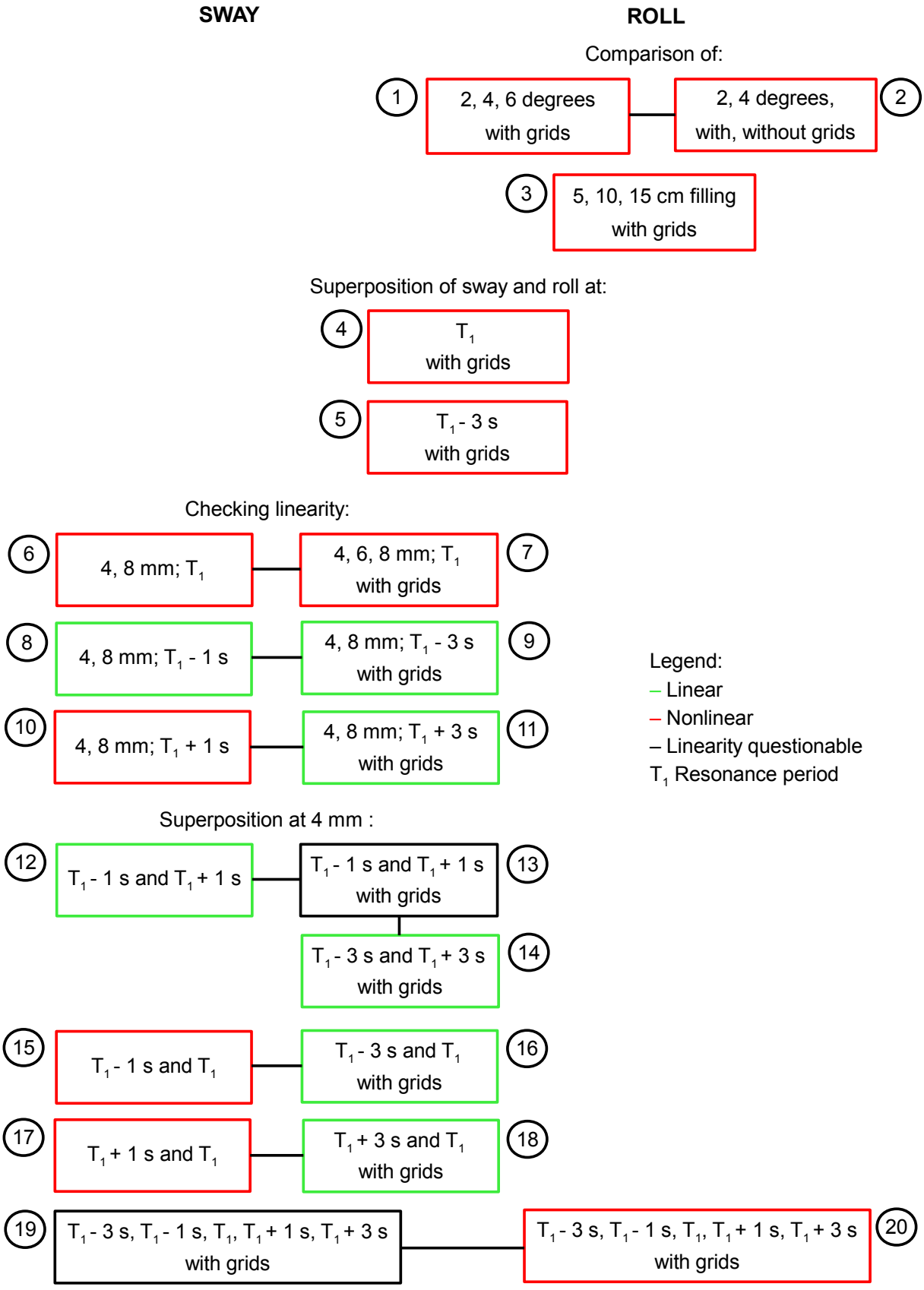

Figure 43: Overview of linearity of the performed experiments

3.4 Error analysis

There are uncertainties in any kind of physical experiment because the equipment might not work 100 % perfectly and environmental conditions can change easily. Every repetition of exact the same experiment will give slightly different results. The question is how large the gap between a measured result and the “true” value is allowed to be. Steen (2012) distinguished between bias errors and precision errors.

Bias errors cannot be revealed by repetition because they are systematic errors which lie e.g. in the test setup, model, and testing facilities. Changing many parts of the experiment like rearranging the setup, building a new model and using a different testing facility would reduce the bias error. Except for the latter mentioned part these changes are seldom realised. Calibration is another key aspect in reducing the bias error which was checked for the tests and described in chapter 3.1.

By repeating a test the precision error can be calculated from the measurements. The uncertainty of the standard deviation decreases with increasing number of repetitions. A systematic uncertainty analysis is a relatively new phenomenon from the past ten years and is more used for verification of computer codes or a new theoretical method. Jin (2013) admitted that tests are normally not repeated for accuracy. It is enough to see trends and main differences between changed parameters when working with a roll damping tank. Doing a detailed uncertainty analysis by calculating precision limits and standard deviations can easily reach a size of an own work. Instead, a qualitative evaluation of the precision from repeated tests is done. The pure roll test with four degrees roll amplitude and ten centimetres water height was repeated five times and plotted in figure 50 in appendix F. The colours show that the last tests are in high accordance with the previous tests. Two main different values were repeatedly reached for the first roll period of four seconds.

Another idea for checking the accuracy of the measured values and data processing is to compare the zero downcrossing with the zero upcrossing periods, suggested by Berget (2013). This symmetry check proves for instance whether a consistent force measurement took place and whether the tank was symmetrically shaped and horizontally placed on the rig. The Matlab code for processing the data had to be changed. Normally, the zero downcrossings[3] were used to define the periods of the sinusoidal wave shaped forces. Now, both the zero downcrossing and the zero upcrossing periods were used in parallel. In general, they should give the same values. The results are plotted in figure 51 in appendix F. Especially for the amplitude of the moment at a roll period of five seconds a discrepancy is noticed. In addition, the periods do not coincide fully in the period range of 18-25 s.

A further error source is the drift of the force transducers mentioned by Steen (2012). Drift occurs when the force output according to a constant load changes slowly over time. It was tried to reduce this error source by a zero reading right before every test.

Errors can also be made with the data processing software and the codes.

3 Point where the wave profile crosses the mean level (zero line) downwards. (Goda, 2010)

4 Discussion

The description of wave phenomena occurring during the tests in chapter 3.3.1 reveals unexpected water behaviour in the tank. It could be observed that water was swinging in x-direction at certain frequencies which shows that nonlinearity plays a roll, even at simple motion patterns. Other nonlinearities due to damping are shown by the comparison of different amplitudes in figure 18 on page 42. The moment curves run relative to each other and a simple addition of them for higher roll amplitudes is not possible which means that the moment increase is not linear. The obtained result is in accordance to an experiment accomplished by Van den Bosch and Vugts (1966). Now it could be shown that this is also the case for a tank with damping grids. Berget (2013) argued that the damping effect of the tank itself is not linear as theory would say because there are nonlinearities when the water passes the grids. In spite of this, MARINTEK further assumes linearity for small roll angles in this issue when analysing model tests by referring to a conclusion from Van den Bosch and Vugts (1966).

One often can read about higher damping moments for higher roll amplitudes, e.g. investigated by Van den Bosch and Vugts (1966), but up until now for tanks without damping grids. With this study it could be shown that it is the same for a tank with damping grids, although not so distinct. As their name says, they hinder the water to flow through the grids. The result is that not enough water reaches the other side of the tank in time to raise a large counteracting moment. As Berget (2013) stated, the roll velocity of the tank is higher for higher amplitudes but the water is less able to follow the tank motions through the grids. The water permeability depends of course on the design of the grids as presented in chapter 2.6. In conclusion, both roll amplitude and design of the grids have to be considered together when looking for the most efficient damping.

For the tests without damping grids as well as for the test with six degrees of roll

motion with grids, very large sloshing against the cover panel was observed. In addition, large side forces were measured. This has to be accounted for when constructing the structure and fixation of the tank.

The phenomenon of a hydraulic jump travelling from one side of the tank to the other was first observed by Van den Bosch and Vugts in 1966 and further illustrated by Faltinsen and Timokha (2009) in figure 4 on page 11. When watching a video of the tank without damping grids, the appearance of a hydraulic jump in the middle of the tank at zero roll angle can be confirmed. Analysing a video of a tank with damping grids as done in figure 21 on page 47, a further delay in the water movement in relation to the tank movement is pointed out in addition to the normal phase shift. The hydraulic jump did not reach the middle of the tank “in time” conditioned by the damping grids. As stated by Van den Bosch and Vugts (1966), the presence of a hydraulic jump is essential for effective damping. Now it could be shown in figure 22 on page 48 that a delay in the jump leads to worse damping performance by creating a lower damping moment. On the other hand, it is beneficial to include damping grids because they smooth the damping curve over the periods and sufficient damping is available over a larger range of periods.

For the tests without damping grids in the second experiment, very large sloshing against the cover panel was observed. This might be the reason for the collapse of the curve for 2 deg roll motion without grids in figure 22 on page 48. One explanation could be that the very fast moving water at a low filling level was running up at the tank sides and splashing back as a wave towards the middle of the tank. The water therefore spent only little time on the tank side which let the counteracting moment not fully develop. On the contrary, this severe sloshing occurred over a large range of periods. The shape of the graph might have other reasons than being related to the severe sloshing because the time series shows no significant changes for this period. The test should be repeated to investigate if the observation was just an artefact.

The first natural period was calculated for the tank. Formula (10) on page 14 is valid

for a tank without grids which could be confirmed in chapter 3.3.3. For tests with grids it was assumed that the resonance period of the tank does not change much such that the same frequencies were tested for a tank with damping grids as without damping grids.

Another issue to discuss is why the roll moments of eight and four millimetres sway amplitude at the resonance period are so close to each other in figure 27 on page 56. Looking first carefully on the water surface elevation of the experiment for one second below the resonance period in figure 30 on page 60 where half the sway amplitude gives half the response, one can see in figure 44 that there is a water level difference along the whole breadth of the tank. Drawing the surface elevation for the tank at resonance, there is only on one side of the tank with a difference in elevation which may lead to the close curves in figure 27.

Wave pattern 1 s below the resonance period

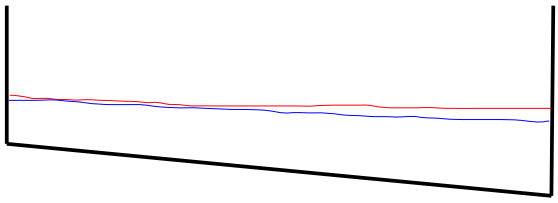

8 mm amplitude
4 mm amplitude

Wave pattern at the resonance period

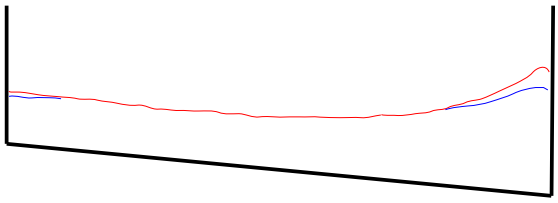

8 mm amplitude
4 mm amplitude

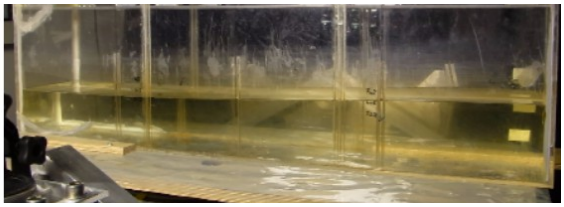

8 mm amplitude

8 mm amplitude

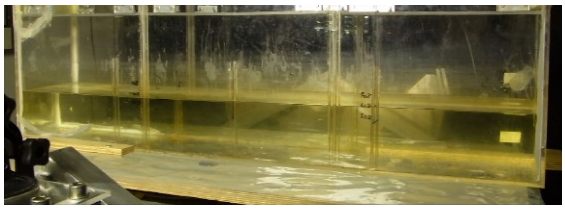

4 mm amplitude

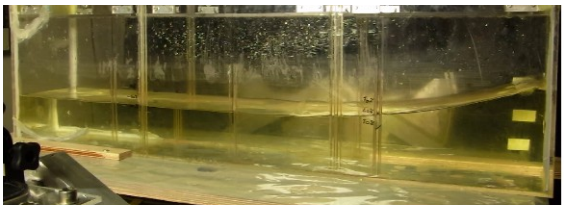

4 mm amplitude

Figure 44: Water surface elevation for a tank without damping grids below and at the resonance period

In the sixth experiment in figure 27 on page 56 the moment curves of different amplitudes at resonance lie close together. As written in chapter 2.7, the DLF and thereby the response amplitude are varying for different frequency ratios and for different damping ratios. For the sixth experiment the period was kept constant (resonance period) but there were no damping grids included such that the damping ratio hardly varied. Consequently, the DLF must be nearly the same in figure 10 on page 22 and thereby the response amplitudes in figure 27. The small difference may be due to viscous boundary-layer flow along the tank walls and other small effects listed by Faltinsen and Timokha (2009) and Solaas (1995). The seventh experiment

in figure 29 on page 58 then had the damping grids included which provided various damping at different sway amplitudes such that the DLF and the response amplitude differed.

Another observation is that the forces and moments in figure 30 on page 60 for a tank motion below the resonance period are exactly 180° opposite in phase with the tank motions. As explained in chapter 2.7 this constellation appears for load frequencies above the natural frequency. The other way around the moments were almost in phase with the tank motions when the tank was excited above the resonance period as in figure 31 on page 62.

When the resonance period is included but the damping grids not, the water movement is no longer linear and superposition is not valid. As soon as the damping grids are mounted, the water behaviour is linear and superposition is possible. Against all apprehensions that the damping grids would introduce more nonlinearities, a new theory is that the grids actually help to keep the water movement in the tank linear by dampening it. By this, Berget (2014) assumed that the nonlinearities must have further sources as slamming, water spray or the roll angle which changes the sloshing pattern at different periods. In spite of the consisting linearity by the damping grids, increasing amplitudes still do not give linear increasing response as the seventh experiment in figure 29 on page 58 shows.

It is surprising that superposition is valid for a tank with damping grids although the resonance period is included and additional viscous effects play a role. This might be a hint that the procedure of superposition at MARINTEK in general might be valid, at least for a combination of the resonance period and periods far away from resonance.

Roll damping tanks are widely used nowadays but still there is only very little understanding of the reaction of such a tank. In chapter 3.3 there were always new results discovered for every new experiment and other combinations of periods will

lead to other results again. As a roll damping tank is difficult to understand by experiments, it is likewise tough to try to simulate sloshing numerically. It is already difficult to simulate the complicated sloshing for a simple tank without damping grids in CFD and Pettersen (2014) added for consideration that it may be difficult to compare test results with CFD results when damping grids are used.

The curves for the moments of the 20th experiment in figure 41 on page 78 where five periods were superposed in roll are slightly more serrated than for the same experiment in sway, even with a high filter frequency of 2.5 Hz. One explanation could be that simply the Matlab code, which was written for the previous tests for the superposition of the different periods, was taken to give direct input to the rig. No sway movement was included to simulate the roll centre on the bottom of the tank like for the first experiments where a code in an Excel sheet was used. So, the centre of roll lay on the roll axis of the rig which was approximately 4.5 cm above the tank bottom and thus nearly in the middle of the 10 centimetres water filling as drawn in figure 14 on page 30. As a consequence, the distance from the tank bottom to the new roll axis had to be added to the otherwise used sway arm which provided the sway force a stronger influence on the overall result. The sway force signal was higher serrated than that of the roll moment. Another explanation of the high serration of the signals could be that the water rolled heavily in the tank by partially hitting the cover panel at maximal 18 degrees roll amplitude.

Overall, the phases match but superposition gives higher moments than the combined motion. This concludes that a prediction of roll moments for a roll damping tank based on superposition would be overestimated because the tank is actually achieving lower roll damping moments in the combined motions. This is for a superposition within roll or sway motions. On the contrary, a superposition of roll and sway together gives lower values than what the tank would actually be able to accomplish with a combined motion in the figures 24 and 25 on page 52.

As soon as the water movement becomes more violent or the hydraulic jump occurs,

nonlinear effects appear at higher frequencies and the superposition principle is no longer valid. Particularly for this frequency range, the prediction of superposed moment amplitudes is of interest, especially at resonance, for which the tank is tuned to work at, to achieve most damping.

There are many possibilities of inserting errors which cannot be fully avoided but kept in an acceptable range. One transducer was drifting such that the discrepancy between the two transducers measuring the vertical forces increased during a test. This could be held to an acceptable minimum by zero settings before each test. This precision error could be reduced by repeating the tests. It was shown that the test results are very consistent except for the first period. Also the comparison of zero crossing periods gives one main discrepancy, this time for a roll period of five seconds. All in all, it could be proved that the accuracy of the tests is good and that they can be used for further comparison.

5 Conclusion

Designing a free surface roll damping tank is not trivial and depends on many factors which might also influence each other. The natural roll period and thereby the performance of the tank can be adjusted to different roll periods of the ship due to changing loading conditions by regulating the water depth in the tank.

The calculated natural period of the tank without grids could be confirmed as well as the fact that the most effective damping occurs at 90° phase shift to the tank motion.

The movement of water through the tank can change very much from period to period and different phenomena occur. The most important phenomenon is the hydraulic jump which plays a roll for efficient roll damping. As a result of installed damping grids, not enough water reaches the other side of the tank in time to raise a large counteracting moment and the hydraulic jump is delayed. This concludes that both roll amplitude and design of the grids have to be considered together when looking for the most efficient damping.

As expected, the occurring moments for the tank without damping grids are much higher than with installed damping grids. The advantage of using damping grids is that the grids are smoothing the damping curve over the periods and that the damping is available over a larger range of periods. This might be more attractive than having excellent damping at specific frequencies.

The comparison of different tank filling heights shows that higher moment amplitudes are reached with a larger amount of water. A high water level gives very high damping at low periods but only within a narrow range.

At the resonance period the tank without damping grids achieved very similar values

no matter of how high the rig amplitudes were.

A first tried superposition of roll and sway gave lower moments than what the tank would actually have been able to accomplish with a combined motion. A roll moment prediction in this case would be underestimated; apart from that the moments also did not coincide in their phase.

For a tank without damping grids and included resonance period among other periods, the water movement is no longer linear and superposition is not valid. As soon as the damping grids are installed, the water behaviour is linear and superposition is possible. A new theory is that the grids help to keep the water movement in the tank linear by dampening it. In spite of this, increasing amplitudes still do not give linear increasing response.

After the systematic analysis of the tank a superposition of five periods just for sway and just for roll was tested with installed damping grids. The neighbouring periods of the resonance period were also included such that the result was nonlinear. In contrast to the first try of superposition described above, the superposition gave higher moments than the combined motion. The roll moment prediction based on this case would be an overestimation.

Every new experiment of a simple case gave new unexpected results. This makes it difficult to discover a pattern especially for the more complicated experiments with two and more periods or even to predict the water behaviour.

It was found out that superposition of periods including the resonance period can be valid for a tank with damping grids, namely for a combination of the resonance period and periods far away from resonance. As a consequence, the procedure of superposition at MARINTEK might be valid when this circumstance is kept in mind. The assumption of linearity of damping moments between different degrees of roll

motion however was refuted.

In practice this would mean for a tank analyses in VERES that the resonance period can be included for a tank with grids but the two neighbouring periods should be excluded to avoid too much excitation near resonance. As the experiments with the damping grids showed, a superposition of the resonance period and periods far away from resonance is no problem whereas a combination of periods near resonance gives questionable results. The values for the excluded periods could then be interpolated.

6 Prospect for further work

The third experiment in chapter 3.3.3 investigated the influence of different filling levels on the damping moment. Since the height of the model tank was not to scale, a h/b ratio was used to decide on the filling height. Now, it would be an idea to compare the received data with data from MARINTEK which has a data base consisting of systematically performed tests in this range. Comparison can be done with tests of other scales, with or without grids and with different grid openings. In addition, this experiment was done for pure roll and it will be interesting to see how the achieved curves fit to the curves of “normal” tests with a different centre of roll.

Next, a tank with normal height to scale could be tested to see how the water movement is influenced by the low tank roof. The impact of severe sloshing and the occurrence of the hydraulic jump can be investigated.

Further investigations can be done to find out why the curve especially for the two degrees of roll amplitude without grids is breaking in. A detailed sloshing analysis could be performed to check whether the break-in comes really from sloshing or whether it has a different source.

Another idea would be to develop the amplitude variation with grids from the first experiment further. A model as a mass-spring system with a damper could be derived to see if it is possible to estimate the moments of the next higher amplitude as their distance between each other is nonlinear. This could give an answer to how the curves for a modal test could be modified.

It was observed that the moment curves of different sway amplitudes are phase shifted to each other for a tank with damping grids in chapter 3.3.5. One might guess that the phase shift in figure 29 on page 58 goes in one direction and that it increases

with decreasing amplitude. Or figuratively speaking, it seems that the smaller peaks are moving further to the right hand side. This trend could be confirmed or refuted by doing further tests with higher and lower amplitudes.

The systematically performed tests in sway could be repeated in roll to prove whether the positive influence of the damping grids is also visible at roll motions. A first superposition of five periods was done which can be analysed further by choosing other periods e.g. to leave the neighbouring periods of the resonance period out and to check for linearity.

After all suggestions the crucial question to solve would be why a prediction of roll moments by using the superposition principle is once underestimated and another time overestimated. It is essential to figure out under which conditions a superposition of roll and sway motions will coincide with a combined motion. A method on how to deal with nonlinear effects should be developed. The high goal would be that 100 frequencies of one sea state can be included at once.

List of figures

List of tables

References

Abramson, H. N.: Slosh Suppression. Washington, D.C.: National Aeronautics and Space Administration NASA, 1969. Monograph.

Berget, K.: Verbal message. Trondheim, Norway: MARINTEK, 2013.

Berget, K.: Verbal message. Trondheim, Norway: MARINTEK, 2014.

Bosch, J. J. van den and Vugts, J. H.: Roll damping by free surface tanks. Delft, Netherlands: Nederlands Scheeps-Studiecentrum TNO, no. 83, 1966

Celebi, Serdar, M. and Akyildiz, H.: Nonlinear Modelling of Liquid Sloshing in a Moving Rectangular Tank. *Ocean Engineering* 29, no. 12, 2002: 1527-1553.

Faltinsen, O. M., Olsen, H. A., Abramson, H. N. and Bass, R. L.: Liquid Slosh in LNG Carriers. Vol. no. 85. Oslo, Norway: Veritas, 1974.

Faltinsen, O. M.: Sea Loads on Ships and Offshore Structures. Vol. 1: Cambridge university press, 1993.

Faltinsen, O. M. and Timokha, A. N.: Sloshing, 2009.

Fathi, D.: ShipX Vessel Responses (VERES) : Motion Control Extension. Trondheim, Norway: MARINTEK, 2012

Goda, Y.: Random Seas and Design of Maritime Structures. Version 3. London, UK: Vol. 33: World Scientific, 2010. URL: http://tinyurl.com/random-seas (last

access 25.11.2013).

Goudarzi, M. A. and Sabbagh-Yazdi, S. R.: Investigation of Nonlinear Sloshing Effects in Seismically Excited Tanks. *Soil Dynamics and Earthquake Engineering* 43, no. 0, 2012: 355-365.

Greco, M.: TMR 4215: Sea Loads : Lecture Notes. Trondheim, Norway: Dept. of Marine Technology, Norwegian University of Science and Technology, 2012: 77-80

Henderson, T.: The Physics Classroom : Fundamental Frequency and Harmonics. Illinois, USA, 2014.
URL: http://www.physicsclassroom.com/class/sound/Lesson-4/Fundamental-Frequency-and-Harmonics (last access 05.04.2014).

Iglesias, A. S., Rojas, L. P. and Rodríguez, R. Z.: Simulation of Anti-Roll Tanks and Sloshing Type Problems with Smoothed Particle Hydrodynamics. *Ocean Engineering* 31, no. 8–9, 2004: 1169-1192.

Jin, J.: Verbal message. Trondheim, Norway: MARINTEK, 2013.

Kramer et. all: Matlab script CheckWaveSignal.m. In: TMR7 – Experimental methods in marine technology : Seakeeping test with a model of an oil tanker. Trondheim, Norway: Norwegian University of Science and Technology, 2013

Larsen, C. M.: Kompendium: TMR4182. Marine dynamics. 18. Trondheim, Norway: Dept. of Marine Technology, Norwegian University of Science and Technology, 2012.

Larsen, C. M.: Forces and motions for marine constructions. In: Offing technology :

An ocean of opportunities (Krefter og bevegelser for marine konstruksjoner. In: Havromsteknologi : Et hav av muligheter). Trondheim, Norway: NTNU, Samarbeidsforum marin, 2013: 169-193

Larsen, C. M.: Verbal message. Trondheim, Norway: Norwegian University of Science and Technology, 2014.

Lee, B. S. and Vassalos, D.: An Investigation into the Stabilisation Effects of Anti-Roll Tanks with Flow Obstructions. *International Shipbuilding Progress* 43, no. 433, 1996: 70-88.

Lewis, E. V.: Principles of Naval Architecture, Volume iii, Motions in Waves and Controllability. Jersey City, NJ: Society of Naval Architects and Marine Engineers, 1989.

MARINTEK: Matlab script StabTank_Analysis_CatMan_compare_amplitudes.m : Stabtank analysis... regular motions taking the difference between two tank series (empty and filled). Trondheim, Norway, 2013.

MARINTEK: Sloshing Laboratory. Trondheim, Norway, 2014. URL: http://www.sintef.no/home/MARINTEK/About-MARINTEK/Departments/Ship-Technology/Laboratories/Sloshing-Laboratory/ (last access 15.05.2014).

Moaleji, R. and Greig, A. R.: On the Development of Ship Anti-Roll Tanks. *Ocean Engineering* 34, no. 1, 2007: 103-121.

Pettersen, B.: Lecture in the Course Marine Dynamics. Trondheim, Norway: Norwegian University of Science and Technology, 2013.

Pettersen, B.: Written message. Trondheim, Norway: Norwegian University of

Science and Technology, 2014.

Solaas, F.: Analytical and Numerical Studies of Sloshing in Tanks. Vol. 1995:103. Trondheim, Norway: NTH., 1995.

Steen, S.: Experimental Methods in Marine Hydrodynamics. Lecture notes. Trondheim, Norway: Norwegian University of Science and Technology, Department of Marine Technology, 2012.

Strandenes, H.: Verbal message. Trondheim, Norway: Norwegian University of Science and Technology, Department of Marine Technology, 2014.

Sæther, A.: Matlab script Frequency_analysis.m : Function reading binary files, analysing and plotting data, for lab 2 - VIV, Experimental methods in Marine Hydrodynamics. Trondheim, Norway, 2013

Winkler, S.: FLUME® Passive Anti-Roll Tanks : Application on merchant and naval ships. Flume GmbH, Hamburg, 2012

Younes, M. F., Younes, Y. K., El-Madah, M., Ibrahim, I. M. and El-Dannanh, E. H.: An Experimental Investigation of Hydrodynamic Damping Due to Vertical Baffle Arrangements in a Rectangular Tank. *Proceedings of the Institution of Mechanical Engineers Part M: Journal of Engineering for the Maritime Environment* 221, no. 3, 2007: 115-123.

Appendix A: Purpose designed damping grids

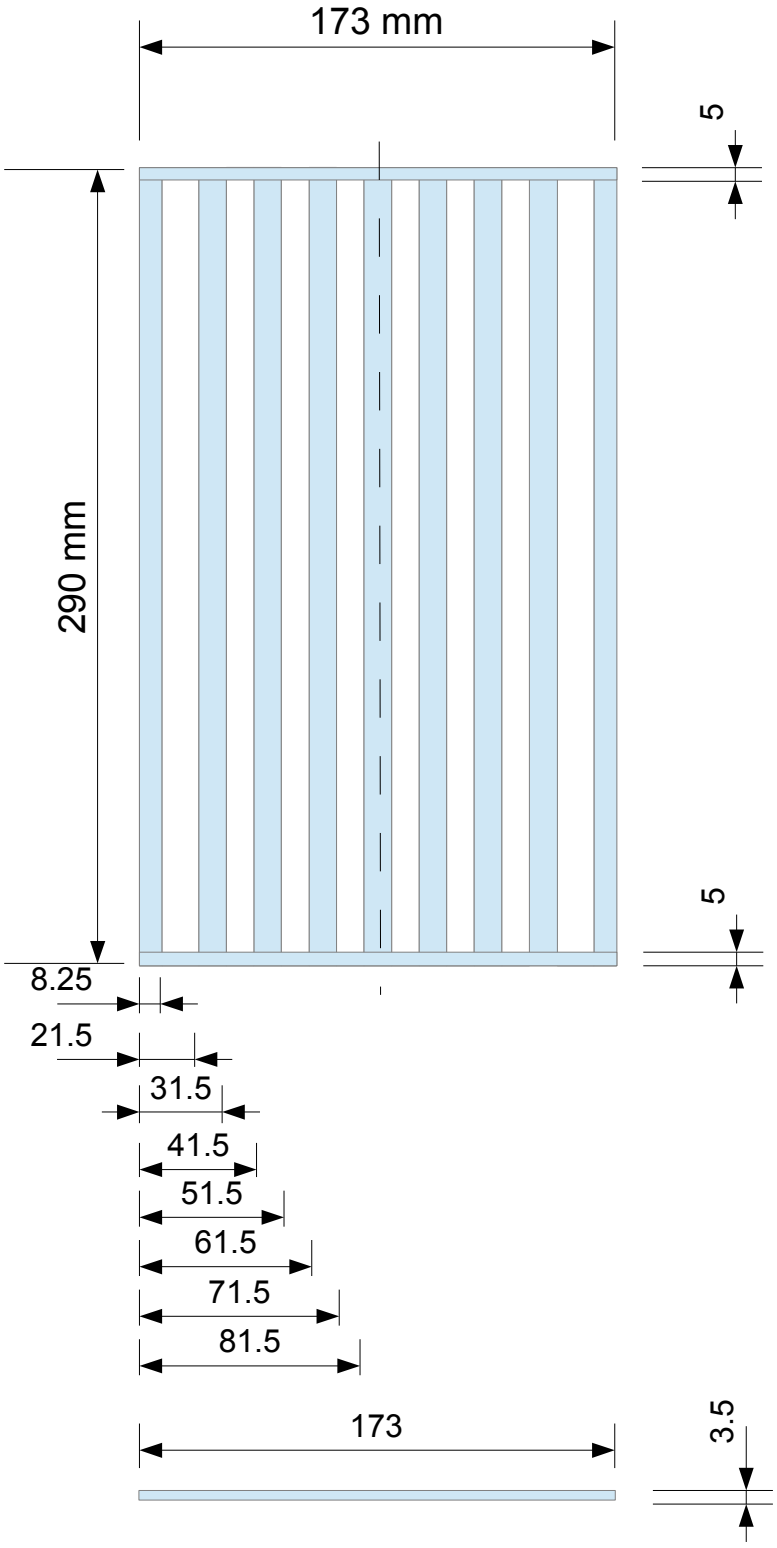

Figure 45: Self-designed damping grid

Appendix B: Complete test matrix

The first tests in table 5 were done with the first method where all 19 periods were performed one after each other. Filling levels and the single rig motions are stated where the distance *s* defines a roll centre below the tank. For all other tests the roll centre was located at the inner tank bottom. Tests were done with and without grids for a comparison. The last column lists in which experiments the test results were used for an analysis. The numbers correspond to the experiment numbering in the overviews on the pages 35 and 82. From test 3001 on each test was accompanied with an empty tank test because a change in period gave different tank inertia forces. These empty tank tests are not extra listed. T_1 is the resonance period of nine seconds in full scale.

Table 5: Complete test matrix

Test number	Periods in full scale [s]	Filling level	Rig motion	Grids	Used in experiment
1103	4-25	Empty	Sway	Yes	4, 5
1104	4-25	Empty	Roll, 4 deg	Yes	1, 2, 3, 4, 5
1105	4-25	Empty	Roll, 2 deg	Yes	1, 2
1106	4-25	Empty	Roll, 6 deg	Yes	1
1107	4-25	Empty	*s* = 10 m; Sway; roll, 4 deg	Yes	4, 5
1108	4-25	10 cm	Roll, 2 deg	Yes	1, 2
1109	4-25	10 cm	Roll, 4 deg	Yes	1, 2
1110	4-25	10 cm	Roll, 6 deg	Yes	1

Test number	Periods in full scale [s]	Filling level	Rig motion	Grids	Used in experiment
1111	4-25	10 cm	*s* = 10 m; Sway; roll, 4 deg	Yes	4, 5
1112	4-25	10 cm	Sway	Yes	4, 5
1113	4-25	10 cm	Roll, 2 deg	No	2
1114	4-25	10 cm	Roll, 4 deg	No	2
1115	4-25	15 cm	Roll, 4 deg	Yes	3
1116	4-25	5 cm	Roll, 4 deg	Yes	3
3001	T_1	10 cm	8 mm sway	No	6
3002	T_1	10 cm	4 mm sway	No	6, 15, 17
3003	T_1	10 cm	8 mm sway	Yes	7
3004	T_1	10 cm	4 mm sway	Yes	7, 16, 18, 19
3005	T_1 - 1	10 cm	8 mm sway	No	8
3006	T_1 - 1	10 cm	4 mm sway	No	8, 12, 15
3008	T_1 - 1	10 cm	4 mm sway	Yes	13, 19
3015	T_1, T_1 - 1	10 cm	4 mm sway	No	15
3017	T_1 - 1, T_1 + 1	10 cm	4 mm sway	No	12
3018	T_1 - 1, T_1 + 1	10 cm	4 mm sway	Yes	13
3021	T_1 + 1	10 cm	4 mm sway	No	10, 12, 17
3022	T_1 + 1	10 cm	4 mm sway	Yes	13, 19
3023	T_1 + 1	10 cm	8 mm sway	No	10
3025	T_1, T_1 + 1	10 cm	4 mm sway	No	17
3028	T_1 - 3	10 cm	4 mm sway	Yes	9, 14, 16, 19
3030	T_1 + 3	10 cm	4 mm sway	Yes	11, 14, 18, 19
3034	T_1, T_1 - 3	10 cm	4 mm sway	Yes	16

Test number	Periods in full scale [s]	Filling level	Rig motion	Grids	Used in experiment
3036	T_1, T_1 + 3	10 cm	4 mm sway	Yes	18
3038	T_1 - 3, T_1 - 1, T_1, T_1 + 1, T_1 + 3	10 cm	4 mm sway	Yes	19
3040	T_1 + 1	10 cm	6 mm sway	Yes	7
3042	T_1 - 3	10 cm	8 mm sway	Yes	9
3044	T_1 + 3	10 cm	8 mm sway	Yes	11
3102	T_1 - 3	10 cm	4 mm roll	Yes	20
3104	T_1 - 1	10 cm	4 mm roll	Yes	20
3106	T_1	10 cm	4 mm roll	Yes	20
3108	T_1 + 1	10 cm	4 mm roll	Yes	20
3110	T_1 + 3	10 cm	4 mm roll	Yes	20
3112	T_1 - 3, T_1 - 1, T_1, T_1 + 1, T_1 + 3	10 cm	4 mm roll	Yes	20

Appendix C: Matlab scripts for the superposition of two tests

The Matlab script for the analysis of the first three experiments is property of MARINTEK (2013) and therefore not published here. Instead, the development of a script for a superposition of two tests and a comparison with the combined test is explained which was used from the fourth test on.

C.1 Matlab script for the superposition of roll and sway motions

In the following it is shortly described how the code was developed and which iteration steps were done to achieve a high accuracy in the data analysis. The first loop in the code for processing the data of different channels is taken from the first mentioned script from MARINTEK (2013). The low pass filter was applied in a simplified form and only on channels which contained measured forces from the strain gauges. It was unnecessary to apply the filter on the recorded movements of the rig because they were very accurate and smooth conducted by the servo motors as could be seen in recorded time series. The relevant channels were plotted for the whole time series for choosing a start and an end point for the investigation of one frequency interval. Besides the forces and rig movements, also the time was recorded. Yet the time was unsuitable for defining start and end points for a further comparison of different tests because the command for starting the rig was given manually after having started the recording. Hence, the time span from starting the record until the first movement of the rig was different for each test. Instead of setting a start point, a local maximum of the performed rig movement in the interval of interest was selected manually and entered into the Matlab script. Still, this method was inaccurate and let to a phase shift in a plotted comparison of the different tests. To find the exact position of the maximum, a small interval containing the first fully

developed rig movement for one period was selected manually, referring to Sæther (2013), and a command from Kramer et. all (2013) was used to find the exact position of the peak. This procedure of finding the start point had to be done for each test. For the tests in roll, a maximum in the roll amplitude was chosen; for the tests in sway a maximum in the sway amplitudes was selected. This explains why roll and sway motions in the figures are always in phase. Indeed, they were almost in phase executed for the combined tests. The following code was used for superposing roll and sway motions in chapter 3.3.4.

```
% Plot CatMan file and superpose the two output signals.
% In a CatMan file the measurement data are stored.
%%%%%%%%%%%%
% For pure roll:

clear all
% Read CatMan data file
filename='1109e_pure_roll4deg_2013_10_21.bin';

[~, water2]=catman_read(filename); % The ~ replaces unused
variables.

nChannels=7; % Data are stored in even channels.

clear dataWater
for iCh= 1:nChannels
        dataWater(:,iCh)=water2(iCh).data;
end

% Filter data
dt = 0.02; % delta t as sampling frequency = 50 Hz

filterFreq = 1.2; % Hz

Sideforce = lpfilt(dataWater(:,4),dt,filterFreq); % channel 4
Roll_moment_Water = lpfilt(dataWater(:,7),dt,filterFreq); % channel
7
% lpfilt = low pass filter

% Total roll moment: adding channel 4 multiplied by the vertical arm
%(from transducer to tank bottom in m) to channel 7 (which has the
% longitudinal arm already included). The arm has to be negative for
% a positive moment.
Total_moment = Roll_moment_Water + Sideforce * (-0.07);
```

```
% Changing dataWater into variables with meaningful names to be able
% to put a dependency on start and end point.
% channel 1 contains time
% channel 2 and 3 contain the two vertical forces Fz
% channel 4 contains side force
% channel 5 contains roll motion of the rig
% channel 6 contains sway motion of the rig
% channel 7 contains roll torque = roll moment from channel 2 and 3
[ch1, ch2, ch3, ch4, ch5, ch6, ch7] = water2.data;

figure(1)
scrsz=get(0,'ScreenSize'); % Get screen size
h=figure('Position',scrsz);  % Open figure in full screen
hold on
plot(ch5, '-k') % It shows, that the rig did not reach an amplitude
% of 4 deg for the first 3 cycles and that it is slightly higher
% towards the end.
plot(Roll_moment_Water, '-b')

% Choose a time interval from figure(1) (to find a local maximum as start
point when superposing in the chapters 3.3.4 until 3.3.7)

t1_start = input('start of small time interval = ')
t1_end = input('end of small time interval = ')
```

Or without query:

```
t1_start = 16700; % for 9. series.
t1_end = 16740;

% Find the local maximum for the start point t1
ch5_start = ch5(t1_start:t1_end);
[peak, locs] = findpeaks(ch5_start);
% where "peak" gives the y-value and "locs" the position within this
% interval, the n-th value, which is then added to the interval
% start point.

% Final start and end points for the interval
t1 = t1_start+locs-1;
t2 = t1 + 500; % for 9. series
% The interval length is then (t2-t1).  For the final plot all
% vectors must be of the same length.

% For checking:
% figure(2)
% hold on
% plot(ch5(t1:t2),'-k')
% plot(Roll_moment_Water(t1:t2), '-b')
% plot(Total_moment(t1:t2), '-r')
% plot(Sideforce(t1:t2), '-g')

%%%%%%%%%%%%%%%%%%%
```

```
% The empty tank forces have to be subtracted for pure roll:

% Read CatMan data files
filename='1104b_empty_pure_roll4deg_2013_10_18.bin';

[~, water2_roll_empty]=catman_read(filename);

clear dataWater_roll_empty
for iCh= 1:nChannels
        dataWater_roll_empty(:,iCh)=water2_roll_empty(iCh).data;
end

Sideforce_roll_empty =
lpfilt(dataWater_roll_empty(:,4),dt,filterFreq);
Roll_moment_Water_empty =
lpfilt(dataWater_roll_empty(:,7),dt,filterFreq);

Total_moment_roll_empty = Roll_moment_Water_empty +
Sideforce_roll_empty * (-0.07);

[~, ~, ~, ~, ch5_roll_empty, ~, ~] = water2_roll_empty.data;

% figure(3)
% scrsz=get(0,'ScreenSize'); % Get screen size
% h=figure('Position',scrsz);  % Open figure in full screen
% hold on
% plot(ch5_roll_empty, '-k')
% plot(Roll_moment_Water_empty, '-b')

% Choose a time interval from the previous figure
% for 9. series:
t1_roll_empty_start = 16930; % = input('start of time interval = ')
t1_roll_empty_end = 16950; % = input('end of time interval = ')

% Find the local maximum for the start point t1
ch5_roll_empty_start =
ch5_roll_empty(t1_roll_empty_start:t1_roll_empty_end);
[peak, locs] = findpeaks(ch5_roll_empty_start);

% Final start and end points for the interval
t1_roll_empty = t1_roll_empty_start+locs-1;
t2_roll_empty = t1_roll_empty + (t2-t1);

% Subtracting the inertia moments of the empty tank from the moments
% of the water movement for achieving the total moment in roll
Total_moment_roll = Total_moment(t1:t2) -
Total_moment_roll_empty(t1_roll_empty:t2_roll_empty);
```

For the pure sway test and the combined motion test this code section has to be repeated but with different variable names. Finally, the total roll moments can be

plotted:

```
figure(7)
scrsz=get(0,'ScreenSize'); % Get screen size
h=figure('Position',scrsz);  % Open figure in full screen
hold on
plot(ch5(t1:t2), '-k')
plot(ch6_sway(t1_sway:t2_sway)*100, '-.k') % in cm
plot(Total_moment_roll, '-b')
plot(Final_moment_sway, '-g')
plot(Total_moment_roll + Final_moment_sway, '-m')
plot(Final_moment_comb, '--r')
title('Moments for pure roll, pure sway, their superposition and
combined; at resonance period')
legend('Roll motion rig','Sway motion rig','Roll moment for
roll','Roll moment for sway','Superposed roll moment','Combined roll
moment',1);
xlabel('Samples')
ylabel('Roll motion [deg], Sway motion [cm], Roll moment [Nm]')
set(findall(h, '-property', 'FontSize'), 'FontSize', 12)
```

C.2 Matlab script for the linearity check and the superposition of different periods

When superposing different periods the start point of each time series could no longer be chosen by an amplitude maximum because the different periods were phase shifted to each other. Therefore a point in the beginning had to be found which was characteristic for all involved periods. This was found to be the first intersection of all periods. The initially created rig sway motions were plotted in one graph to find the x-value where all periods went through. Next, the executed rig sway motions with different time delay in the beginning were plotted and the previously established point had to be detected roughly. Finally, the theoretical and the measured rig motions were overlaid with the intersection as starting point and fine tuned until they matched. A correct superposition was secured by this method. A separate script was used for this analysis. The in this manner established starting points could then be entered into the script used for superposing the periods. This procedure had to be repeated for the tests with the empty tank. In this way the rig motions were proportioned and

the measured forces according to these motions could be plotted and superposed.

The following script is based on the first one but the code was modified for the experiments with a superposition of different periods in chapter 3.3.8 and further on. In addition, a mean value for each roll moment and sway force had to be estimated because the transducers did not start with zero values at zero load. Later on, the procedure of finding the mean value was automated. Moreover, the filter frequency was adjusted for each test.

```
% For the first test:

clear all
% Read CatMan data file
filename='Test3001_0.008_2.02_2014.03.11.bin';

[~, water2]=catman_read(filename); % The ~ replaces unused
variables.

nChannels=7; % Data are stored in even channels.

clear dataWater
for iCh= 1:nChannels
        dataWater(:,iCh)=water2(iCh).data;
end

% Changing dataWater into variables with meaningful names to be able
% to put a dependency on start and end point. NOTE: CHANNEL CONTENT
% CHANGED!!! --> words like "roll" are no longer correct in
% combination with a channel.
% channel 1 contains time
% channel 2 contains roll motion of the rig
% channel 3 contains sway motion of the rig
% channel 4 contains side force
% channel 5 and 6 contain the two vertical forces Fz
% channel 7 contains roll torque = roll moment from 5 and 6
[ch1, ch2, ch3, ch4, ch5, ch6, ch7] = water2.data;

% Filter data
dt = 0.02; % delta t is sampling frequency = 50 Hz

filterFreq = 1.2; % Hz, normally 1.2, 2 Hz for test 3023, 2.5 Hz for
% test 3028
filterFreq2 = 2.5; % 2.5 for the high serrated side force signal in
% general, 1.2 Hz for test 3023 without double peak
```

```
% for test 3001:
Sideforce = lpfilt(dataWater(:,4),dt,filterFreq2) +0.62;
Roll_moment_Water = lpfilt(dataWater(:,7),dt,filterFreq) -0.45;
% lpfilt = low pass filter

% The measurements start not with zero values at zero load! → Use
% figure 1 to determine for each test separately: here, ch7 with
% -0.45 and ch4 with +0.62 (values are the gap to half the
% difference between a maximum and the following minimum)

Total_moment = Roll_moment_Water + Sideforce * (-0.07);

figure(1)
scrsz=get(0,'ScreenSize'); % Get screen size
h=figure('Position',scrsz);  % Open figure in full screen
hold on
plot(ch3*100, '-k')
% plot(Roll_moment_Water , '-b')
% plot(ch7 -0.45,'r')
plot(ch4 +0.62,'r')
plot(Sideforce ,'b')
```

For adding two periods, the start point was found in a different way:

```
t1 = 784; % for test 3002b when analysing T_1 + T_2 (resonance, 1 s
% below)
t2 = t1 + 7200;
% The interval length is then (t2-t1).

% For the final plot all vectors must be of the same length.
Sway_rig = ch3(t1:t2);
```

The variable name is kept although different periods instead of sway and roll motions are now superposed.

Instead of determining the mean value manually as shown a few lines before, a further development was to get the mean value automatically:

```
% The measurements start not with zero values at zero load. Use
% figure 1 to find a range where you want to get the mean value
% from.
S = mean(ch4(1:250));
R = mean(ch7(1:250));
% (1:300) for test 3023, (1:60) for test 3008b, (1:250) for test
% 3028

Sideforce = lpfilt(dataWater(:,4),dt,filterFreq2) -S;
Roll_moment_Water = lpfilt(dataWater(:,7),dt,filterFreq) -R;

figure(1)
scrsz=get(0,'ScreenSize'); % Get screen size
h=figure('Position',scrsz);  % Open figure in full screen
hold on
```

```
plot(ch3*100, '-k')
% plot(Roll_moment_Water , '-b')
% plot(ch7 -R,'r')
plot(ch4 -S,'r')
plot(Sideforce ,'b')

%%%%%%%%%%%%%%%%%%%
% The empty tank forces have to be subtracted:

% Read CatMan data files
filename='Test4001_2014.03.12.bin';

[~, water2_roll_empty]=catman_read(filename);

clear dataWater_roll_empty
for iCh= 1:nChannels
        dataWater_roll_empty(:,iCh)=water2_roll_empty(iCh).data;
end

[~, ~, ch3_roll_empty, ch4_roll_empty, ~, ~, ch7_roll_empty] =
water2_roll_empty.data;

S = mean(ch4_roll_empty(1:180));
R = mean(ch7_roll_empty(1:180));
% (1:100) for test 4023, % (1:40) for test 4008, (1:180) for test
% 4028

Sideforce_roll_empty =
lpfilt(dataWater_roll_empty(:,4),dt,filterFreq2) -S;
Roll_moment_Water_empty =
lpfilt(dataWater_roll_empty(:,7),dt,filterFreq) -R;

Total_moment_roll_empty = Roll_moment_Water_empty +
Sideforce_roll_empty * (-0.07);

figure(3)
scrsz=get(0,'ScreenSize'); % Get screen size
h=figure('Position',scrsz);  % Open figure in full screen
hold on
plot(ch3_roll_empty*100, '-k')
% plot(ch7_roll_empty -R,'r')
% plot(Roll_moment_Water_empty, '-b')
plot(ch4_roll_empty -S,'r')
plot(Sideforce_roll_empty,'b')

% Choose a time interval from the previous figure
% t1_roll_empty_start = 960; % for test 4001
% t1_roll_empty_end = 1005;

% Find the local maximum for the start point t1
% ch3_roll_empty_start =
% ch3_roll_empty(t1_roll_empty_start:t1_roll_empty_end);
% [peak, locs] = findpeaks(ch3_roll_empty_start);
```

```
% Final start and end points for the interval
% t1_roll_empty = t1_roll_empty_start+locs-1;
t1_roll_empty = 465; % for test 4002b when analysing T_1 + T_2
t2_roll_empty = t1_roll_empty + (t2-t1);

% Subtracting the inertia forces from the empty tank from the water
% forces
Total_Sideforce = Sideforce(t1:t2) -
Sideforce_roll_empty(t1_roll_empty:t2_roll_empty);
Total_Roll_moment_Water = Roll_moment_Water(t1:t2) -
Roll_moment_Water_empty(t1_roll_empty:t2_roll_empty);
Total_moment_roll = Total_moment(t1:t2) -
Total_moment_roll_empty(t1_roll_empty:t2_roll_empty);
```

As for the previous code this code section has to be repeated for every period which shall be superposed to this period. In addition, the same analysis has to be done for the combined test until a comparison can be plotted:

```
figure(7)
scrsz=get(0,'ScreenSize'); % Get screen size
h=figure('Position',scrsz);  % Open figure in full screen
subplot(2,1,1)
grid on
hold on
plot(Sway_rig(14000:14500) + Sway_rig_sway(14000:14500), '-g')
plot(Sway_rig_comb(14000:14500), '-b')
title('Roll moments for tests at 4 mm sway amplitude, 3 s below and
above the resonance period, their superposition, and in one test
combined')
legend('Superposed sway motion rig','Combined sway motion rig',1);
ylabel('Sway motion [mm]')
subplot(2,1,1)
grid on
hold on
plot(Total_moment_roll(14000:14500) +
Final_moment_sway(14000:14500), '-b')
plot(Final_moment_comb(14000:14500), '-r')
legend('Superposed roll moment','Combined roll moment',4);
xlabel('Samples')
ylabel('Total roll moment [Nm]')
```

Appendix D: Graphs to the linearity check

Figure 46 belongs to the ninth experiment described in chapter 3.3.6 Linearity check below the resonance period. The tank performance at three seconds below the resonance period with included damping grids is shown. The result was a linear water movement.

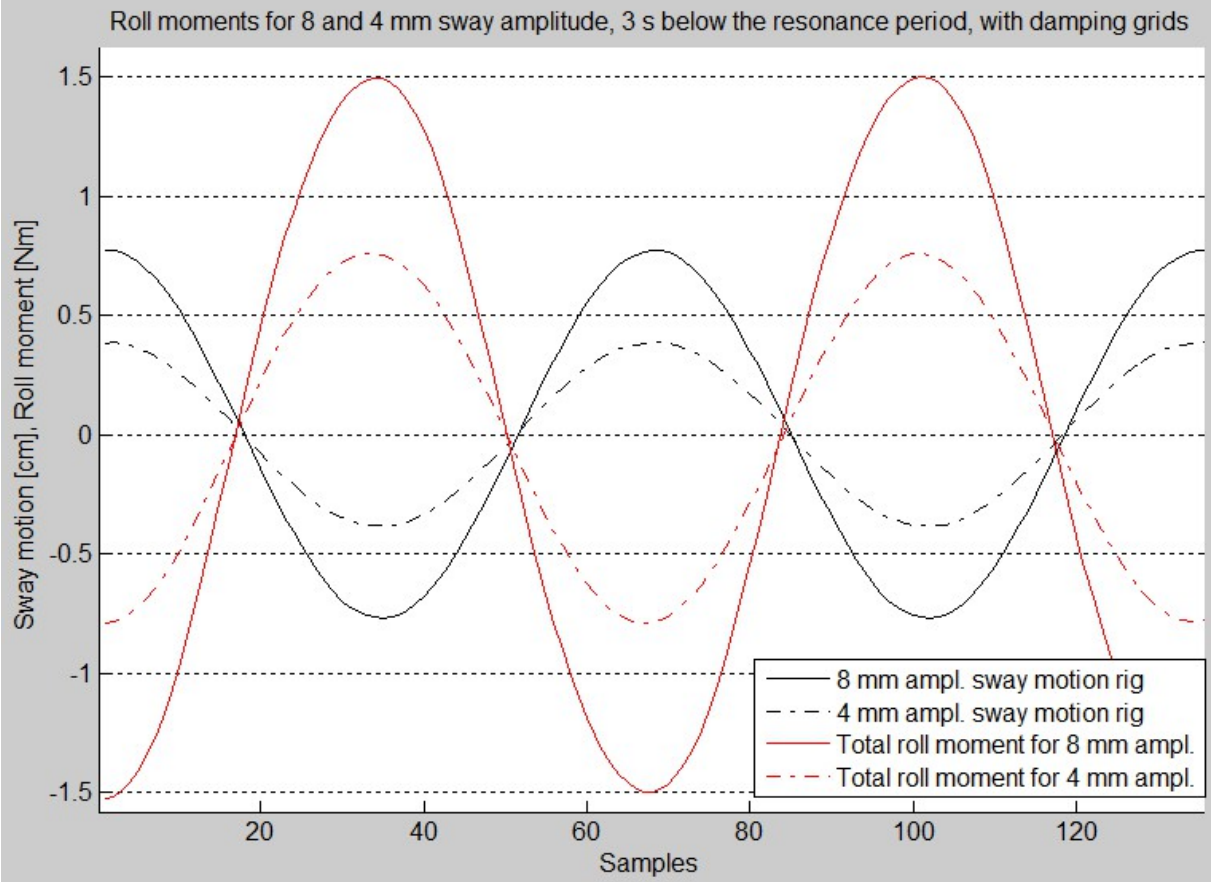

Figure 46: Roll moments for eight and four millimetres sway amplitude at three seconds below the resonance period, with damping grids; ninth experiment

Figure 47 belongs to the eleventh experiment described in chapter 3.3.7 Linearity check above the resonance period. The tank performance at three seconds above the resonance period with included damping grids is shown. The result was a linear water movement.

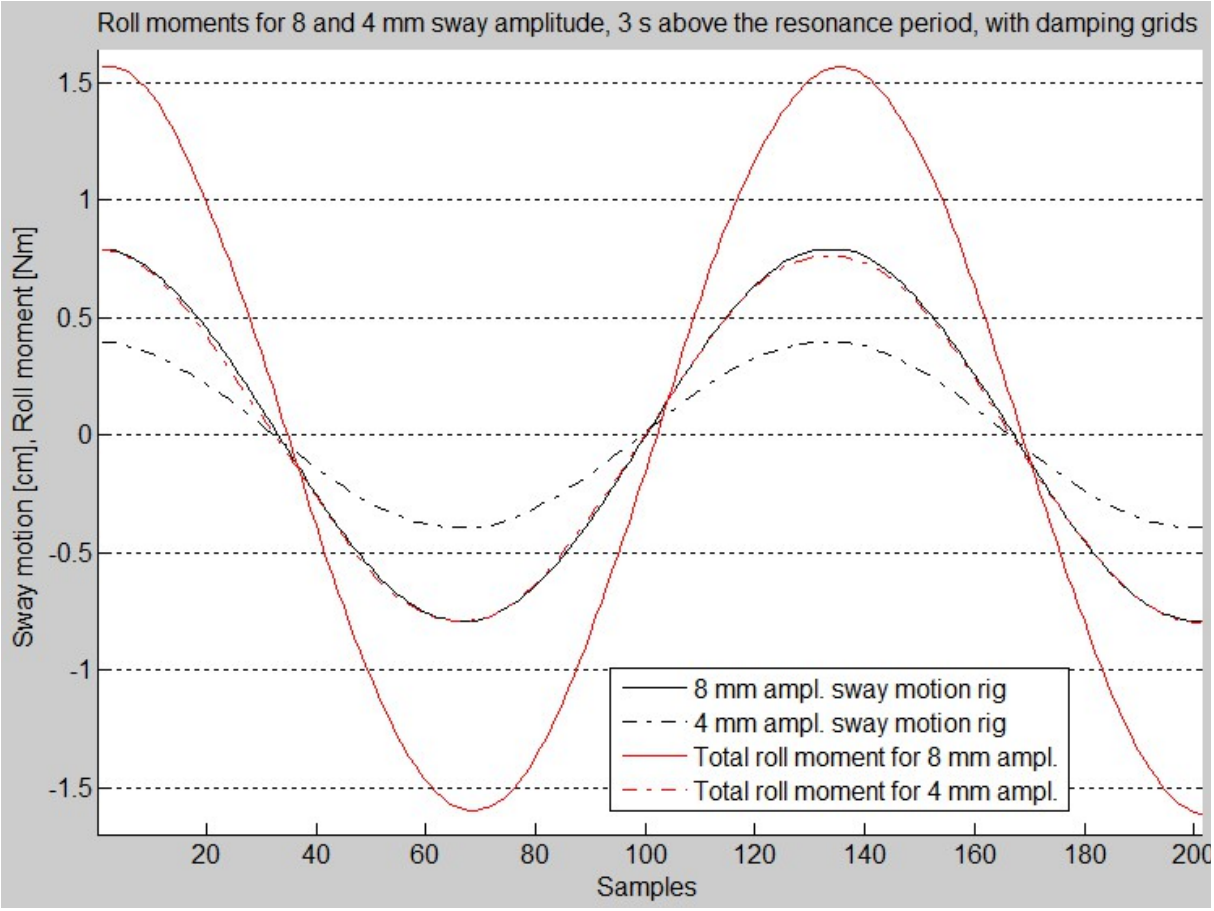

Figure 47: Roll moments for eight and four millimetres sway amplitude at three seconds above the resonance period, with damping grids; 11th experiment

Appendix E: Graphs to the superposition of two signals

Two different frequencies are combined in figure 48. The outcome is a signal in the bottom graph of the figure where frequency and amplitude change in time but the originated pattern is repeating itself periodically.

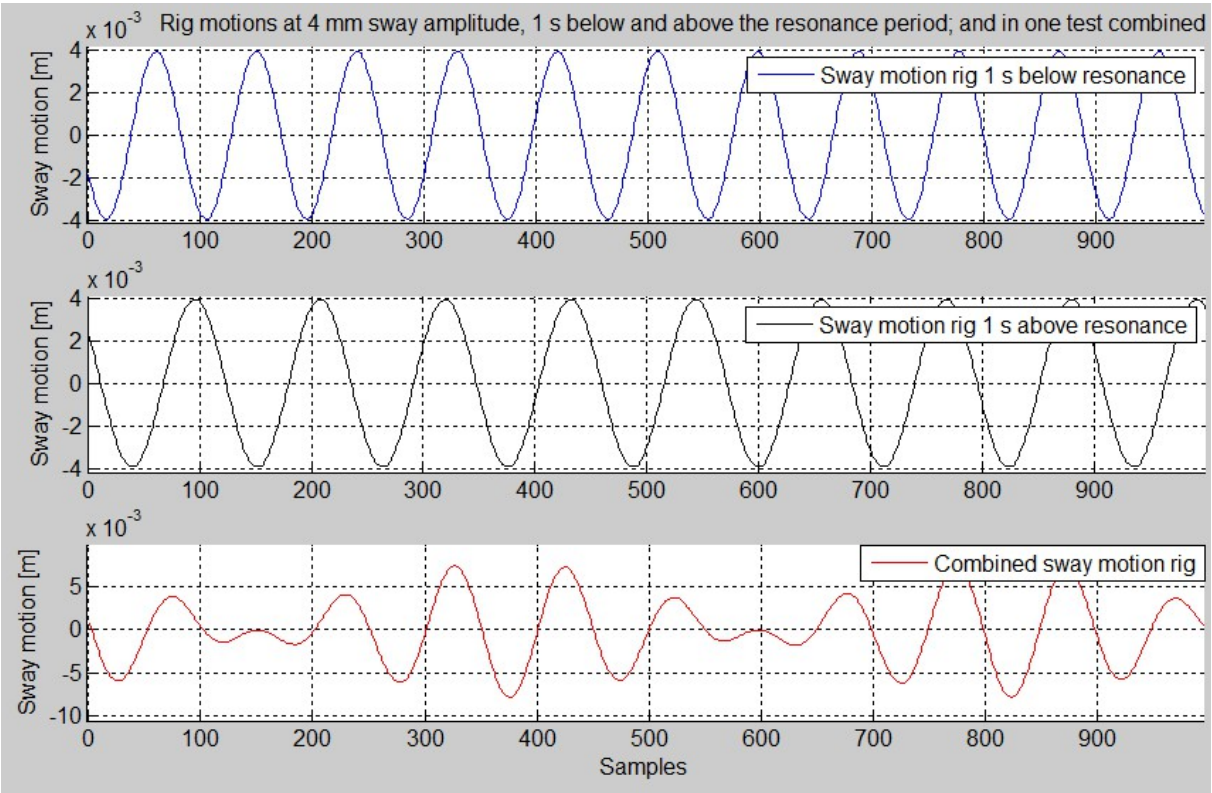

Figure 48: Performing a superposition of two signals with different frequencies

Figure 49 documents the validity of superposition of roll moments in a tank with damping grids at three seconds above and at the resonance period. Superposition is valid. The figure belongs to the 18th experiment described in chapter 3.3.10 Superposition of sway motions above and at the resonance period.

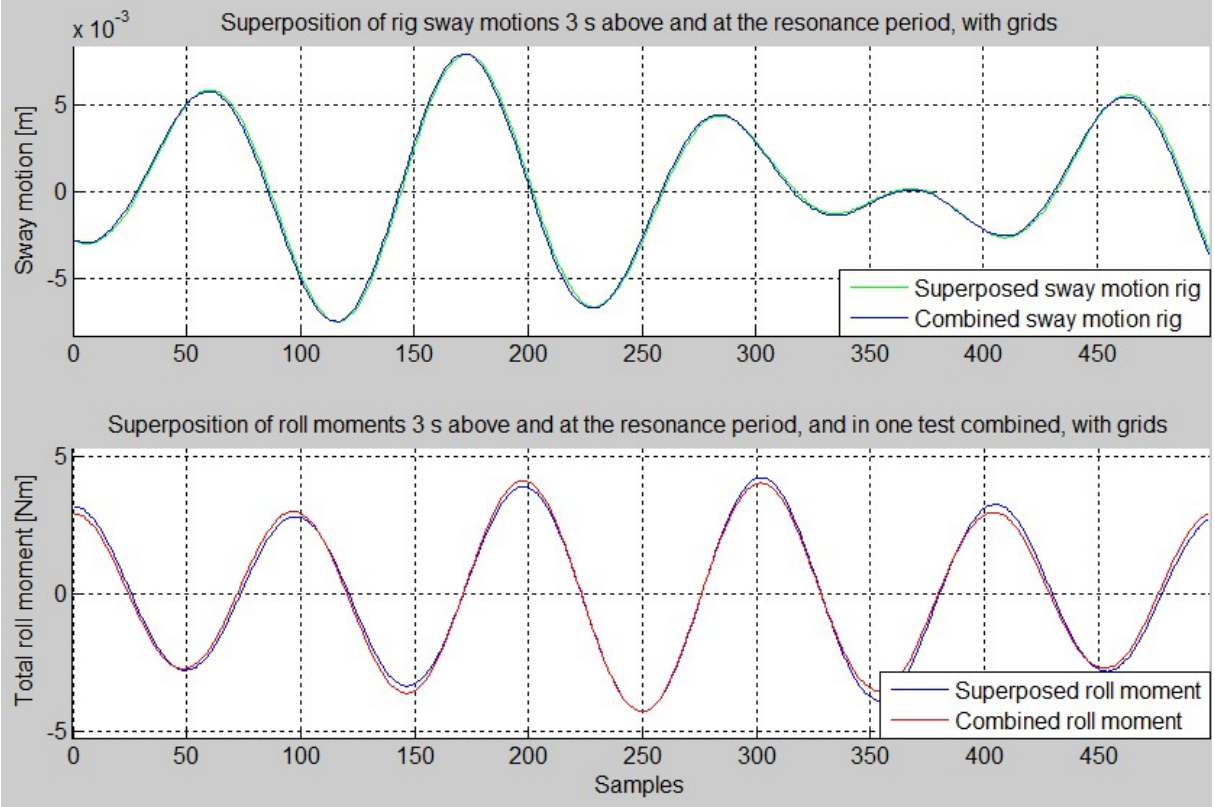

Figure 49: Superposition of sway motions (upper graph) and roll moments (lower graph) at four millimetres amplitude, three seconds above and at the resonance period, with damping grids; 18th experiment

Appendix F: Graphs to the error analysis

One test was repeated five times. Damping grids were included. The recorded values of the single tests in figure 50 are in high accordance to each other. This figure and the next one belong to chapter 3.4 Error analysis.

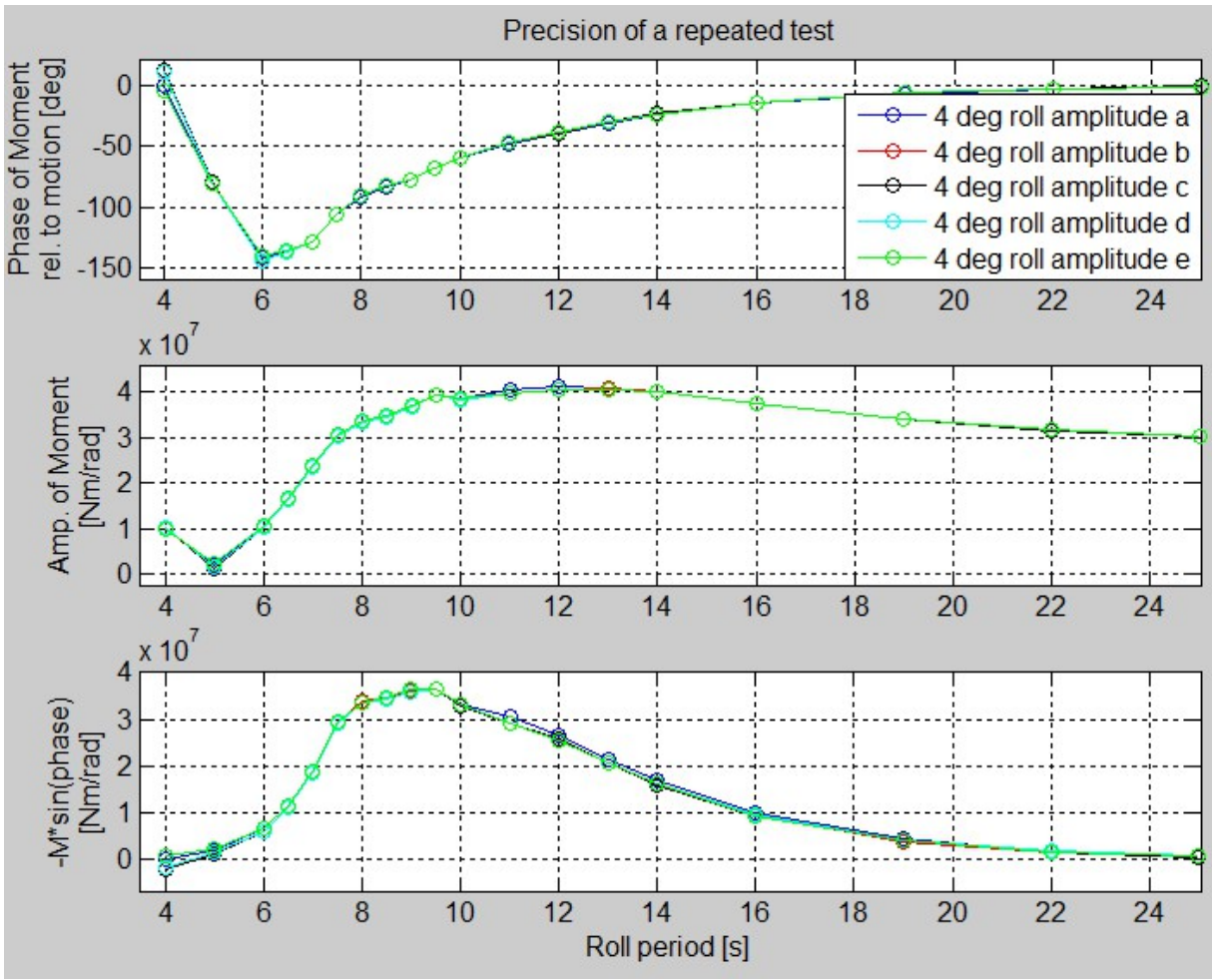

Figure 50: Precision of a five times repeated test

The second method applied for an error analysis described in chapter 3.4 was to use both the zero downcrossing and the zero upcrossing periods. In figure 51, they result in almost the same values.

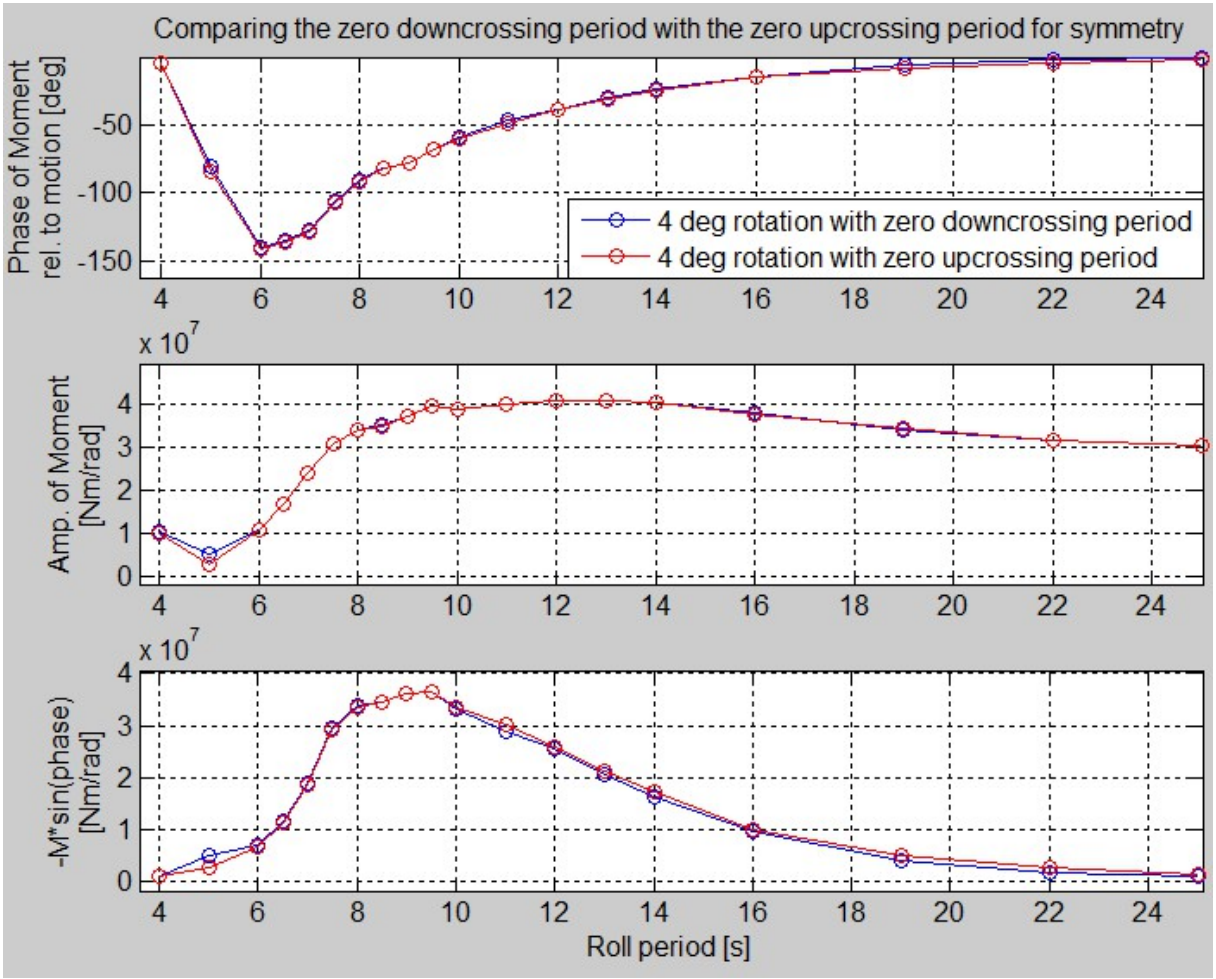

Figure 51: Comparing the zero downcrossing with the zero upcrossing period for a symmetry check